



FE20064

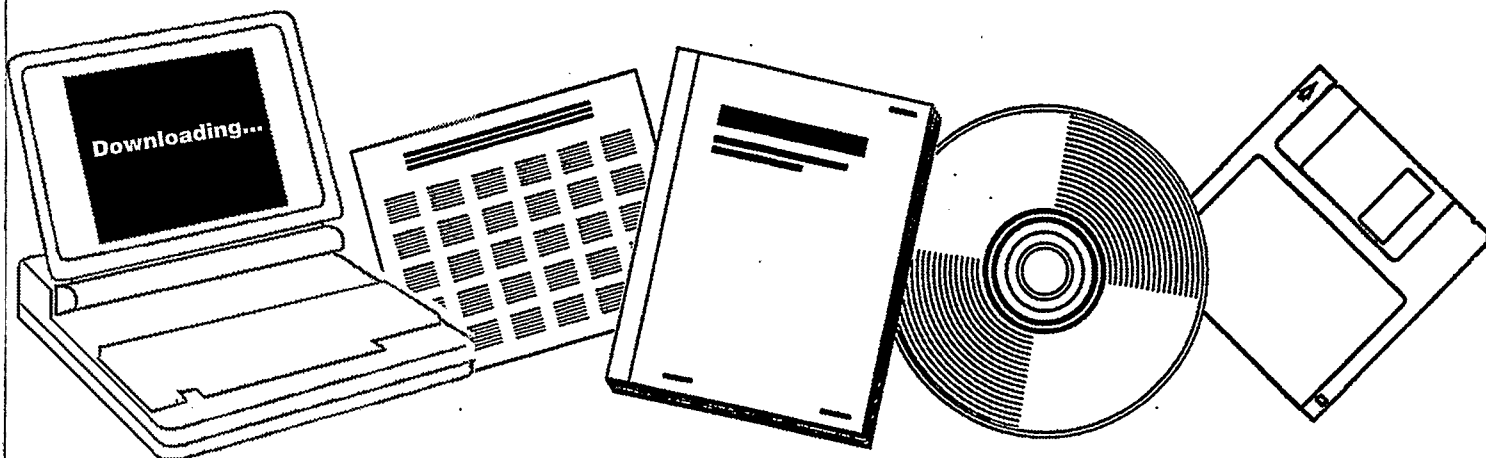
NTIS

One Source. One Search. One Solution.

**APPLIED RESEARCH AND EVALUATION OF PROCESS
CONCEPTS FOR LIQUEFACTION AND GASIFICATION
OF WESTERN COALS. QUARTERLY PROGRESS
REPORT, APRIL--JUNE 1976**

UTAH UNIV., SALT LAKE CITY. DEPT. OF
MINING, METALLURGICAL AND FUELS
ENGINEERING

OCT 1976



U.S. Department of Commerce
National Technical Information Service

One Source. One Search. One Solution.

NTIS



Providing Permanent, Easy Access to U.S. Government Information

National Technical Information Service is the nation's largest repository and disseminator of government-initiated scientific, technical, engineering, and related business information. The NTIS collection includes almost 3,000,000 information products in a variety of formats: electronic download, online access, CD-ROM, magnetic tape, diskette, multimedia, microfiche and paper.



Search the NTIS Database from 1990 forward

NTIS has upgraded its bibliographic database system and has made all entries since 1990 searchable on www.ntis.gov. You now have access to information on more than 600,000 government research information products from this web site.

Link to Full Text Documents at Government Web Sites

Because many Government agencies have their most recent reports available on their own web site, we have added links directly to these reports. When available, you will see a link on the right side of the bibliographic screen.

Download Publications (1997 - Present)

NTIS can now provide the full text of reports as downloadable PDF files. This means that when an agency stops maintaining a report on the web, NTIS will offer a downloadable version. There is a nominal fee for each download for most publications.

For more information visit our website:

www.ntis.gov



U.S. DEPARTMENT OF COMMERCE
Technology Administration
National Technical Information Service
Springfield, VA 22161

FE-2006-4

Distribution Category UC-90

Applied Research and Evaluation of
Process Concepts for Liquefaction
and Gasification of Western Coals

Quarterly Progress Report
for the Period April-June 1976

Dr. Wendell H. Wiser

University of Utah - Department of Mining
Metallurgical and Fuels Engineering
Salt Lake City, Utah 84112

Date Published - Oct 1976

Prepared for
Energy Research and Development Administration

Under Contract No E (49-18) - 2006

CONTENTS

I	Cover Sheet	1
II	Objective and Scope of Work	3
III	Summary of Progress to Date	5
IV A-1	Catalytic Gasification of Coal to High BTU Gas	6
A-2	Dissolution of Coal in Hydrogen Donor Solvents with Application of Catalysts and Energized Conditions to Produce Clean Fuels	27
A-4	Steam Reforming of Aromatic Compounds	43
A-6	Production of Hydrogen from Char Produced in Coal Hydrogenation under High Pressure	43
A-7	Study of Thermal and Vapor Phase Catalytic Upgrading of Coal Liquids	44
A-8	Synthesis of Light Hydrocarbons from CO and H ₂	45
A-9	Development of an Inexpensive Recycle Pump	69
B-1	Development of Optimum Catalysts and Supports	69
B-2	Fundamental Studies on Adsorption of Catalytic Materials on Coal	79
B-3	Fundamental Studies on Hydrogen Transfer over Coal Conversion Catalysts	91
B-4	Mechanism of Catalytic Hydrogenation by Metal Halide Catalysts	93
C-1	The Mechanism of Pyrolysis of Bituminous Coal	104
C-2	Heat Transfer to Gas-Solids Suspension in Vertical Cocurrent Downflow	103
D-1	Coal Particle and Catalyst Characteristics for Hydrogenation Evaluation and Testing	106
D-2	The Effect of Structure on Coal Reactivity	113
D-4	Pyrolytic Studies and Separation and Characterization of Coal-Derived Liquids	115
V	Conclusion	127

II. OBJECTIVE AND SCOPE OF WORK

The research reported herein is all of fundamental importance in support of either a process for development of liquefaction of coal, catalysis or some related research. The information which will be gained by research on this contract should materially assist the application of coal in the solution of the energy problems now facing the United States and the world. In particular, the projects reported herein are intended to apply the expertise developed by the coal research team at the University of Utah to problems in four general areas:

- a) Evaluation of process concepts in relation to liquefaction and gasification of coal,
 - b) Catalysis studies of fundamental importance in liquefaction and gasification of coal,
 - c) Studies of fundamental principles involved in processes for liquefaction and gasification of coal,
 - d) Properties of coal and coal conversion products of significance in liquefaction and gasification of coal.
-
- A-1 Coal will be gasified by direct catalytic hydrogenation to produce a high-BTU gas. A liquid will be produced in a first stage reaction at 400-450°C. This product will be further hydrogenated to produce a high-BTU gas. Catalysts and reaction conditions for each stage will be studied.
 - A-2 Kinetics, yields and optimum reaction conditions for extraction of coal will be determined. Hydrogen donor solvents, ultrasonic energy, hydrogen pressures and catalysts will be employed. Extraction products will be analyzed and characterized.
 - A-4 Aromatic liquids derived from coal hydrogenation or extraction will be considered as feedstocks for steam reforming to make a high-BTU gas. Optimum conditions for the production of hydrogen or high-BTU gas, optimum catalysts, the effects of poisons and the degree of coke formation will be determined.
 - A-6 The gasification of coal char will be studied at 2000-3000 psi to produce hydrogen for coal hydrogenation. Steam and oxygen will be used for gasification. The thermal efficiency of producing hydrogen at the pressure at which it will be used will be studied.
 - A-7 Thermal hydrogenolysis of coal slurried with recycle solvent will be studied as such or in the presence of a vapor-phase catalyst to determine the extent of upgrading.
 - A-8 Fischer-Tropsch synthesis of C₂-C₄ hydrocarbons will be studied. New catalysts will be developed and a continuous test unit for long-term catalyst testing will be constructed.
 - A-9 The capacity and durability of a previously developed high-pressure gas recycle pump will be increased. A goal of 3000 psi operating pressure at 500°C is desirable.

- B-1 Adsorption properties and penetration of aromatic molecules on typical cracking catalysts will be determined. These properties will be used to evaluate the ability of such catalysts to crack the large molecules present in coal-derived liquids.
- B-2 (alternate) The mechanism of deactivation of molybdena hydrodesulfurization catalysts by coal-derived liquids will be studied. Kinetic studies involving the model compound benzothiophene will be employed.
- B-3 Hydrogen transfer by metal halide catalysts during coal hydrogenation will be studied. Deuterium labeled hydrocarbons will be used to elucidate reaction mechanisms.
- B-4 The mechanism of catalytic hydrogenation of coal by metal halide catalysts will be investigated. The nature of active catalyst sites will be studied. Changes in properties of the reacting coal will be determined and the nature of reaction products will be determined. Catalyst regeneration will also be studied.
- C-1 The mechanism of pyrolysis of coal will be studied by the use of isotopically labeled model compounds. Products of pyrolysis will be examined to determine their precursors in coal.
- C-2 Fluid mechanics and heat transfer studies involving gas-solid suspensions in vertical downward cocurrent flow systems will be conducted to obtain information on the effect of these variables in the University of Utah coal hydrogenation reactor.
- D-1 The effect of coal and catalyst properties and pretreatment on the hydrogenation of western coals will be studied in the University of Utah short-residence-time, entrained-flow reactor.
- D-2 The effect of coal structure on reactivity to hydrogenation, pyrolysis and dissolution will be studied. Pretreatment of the coal by specific reactions will be used to obtain samples with special structural features.
- D-4 Liquid products from coal hydrogenation in the University of Utah reactor will be separated and characterized. Coal pyrolysis and hydrogenation mechanisms and model compound reactions will also be studied.

III. Summary of Progress to Date

Research Highlights

The second stage of a two-stage direct coal gasification system for production of high-BTU gas was studied. The effect of variables was determined.

Catalysts for the hydrogenation of CO to produce C₂-C₄ hydrocarbons have been prepared and tested to determine the effect of cobalt and copper in Co-Cu catalysts, the effect of pretreatment and the effectiveness of iron catalysts.

Adsorption capacities of aromatic compounds on Al₂O₃ for several non-polar solvents were found to be different. The reasons for this phenomenon are being investigated.

Preliminary results show that the rate of hydrodesulfurization of benzothiophene over a CoMo/Al₂O₃ catalysts is greatly retarded by the presence of aromatic nitrogen compounds, but not by aromatic compounds or water.

The experimental heat transfer unit is nearly completed and ready for initial testing.

Carbon-13 nuclear magnetic resonance spectra of fractions of coal-hydrogenation liquids have been obtained and interpreted.

Special Activities

Drs. Wendell H. Wiser, Larry L. Anderson and Alex G. Oblad attended the April meeting of the American Chemical Society in New York. Dr. Wiser is serving as chairman of the Fuels Chemistry Division. Dr. Anderson served as a symposium chairman.

A meeting of the advisory council was held in May.

Dr. David M. Bodily presented a paper at the Western Regional Meeting of the American Chemical Society in Laramie, Wyoming in June.

Drs. Wendell H. Wiser, Larry L. Anderson and David M. Bodily attended the Gordon Research Conference on Coal Chemistry. Dr. Alex G. Oblad attended the Gordon Research Conference on Catalysts.

Project A-1

Catalytic Gasification of Coal to High BTU Gas

Two-stage Coal Gasification

Faculty Advisor: Wendell H. Wiser
Graduate Student: Ying-Hsiao Li

Introduction

The general approach to the production of high BTU gas from coal has been to react the coal with oxygen and steam to produce a synthesis gas composed of carbon monoxide and hydrogen. This gas is then passed through a catalytic shift reaction to adjust the hydrogen-carbon monoxide ratio to about 3.1. This synthesis gas is then purified and catalytically methanated. Of the processes which have shown sufficient promise to enter the pilot plant stage or to be seriously considered for scale-up, all except the Hydrane process rely heavily upon this reaction scheme of producing a synthesis gas. In these processes more than 50% of the carbon from the coal which ultimately appears as methane passes from the reduced state in the coal to the oxidized state in carbon monoxide then to the reduced state again in methane. Since the carbon-steam reaction is highly endothermic, temperatures above 900°C are normally required in the first stage. At the required pressures, generally above 1000 psi, the materials demand can become rather severe.

The objective of this research is to investigate the potential of a two stage catalytic gasification to high BTU gas with the maximum temperature in both stages being below 600°C. The previous progress report contained a description of the first stage. The following report describes the operation of the second stage.

Project Status

Hydrogasification Process (second stage)

The second stage is a fixed bed continuous flow system. The coal oil from the first stage is used as a feedstock. Hydrogasification of coal oil is a hydrogenolysis process involving cleavage of a molecule by combining with hydrogen in the presence of a hydrogenation catalyst. The major difficulty with the production of methane-rich gas from coal oil is carbon deposition which occurs during the gasification step. One technique, developed by the British Gas Council, has been to conduct thermohydrogasification in a fluidized bed of coke, continuously withdrawing material from the bed to avoid carbon build up. The Institute of Gas Technology's approach to the problem of carbon deposition is to eliminate the carbon forming material by hydrocracking the heavy oil prior to thermohydrogasification.

In this study, in the presence of a Ni-Mo catalyst, a temperature of 525°C to 625°C produced a high yield of gas and a low yield of coke.

The main operating variables in this process are hydrogen-to-feed ratio, temperature, pressure and liquid hourly space velocity. The individual effects of each operating variable are discussed first, then a comparison is made of the effects of these variables.

Effect of Hydrogen-to-Feed Ratio

The most important variable affecting product distribution is the hydrogen-to-coal oil ratio. The amount of carbon deposition upon the catalyst decreases with increasing hydrogen-to-feedstock ratio and the gas yield increases with an increasing ratio. To find the optimum ratio of hydrogen-to-coal oil, three experiments were performed at a constant temperature of 600°C, a constant pressure of 1750 psi and a constant space velocity of 1 but with different hydrogen-to-coal oil ratios. The amount of carbon deposition from the coal oil on the catalyst was significantly affected by the hydrogen-to-coal oil ratio, dropping from 15.4% at 75% of stoichiometric ratio to 9.4% at 150% of stoichiometric ratio and 7.4% at 250% of stoichiometric ratio. It was found that at a ratio greater than 250% the amount of carbon deposition did not decrease. All data presented in the following were produced at 300% of stoichiometric ratio to ensure that excess hydrogen was always present.

Effect of Temperature

Five experiments were carried out to determine the ideal reaction temperature with a relatively high conversion. In Table 1, Figure 1 and Figure 2 the effects of temperature on hydrogasification are shown. The data were obtained at a constant space velocity, a constant hydrogen pressure and a constant hydrogen-to-feed ratio. Conversions increased linearly with temperature. The percent conversions are 59.08% at 525°C, 76.12% at 575°C, and 75.85% at 625°C. As the reaction temperature increased the gas product yield also increased rapidly from 52.53% at 525°C to 66.80% at 625°C. The methane yield, as weight percent, increased linearly with temperature from 44.66% at 525°C to 64.45% at 625°C. The ethane yield decreased with an increase in temperature from 2.83% at 525°C to 1.62% at 625°C. The methane-to-ethane ratio varied from 15.78 at 525°C to 39.78 at 625°C. The propane and the butane curves show convex downward trends. Although the quantity of gaseous product increased with increasing temperature, the undesired byproduct of coke also increased slightly with increasing temperature.

The properties of the unconverted liquid product are shown in Table 2. The yield of gasoline remained nearly constant but the yields of middle oil and residue decreased as the temperature increased. Gas and gasoline were formed at the expense of middle oil and residue. The gasoline formed contained 79% to 64% saturates and 21% to 30% aromatics. In the middle oil one sample obtained at 575°C showed 10% of saturates. The olefins were almost completely hydrogenated under the experimental conditions employed.

The composition of the reacting species continuously change with increasing conversion. At high conversion levels the more refractory

components such as aromatics remain in the liquid fraction or condense to form additional coke. Therefore, a slight increase of coke and the formation of aromatics in the liquid were observed with an increase in temperature and conversion. The aromatics in the gasoline were probably formed by the dealkylation of alkylaromatics and the hydrogenolysis of saturated rings in heterocyclic compounds.

Effect of Pressure

There were five experiments performed to study the effects of pressure on the conversion of coal oil to hydrocarbon gas. The data were obtained at a constant temperature, a constant space velocity and a constant hydrogen-to-feed ratio with an increase of pressure from 750 psi to 1750 psi. Table 3, Figure 3 and Figure 4 show the effects of pressure on conversion. As the pressure increased, the conversion decreased from 78.70% at 750 psi to 70.83% at 1750 psi while the coke decreased dramatically from 16.31% to 7.12%. The hydrocarbon gas remained nearly constant and methane and ethane yields passed through a broad maximum in the range of pressure from 1250 psi to 1500 psi. The yields of propane and butane remained constant over the entire pressure range. Cottingham, from the studies of catalytic hydrogasification of crude shale oil at the Laramie Petroleum Research Center, also showed that pressures in excess of 2000 psi greatly suppressed the formation of methane, ethane and coke deposit. At low pressures, such as 500 psi, coke deposit became excessive.²

The properties of the liquid product are shown in Table 4. As the pressure increased, the liquid product yield increased markedly in the pressure range from 750 psi to 1750 psi. The yield of gasoline slightly increased with increasing pressure. The yields of middle oil and residue increased as the pressure increased. The increase in the liquid product, including the middle oil and the residue, is due to the suppression of the coke forming reaction. The densities of the liquid product changed from 0.85 at 750 psi to 0.91 at 1750 psi. Considering the composition of the liquid the aromatic content in the gasoline increased from 11% to 28% in the range of pressure from 750 psi to 1750 psi.

If Le Chatelier's principle is applied to the gas phase reaction $8C_xH_y + (16x-4y)H_2 = 8xCH_4$, an increase of pressure will cause the reaction to shift to the formation of CH_4 . In other words the equilibrium shifts in the direction that tends to minimize the effect of the applied change. The reaction rate of hydrocarbon hydrogenation is also proportional to the hydrogen pressure. Considering the product distribution, it was noted that the increase of pressure did not improve the yield of gas. Table 7 lists the properties of several aromatic compounds mainly existing in the coal oil. It is probable that the high molecular weight portion of the feedstock passed through the reaction zone as a liquid. The increase of pressure only increased the liquid phase hydrogenation and suppressed the formation of carbon on the catalyst. Decreasing the pressure accelerated the vapor phase hydrogenation, so the concentration of unsaturated C_4 compounds at low pressure was lower than that at high pressure. The saturate content in the gasoline also increased with

decreasing pressure.

Effect of Liquid Hourly Space Velocity

Decreasing the space velocity, which will increase the contact time of catalyst and oil, has much the same effect as increasing the reaction temperature. For this work, the weight hourly space velocity was defined as

$$\text{WHSV (hr}^{-1}\text{)} = \frac{\text{weight feed rate of coal oil (wt/hr)}}{\text{weight of catalyst wt}}$$

This definition was used as a relative measurement of the contact time. Table 5, Figure 5 and Figure 6 show the effects of space velocity on conversion and product distribution. The data were obtained at a constant temperature, a constant pressure and a constant hydrogen-to-feed ratio. The results show that a greater methane yield and a greater total gas yield were obtained at the lower space velocity. Conversions of the coal oil varied from 77.81% at a WHSV of 0.5 to 66.72% at a WHSV of 2.0. The quantity of gas and coke decreased as the WHSV was increased. The only disadvantage of a relatively low WHSV operation, as also with a relatively high temperature operation, is that the coke formation increases and the selectivity to gas decreases. The selectivity to gas is increased and the amount of coke is decreased as the WHSV is increased. Except for the methane curve which shows a concave downward trend, all the curves of ethane, propane and butane in Figure 6 show convex upward trends.

Table 6 shows the properties of the liquid product. The liquid properties were improved by decreasing the WHSV. The gasoline yield increased as the WHSV decreased. The content of aromatics in the gasoline varied from 17% at a WHSV of 0.5 to 29% at a WHSV of 2.0.

The effects of space velocity on product distribution are due mainly to the contact time and the severity of hydrogenation. Additional reaction time added slightly to further gasification but allowed more gas phase conversion to produce methane. The yield of total gas increased only 4.16% but the methane yield increased 6.54% in the range of WHSV from 2.0 to 0.5. The yield of unsaturated C₄'s obtained at a low WHSV was lower than that at a high WHSV.

Comparison of Effects of Operating Variables

The desired goal of this project has been the production of a synthetic natural gas. This means an emphasis on maximum production of gas with a minimum formation of coke. Therefore, a comparison was made to evaluate the effects of each operating variable on selectivities. The data for the selectivities and the conversion were obtained from Tables 1, 3 and 5. The point, which has a conversion level of 70.83%, obtained at a temperature of 600°C, a hydrogen pressure of 1750 psi, a WHSV of 1 and a hydrogen-to-feed ratio of 6000 (volume basis), is a common point for each curve on Figure 7. The curves were formed by holding two variables constant and allowing the third to change. For example, the temperature curve has a constant pressure of 1750 psi and a constant WHSV of 1.

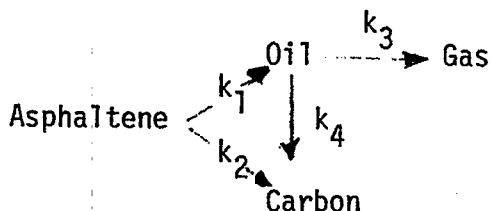
In Figure 7, the selectivity to gas versus conversion is shown. The selectivity to gas decreased as the conversion level, with changing WHSV and pressure, increased. Both curves show convex downward trends. The curve of the temperature effect, which passed through a maximum conversion level of 70.83%, shows a convex downward trend. Below the conversion level of 70.83%, a relatively low temperature was applied. As in the discussion of coke formation on catalyst in the hydrosolvation process (first stage), the high molecular weight portion of the coal-derived liquid fouled the catalyst and an increase of temperature increased the breakdown of those materials to less viscous small units. In this stage some liquid phase hydrogenation also occurred. At temperatures below 600°C or conversion levels below 70.83%, the selectivity to gas increased due to the breakdown of high molecular weight material. Above 600°C, conversion still increased but the rate of condensation or overcracking was also accelerated and excess carbon was deposited upon the catalyst.

The pressure curve is the most convex which indicates that pressure has the greatest effect on the selectivity to gas. At a given conversion level with a temperature higher than 600°C, the best combination of the highest pressure and the lowest WHSV gives the highest yield of gas. The following table shows the results of two sets of experiments. They have different WHSV and different pressures but have approximately the same conversion levels of 78.70% and 77.81% at the same reaction temperature of 600°C.

The selectivity to gas increased from 0.77 at 750 psi and the WHSV of 1, to 0.84 at 1750 psi and the WHSV of 0.5. The selectivity to coke decreased from 0.21 to 0.14 in the same operating range defined above.

Catalyst	NiMo	NiMo
Reactor Temperature (°C)	600	600
H ₂ /Feed Ratio (volume basis)	6000	6000
H ₂ Pressure (psi)	750	1750
WHSV (wt/wt/hr)	1.0	0.5
Conversion (wt %)	78.696	77.810
Selectivity (%)		
Gas/Conversion	77.399	84.249
Coke/Conversion	20.719	13.996

In this work there is no intention to derive a theoretical mechanism and a kinetic expression, but by elaborating on the following simple model, the observed facts can be explained.



In the coal oil some of the constituents, saturates and olefins, are quite susceptible to hydrogenation, whereas the aromatics tend to be more refractory. The susceptible molecules in the feedstock were cracked quite rapidly resulting in a high value of k_1 . The ratio of k_1/k_2 was increased by raising the reaction temperature to 600°C. This is due to the acceleration of the breakdown of weak bonds in the high molecular weight, coke-forming material. This also results in the higher selectivity to gas. As the reaction temperature and conversion level increased, the more resistant molecules remained unconverted. The k_3/k_4 ratio decreased as the temperature exceeded 600°C. As the reaction proceeded the remaining resistant molecules became progressively more difficult to hydrogenate, resulting in a decrease of the rate constant k_3 . On the other hand overcracking continuously increased with increasing conversion or temperature.

References

1. J. Heubler, J. Janka, G. Seay and P. Tarman, Chem. Eng. Progr., **69** (5), 19 (1973).
2. P.L. Cottingham and H.C. Carpenter; "Fuel Gasification," Advances in Chemistry Series, No. 69, American Chemical Society, Washington, D. C., 1967, Chapter 12.

Table 1. Effect of Temperature on Conversion and Production Distribution in Hydrogasification Process

Catalyst	NiMo	NiMo	NiMo	NiMo	NiMo
Preheater Temperature (°C)	500	500	500	500	500
Reactor Temperature (°C)	525	550	575	600	625
H ₂ Pressure (psi)	1750	1750	1750	1750	1750
H ₂ /Feed Ratio (cc/cc)	6000	6000	6000	6000	6000
WHSV (wt/wt/hr)	1	1	1	1	1
<hr/>					
Conversion (wt %)	59.081	62.864	67.116	70.832	75.848
<hr/>					
Yield (wt %)					
CH ₄	47.660	52.069	56.332	60.327	64.451
C ₂ H ₄	--	--	--	--	--
C ₂ H ₆	2.834	2.430	2.288	1.951	1.616
C ₃ H ₆	--	--	--	--	--
C ₃ H ₈	0.958	0.913	0.914	0.904	0.468
tran-2-C ₄ H ₈	0.295	0.200	0.160	0.120	0.094
cis-2-C ₄ H ₈	0.255	0.110	0.085	0.024	0.025
i-C ₄ H ₁₀	0.198	0.175	0.124	0.079	0.051
n-C ₄ H ₁₀	0.328	0.316	0.347	0.275	0.095
<hr/>					
Total Gases	52.528	56.213	60.250	63.680	66.800
Liquid	40.920	37.124	32.885	29.197	24.695
Coke	6.552	6.663	6.865	7.123	8.505
<hr/>					
Selectivity (%)					
Gases/Conversion	88.908	89.420	89.770	89.903	88.071
Coke/Conversion	11.090	10.599	10.228	10.056	11.213

Table 2. Effect of Temperature on Properties of Liquid Product in Hydrogasification Process

Catalyst: NiMo

H₂ Pressure: 1750 psi

H₂/Feed Ratio: 6000 cc/cc

WHSV: 1

Temperature (°C)	575	600	625
Yield (wt %)	32.885	29.197	24.695
Specific Gravity (25-25°C)	0.919	0.909	0.913
Distillation Data (wt %)			
<200°C (gasoline)	15.780	15.090	16.052
200-300°C (middle oil)	12.859	10.876	5.433
>300°C (residue)	4.246	3.231	3.210
Hydrocarbon Types in Oil below 200°C (vol %)			
Saturates	79	72	64
Aromatics	21	28	36

Table 3. Effect of Pressure on Conversion and Product Distribution in Hydrogasification Process

Catalyst	NiMo	NiMo	NiMo	NiMo	NiMo
Preheater Temperature (°C)	500	500	500	500	500
Reactor Temperature (°C)	600	600	600	600	600
H ₂ Pressure (psi)	750	1000	1250	1500	1750
H ₂ /Feed Ratio (cc/cc)	6000	6000	6000	6000	6000
WHSV (wt/wt/hr)	1	1	1	1	1
Conversion (wt %)	78.696	76.178	74.499	73.542	70.832
Yield (wt %)					
CH ₄	58.396	59.229	61.142	61.145	60.327
C ₂ H ₄	--	--	--	--	--
C ₂ H ₆	1.445	1.900	1.958	2.047	1.951
C ₃ H ₆	0.005	--	--	--	--
C ₃ H ₈	0.938	1.024	1.129	0.926	0.904
1-C ₄ H ₈	0.003	--	--	--	--
trans-2-C ₄ H ₈	0.003	0.035	0.048	0.066	0.120
cis-2-C ₄ H ₈	0.001	0.035	0.029	0.027	0.024
i-C ₄ H ₁₀	0.062	0.077	0.084	0.085	0.079
n-C ₄ H ₁₀	0.057	0.042	0.103	0.226	0.275
Total Gases	60.910	62.342	64.493	64.523	63.680
Liquid	22.785	24.635	25.811	27.026	29.197
Coke	16.305	13.023	9.696	8.451	7.123
Selectivity (%)					
Gases/Conversion	77.399	81.837	86.569	87.736	89.903
Coke/Conversion	20.719	17.095	13.015	11.491	10.056

Table 4. Effect of Pressure on Properties of Liquid Product in Hydrogasification Process

Catalyst: NiMo		Temperature: 600°C		
H ₂ /Feed Ratio: 6000 cc/cc		WHSV: 1		
Pressure (psi)	750	1250	1750	
Yield (wt %)	22.785	25.811	29.197	
Specific Gravity (25-25°C)	0.850	0.877	0.909	
Distillation Data (wt %)				
200°C (gasoline)	15.952	15.511	15.090	
200-300°C (middle oil)	5.013	8.001	10.876	
300°C (residue)	1.820	2.299	3.231	
Hydrocarbon Types in Oil Below 200°C (vol %)				
Saturates	89	84	72	
Aromatics	11	16	28	

Table 5. Effect of Space Velocity on Conversion and Product Distribution in Hydrogasification Process

Catalyst	NiMo	NiMo	NiMo	NiMo	NiMo
Preheater Temperature (°C)	500	500	500	500	500
Reactor Temperature (°C)	600	600	600	600	600
H ₂ Pressure (psi)	1750	1750	1750	1750	1750
H ₂ /Feed Ratio (cc/cc)	6000	6000	6000	6000	6000
WHSV (wt/wt/hr)	0.5	0.75	1.0	1.5	2.0
Conversion (wt %)	77.810	73.689	70.832	68.649	66.716
Yield (wt %)					
CH ₄	63.852	61.927	60.327	58.657	57.318
C ₂ H ₄	--	--	--	--	--
C ₂ H ₆	1.179	1.907	1.951	2.272	2.359
C ₃ H ₆	--	--	--	--	0.003
C ₃ H ₈	0.397	0.828	0.904	0.951	0.902
i-C ₄ H ₈	--	--	--	--	0.016
1-C ₄ H ₈	--	--	--	--	0.006
trans-2-C ₄ H ₈	0.010	0.056	0.200	0.148	0.185
cis-2-C ₄ H ₈	0.005	0.028	0.024	0.063	0.121
i-C ₄ H ₁₀	0.055	0.064	0.079	0.129	0.184
n-C ₄ H ₁₀	0.056	0.153	0.275	0.314	0.292
Total Gases	65.554	64.963	63.680	62.534	61.386
Liquid	23.556	26.875	29.197	30.979	32.567
Coke	10.890	8.162	7.123	6.487	6.047
Selectivity (%)					
Gases/Conversion	84.249	88.158	89.902	91.092	92.011
Coke/Conversion	13.996	11.076	10.056	9.450	9.064

Table 6. Effect of Space Velocity on Properties of Liquid Product in Hydrogasification Process

Catalyst: NiMo

H₂ Pressure: 1750 psi

Hydrogen/Feed Ratio: 6000 cc/cc

Temperature: 600°C

WHSV (wt/wt/hr)	0.5	1.0	2.0
Yield (wt %)	23.556	29.179	32.567
Specific Gravity (25-25°C)	0.885	0.909	0.920
Distillation Data (wt %)			
< 200°C (gasoline)	18.609	15.090	14.302
200-300°C (middle oil)	2.356	10.876	12.896
> 300°C (residue)	2.591	3.231	5.369

Hydrocarbon Types in Oil
Below 200°C (vol %)

Saturates	83	72	71
Aromatics	17	28	29

Table 7. Properties of Several Aromatics

Name	Structure	Formula	M.W.	B.T. (°C)	C.T. (°C)	C.P. (psi)
Benzene		C_6H_6	78	80.0	288.5	701.2
Tetralin		$C_{10}H_{12}$	132	207.2	430.0	564.5
Naphthalene		$C_{10}H_8$	128	217.8	475.0	446.9
Anthracene		$C_{14}H_{10}$	178	341.1	610.5	323.0
Penanthrene		$C_{14}H_{10}$	178	339.0	593.7	322.0
Pyrene		$C_{16}H_{10}$	202	393.0	662.4	241.8
Chrysene		$C_{18}H_{12}$	228	441.6	--	252.8

M.W. (Molecular Weight)

B.T. (Boiling Point)

C.T. (Critical Temperature)

C.P. (Critical Pressure)

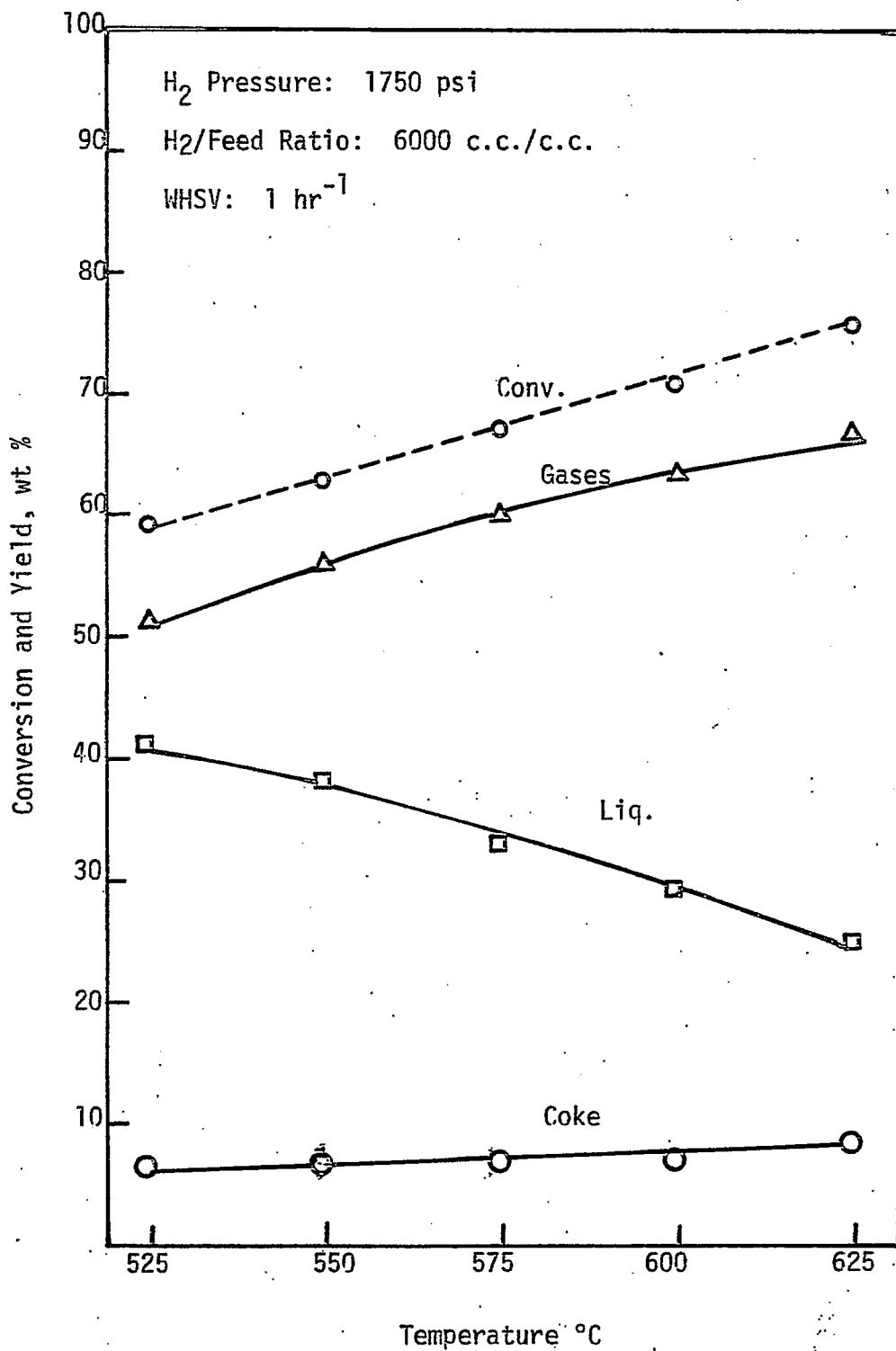


Figure 1

Effect of Temperature on Conversion and Product Distribution

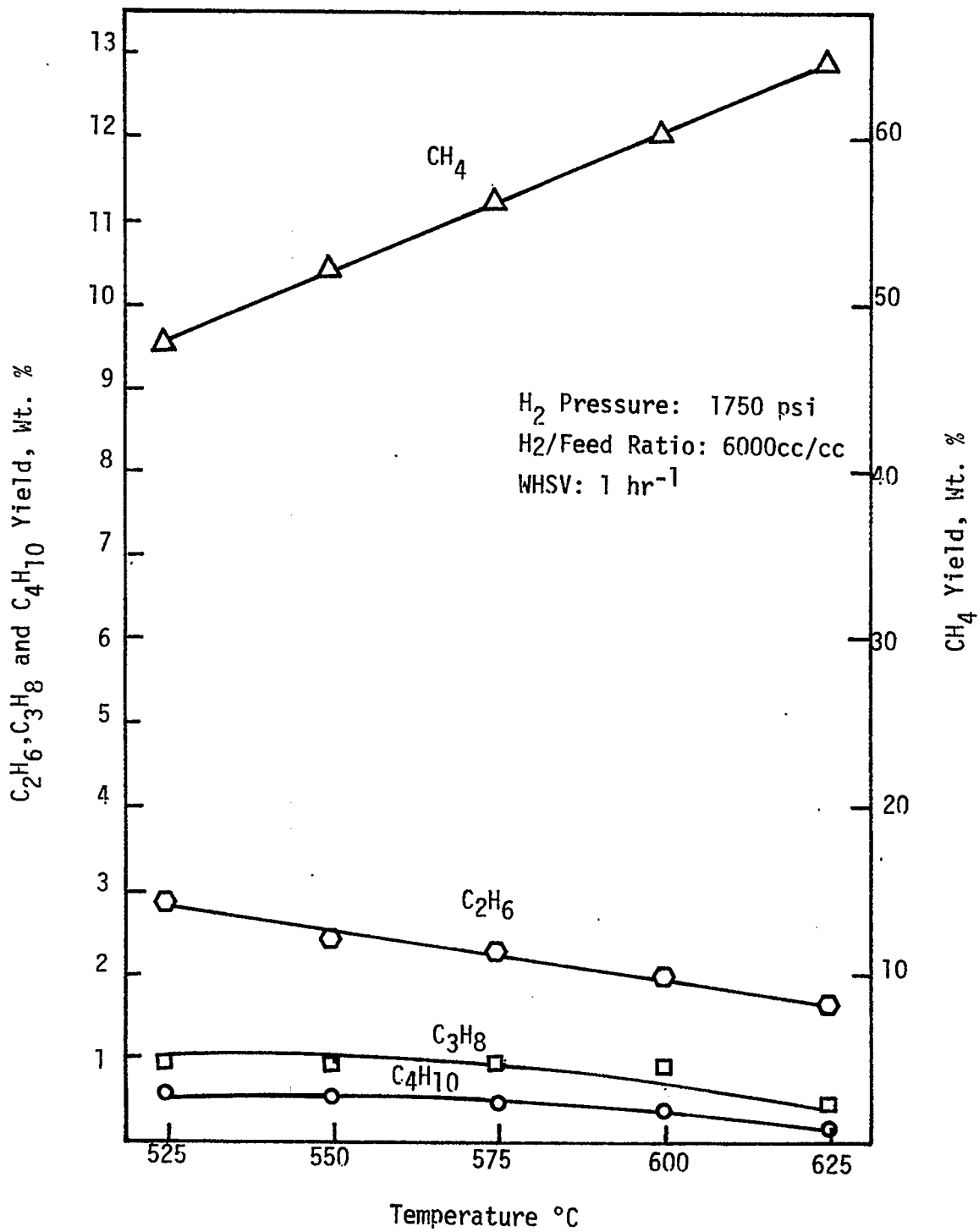


Figure 2
Effect of Temperature on Gases Yield

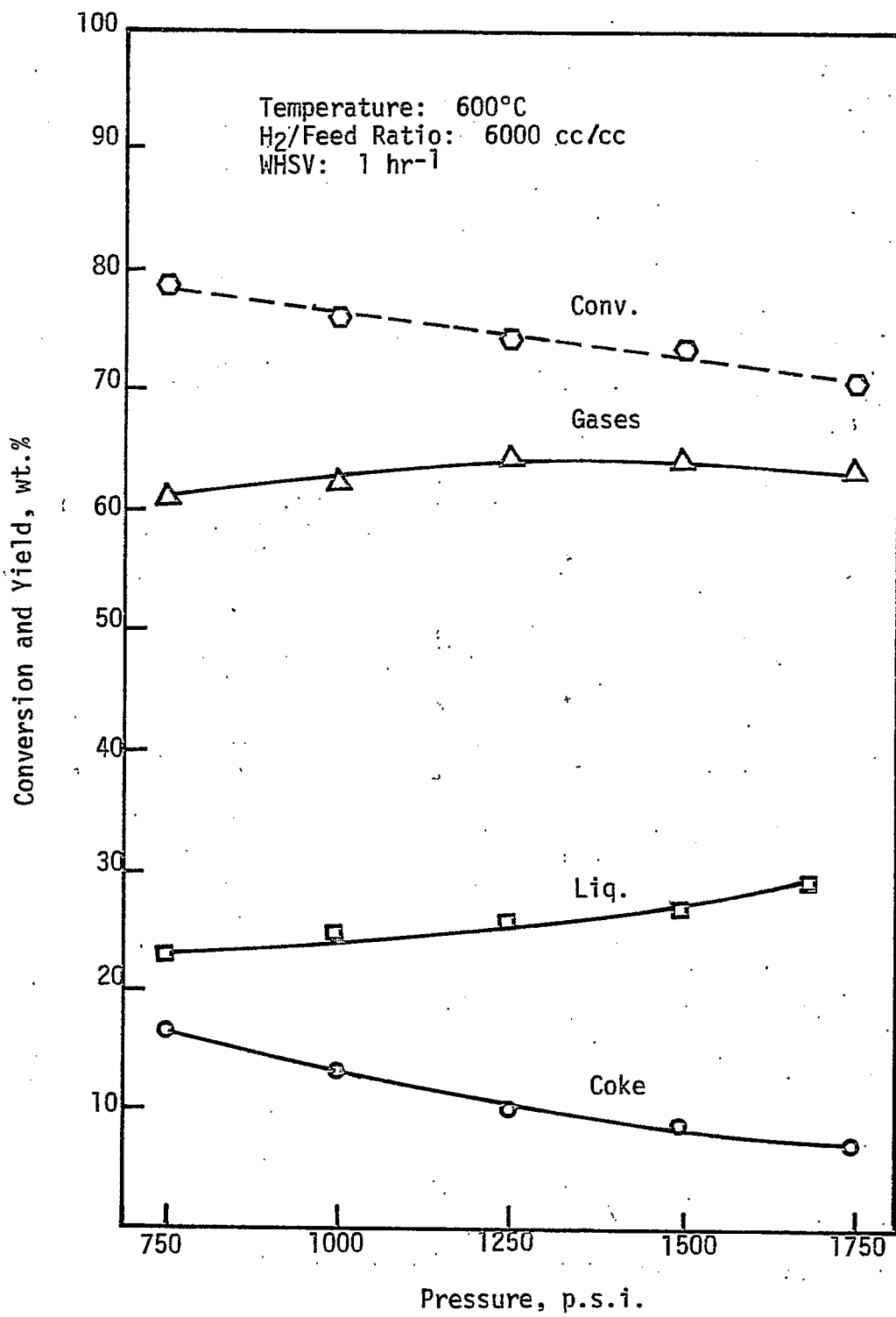


Figure 3
Effect of Pressure on Conversion and Product Distribution

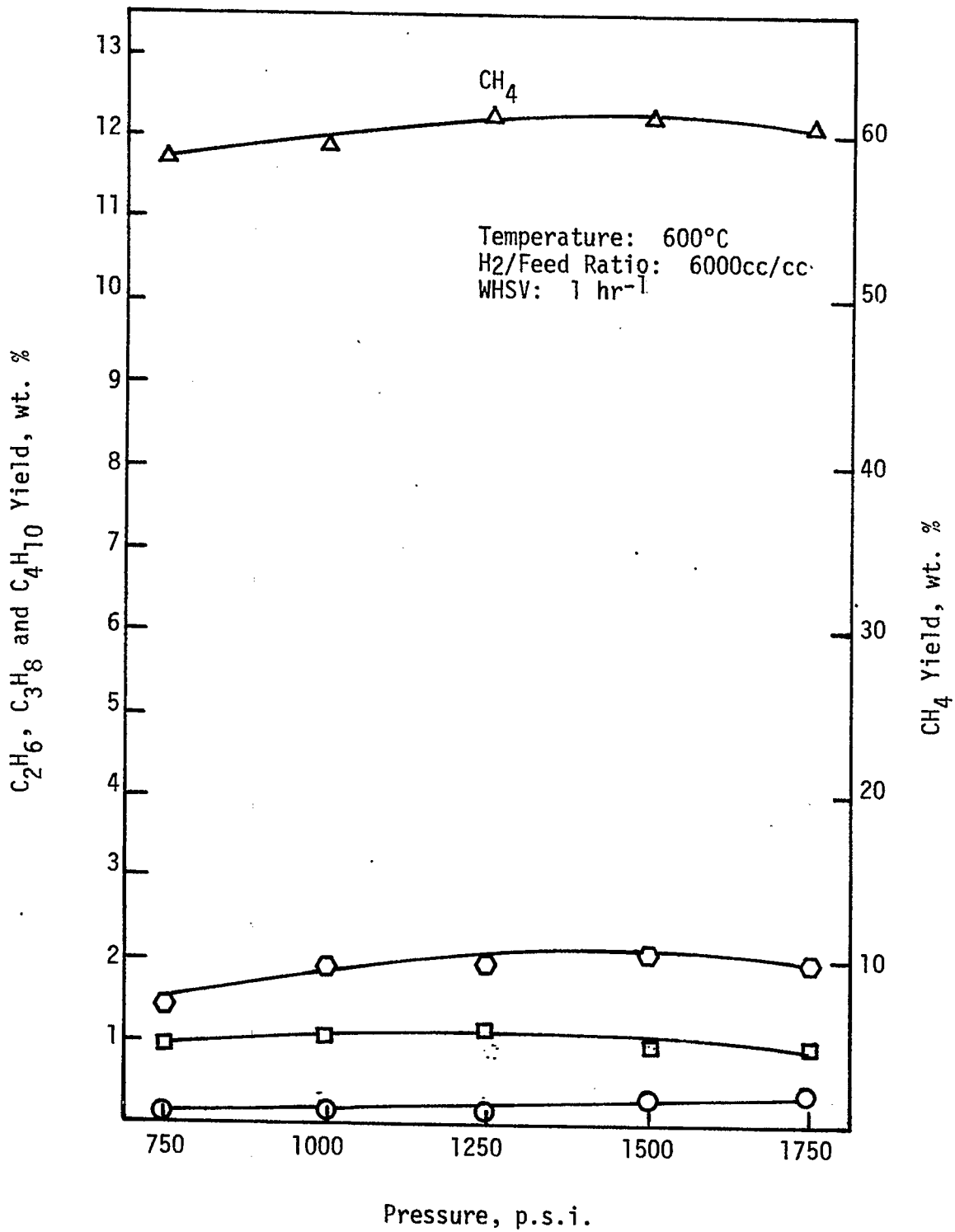


Figure 4
Effect of Pressure on Gases Yield

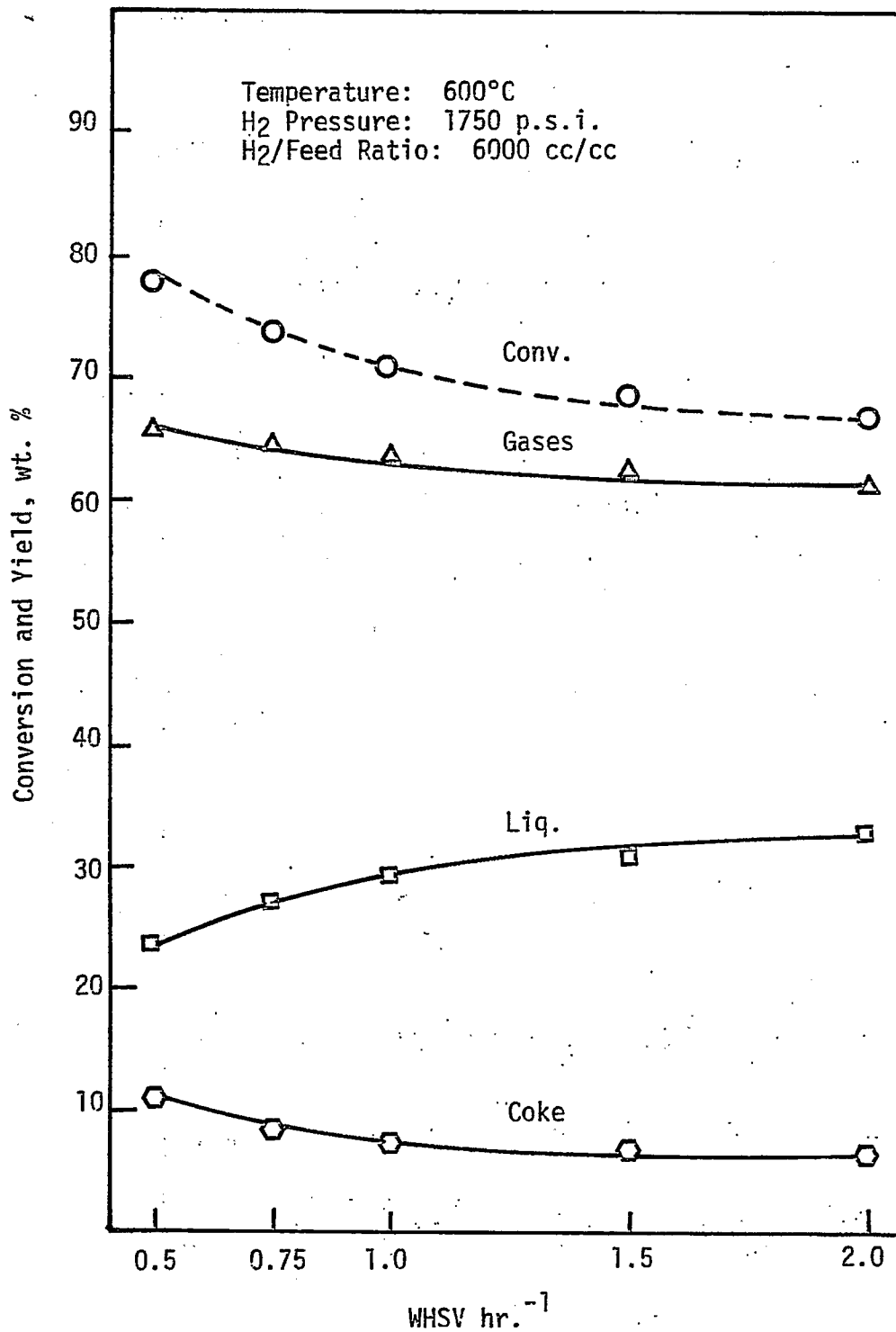


Figure 5
 Effect of Space Velocity on Conversion and Product Distribution

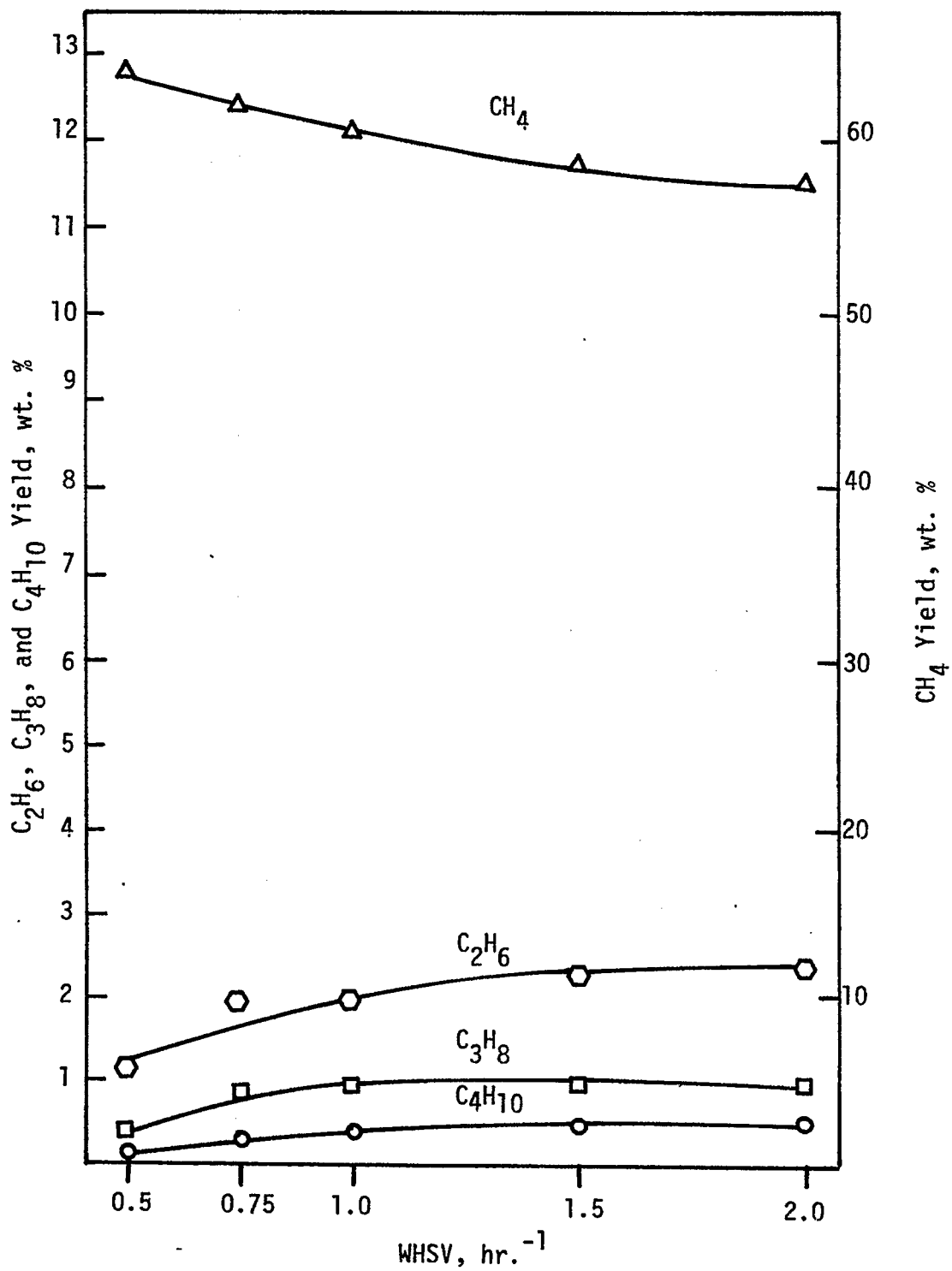


Figure 6
Effect of Space Velocity on Gases Yield

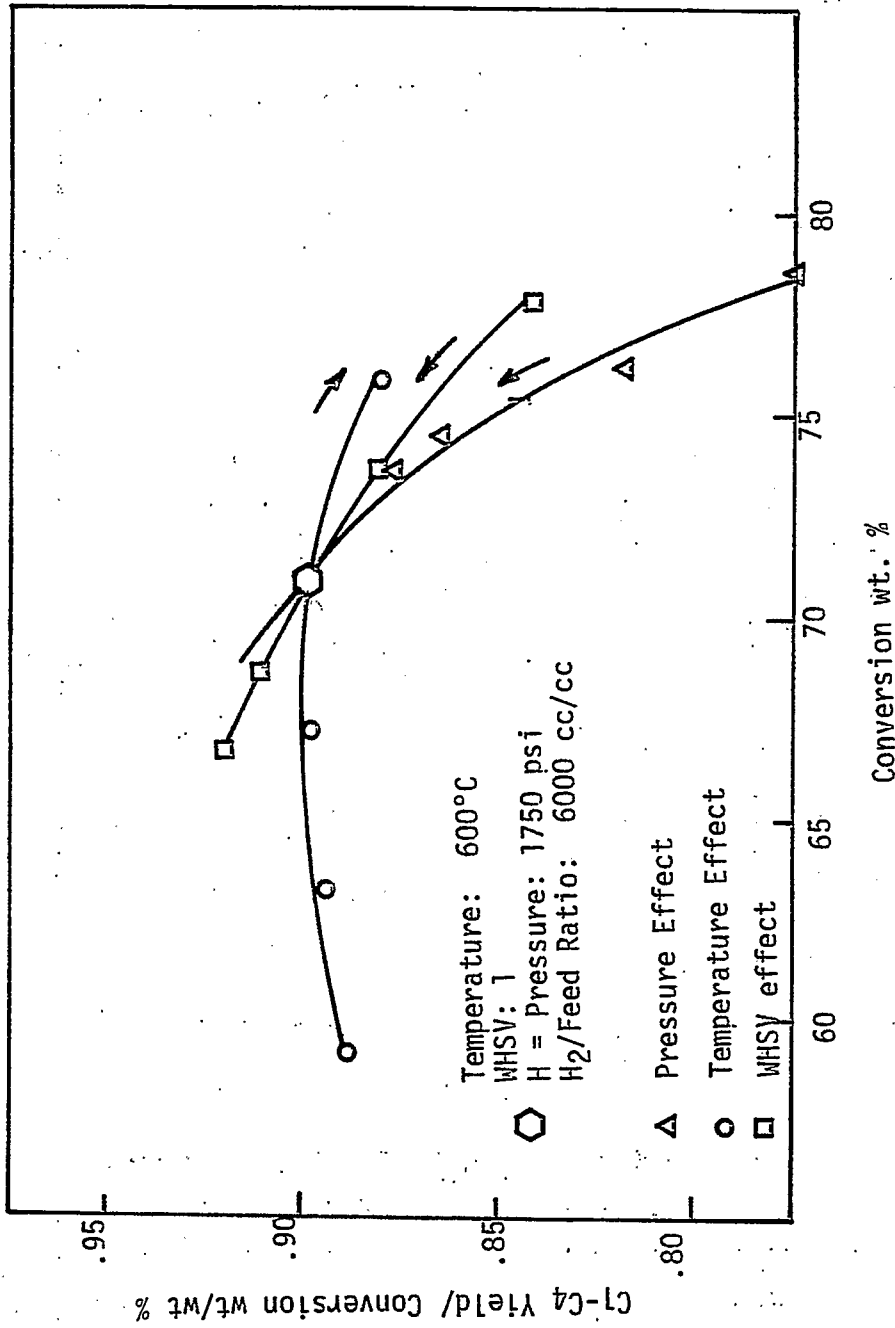


Figure 7.
 The Comparison of Effect of Operating Variables
 on Selectivity of Hydrocarbon Gases (C₁-C₄)

Project A-1

Catalytic Gasification of Coal to High BTU Gas

Single Stage Coal Gasification

Faculty Advisor: Wendell H. Wiser
Graduate Student: Subhash Kithany

Introduction

The objective of this research was originally to investigate the potential of two stage catalytic gasification to high BTU gas with the maximum temperature in both stages being below 600°C. As this work progressed it was observed that high yields of methane could be obtained utilizing the same catalyst in both stages. Accordingly the objective has now become an investigation of the potential of obtaining high methane yields by the direct catalytic hydrogenation of coal in a single stage with maximum temperature to be in the range of 550°C. A significant reduction in complexity of the equipment will result if the work is successful.

A single stage reactor concept for making substitute natural gas (SNG) from coal is relatively new in coal gasification technology. This concept involves charging slurried coal in a hydrogen donor solvent together with hydrogen and/or steam into a single reactor to generate a gas that contains methane as the primary combustible constituent. This will be a catalytic process. As mentioned in an earlier progress report, the thermodynamic simulation studies for this process have been completed. The results are encouraging.

Project Status

A process flow sheet for the experimental model has been developed and included in a previous report. The design, almost completed, is based on a feed rate of 25 to 100 g/hr of coal slurry. The coal slurry will be prepared by dispersing 100 g of coal in 200 g of hydrogen donor solvent, preferably tetralin, giving a solvent to coal ratio of 2:1. Various ratios of solvent to coal will be tested.

Most of the units have been ordered. The condenser, separator, preheater and steam generator will be fabricated at the University workshop. Two pumps will be required, one for feeding the coal slurry and the other for feeding water to the steam generator.

Future Work

The work to be done in the next quarter will involve setting up the various units as they are acquired. Some minor items may have to be ordered as the need arises.

Project A-2

Dissolution of Coal in Hydrogen Donor Solvents with Application of Catalysts and Energized Conditions to Produce Clean Fuels

Solvent Extraction of Coal Utilizing Sonic Energy

Faculty Advisor: L. L. Anderson
Graduate Student: Doohee Kang

Project Status

During the last quarter, there was an emphasis on defining the conversion and analysis of products. This was due to poor conversion results compared to the material balances based on solid residue. These fluctuations are probably due to the small amounts of the samples. In order to define a reliable method of determining conversion (dissolution) and product analysis, gas chromatographic techniques have been extensively studied during this period.

For the evaluation of conversion, solvent peak changes on the extracts have been quantitatively compared with internal standards. The internal standards had been premixed with the solvent extract mixture before analysis. The amount of solvent associated with the extract is, however, too large in comparison with the extracts dissolved to give reliable quantitative data (coal: solvent ratio is 1:9 and 1:6). Even if chromatographic results are precise to one or two percent for each corresponding peak, results of analysis involve unavoidable magnification of errors since large solvent peaks are the basis of the calculations. Even one percent fluctuation in the area of the solvent peak can produce too large an error in the smaller peaks.

This problem arises in part, if the measure of extract is used to calculate solubility or yield. (If C grams of coal are charged with T grams of solvent which result in S grams of solution, E grams of extract and R grams of residue the solubility can be expressed as E/C ; $E/(S-T)$ or $\frac{C-R}{C}$). Since E/C is being used to calculate the solubility the extract area needs to be measured accurately.

During the analysis, changes of compounds derived from the solvent can be seen clearly as conversions proceed. Typical chromatograms are compared in Figure 1. Decalins (cis and trans) are formed to their limiting compositions and appear to be unchanged above this level. Formation of naphthalene increases gradually as conversion develops, as shown in Figure 3, but the increase is somewhat different at 300°C and 350°C. Formation of 1,2-dihydronaphthalene in sizable amounts was difficult to

evaluate because its separation from tetralin was hampered by the large quantities of the tetralin. These data remain to be confirmed for the explanation of the intermediate step in the dehydrogenation of tetralin to naphthalene.

As seen in a typical chromatogram, most of the components of coal extract remain in the OV-17 column even at an oven temperature of 280°C. Components will be separated into two parts by flash distilling the solvent out of the extracts. Other means of analysis under investigation include GC-MS, NMR, IR and elemental analysis.

Even though the problems of high temperature application of an ultrasonic device have been solved, the operation is still hazardous at high pressures. The bolts connecting the probe and reactor cell are loosened by severe vibration and by thermal expansion. Modification of the design is under investigation. Experiments without ultrasound are to be carried out until a new design is completed. Future work will involve ultrasonic and catalytic effects on dissolution of coal.

Results shown in Figure 2 indicate that ultrasound significantly enhances the initial conversion rate and some slight increase in the ultimate yields can also be seen. Percent yield shown in Figure 2 is based on the amounts of solidified extract after the removal of solvent by evaporation. Better conversion data will be reported in the future after correcting this method through thorough analysis of the solvent.

Figure 1

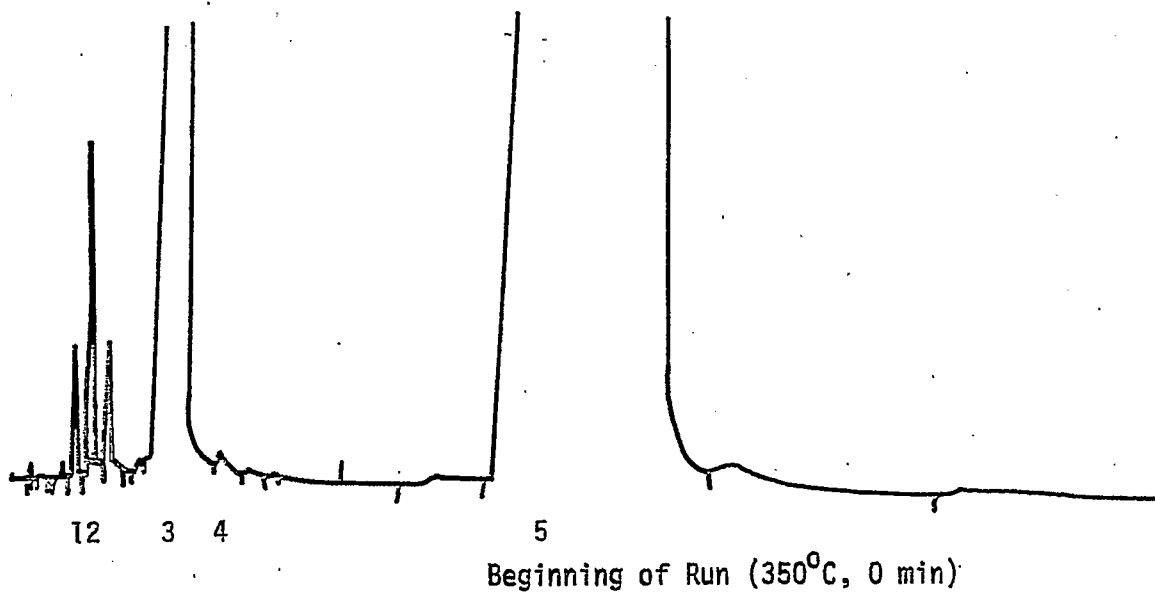
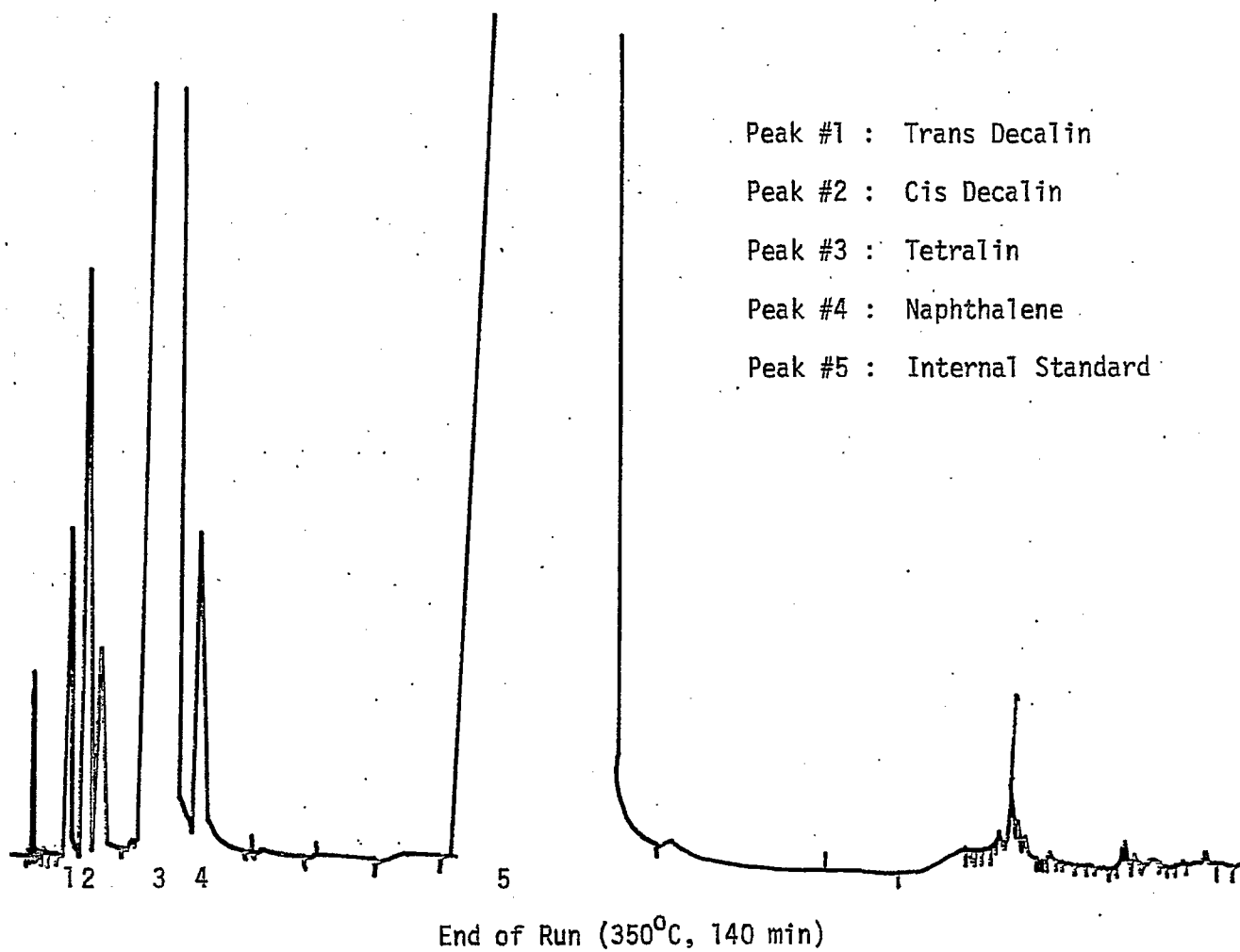
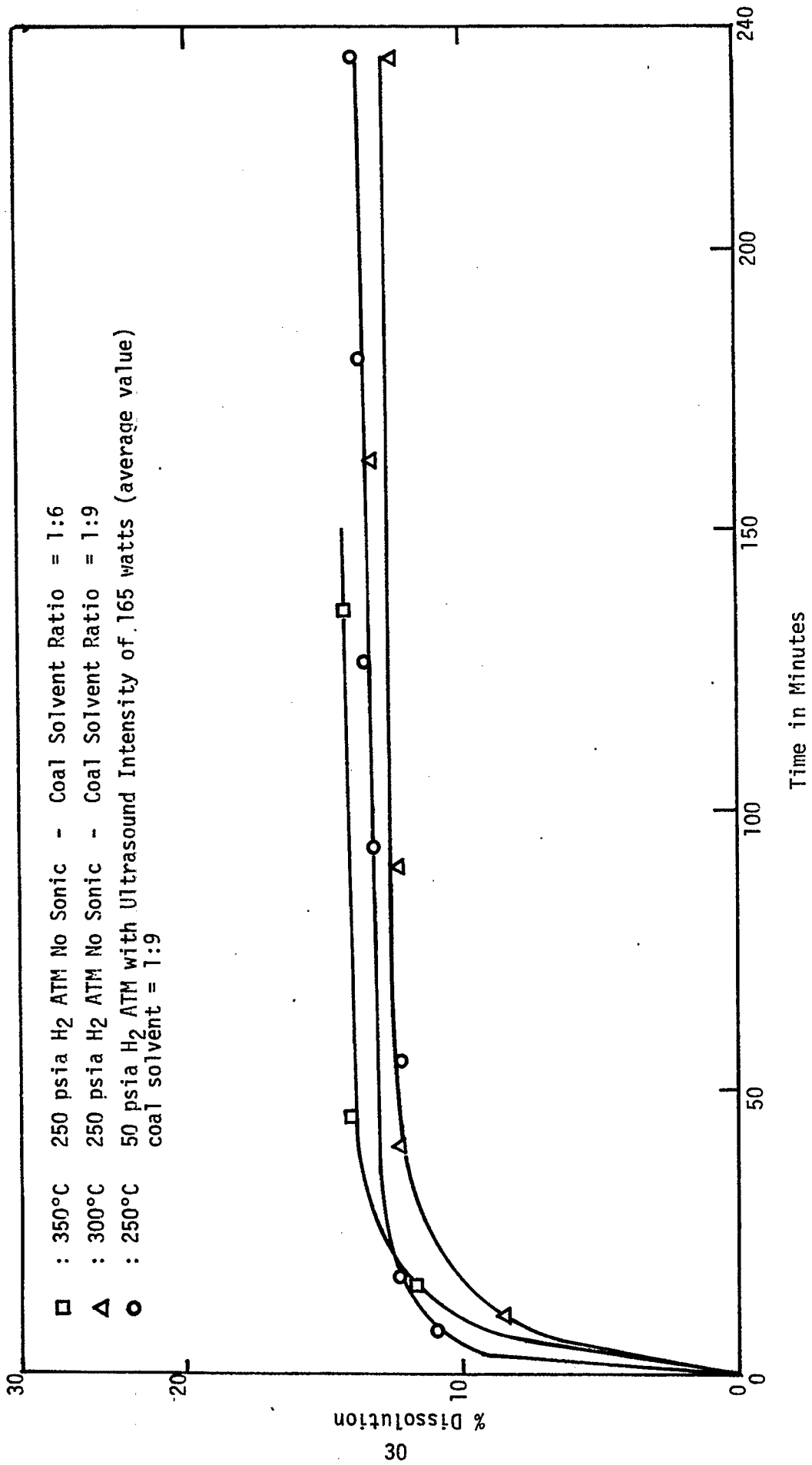


Figure 2



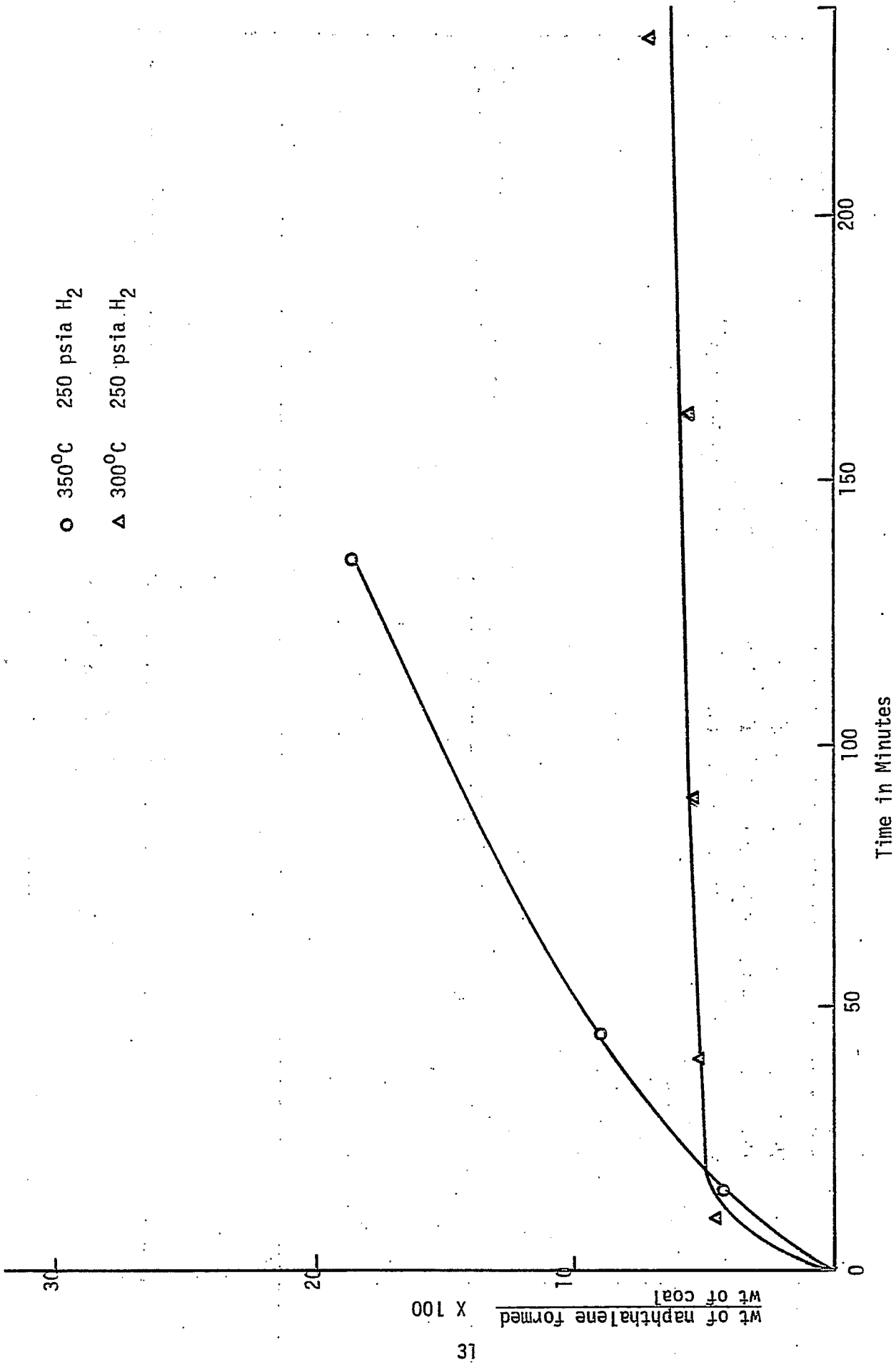


Figure 3

Project A-2

Solvent Extraction of Coal for Separation and Identification of Chemical Species in Coal

Faculty Advisor: L. L. Anderson
Graduate Student: S. Jackson

Introduction

For many years various solvents have been used to extract chemicals from coal and to improve the properties of coal. More recently solvent extraction of coal has been used to study the structure, composition and the chemistry of coal. The purpose of this project is to supplement work done in the area of coal characterization.

This project is a study of the effects that chemically related solvents have upon different coal types and the extracts. Past work has included a literature search and experiments have been done to determine the best method for extraction and extraction conditions.

Project Status

This last quarter involved characterizing the extracts derived from two different coals. Four different solvents were used with each type of coal. The solvents used were benzene, benzaldehyde, anisole and benzyl alcohol. The last three solvents were chosen because each contains an oxygen atom which is electronically different from the others, thus making it possible to correlate extraction results with linear free energy relationships. Two Utah coal samples were used in this work, Clear Creek and Coalville coal, ground 60-100 mesh.

Five grams of dried coal was added to 25 grams of solvent. The coal/solvent mixture was stirred for 24 hours at a constant temperature after which the sample was passed through a fine glass frit. The solvent was then removed by vacuum distillation and the extract was recovered for analysis.

Since anisole, benzyl alcohol, and particularly benzaldehyde were difficult to remove by vacuum distillation, the alternative method of steam distillation will be used to see if improved separation can be achieved.

All filtered solvents displayed different characteristics, the color being the most noticeable. The benzene extract was a honey color, the anisole extract a light brown, the benzyl alcohol extract a darker brown and the benzaldehyde extract a bright red. Eventually all samples, except

the benzene extract, became dark brown. The benzaldehyde sample changed most rapidly, though the change was slower if the sample was stored in the dark.

Analysis of Extracts Recovered by Benzene

Spectral grade benzene was used to redissolve the extract. This solution was then placed on a salt crystal (KBr) and the benzene was allowed to evaporate. The viscous remainder was analyzed in an IR spectrophotometer.

Figure 1 is the spectrum of the benzene extract from Clear Creek coal. Especially noticeable is the lack of any olefinic or aromatic bands. The bands at 2860, 2930 and 2960 cm^{-1} are strong indications of alkanes. Further evidence of aliphatic molecules are the peaks at 1460 and 1380 cm^{-1} which represent methylene and methyl groups. The band at 740 cm^{-1} may be due to methylene rocking in long chained molecules. Also present in the spectrum is a carbonyl peak at 1730 cm^{-1} due to either an aldehyde or ketone.

The bands at 1270 to 1290 and 1120 cm^{-1} are difficult to interpret. This first is probably due to carbon-carbon stretching between carbon atoms close to the carbonyl group. The second may be due to carbon-carbon vibrations from a highly branched molecule. However, it is shifted too far downfield for a definite assignment.

Figure 2 is the spectrum of the benzene extract from Coalville coal. It is essentially identical to the spectrum in Figure 1, thus the above discussion also applies to Figure 2.

Temperature programmed gas chromatograms were obtained using the benzene extract from Clear Creek coal. The Coalville coal extract has not yet been analyzed by GC. The chromatogram in Figure 3 was done on a column packed with OV-17. The extract was diluted with spectral grade benzene before injection. The chromatogram indicates the possibility that a homologous series of hydrocarbons is present in the extract. Indeed, over 56% of the peaks have elution intervals which are identical. The other peaks may be isomers.

The GC and IR results indicate that the benzene extractable portion of the two coals are similar in nature, if not in composition. Actual similarities will be further studied.

The infrared studies show benzene removes paraffinic materials that may contain carbonyl groups. The IR does not indicate whether these carbonyl groups are attached to the paraffins. The true form in which carbonyl groups appear is yet to be determined.

Future Work

Arrangements are being made to use a GC-MS equipped for chemical ionization mass spectrometry with a computer terminal and data bank.

This equipment will aid in the interpretation and characterization of the extracts. This will enable the assignment of molecular weights to chromatographic peaks, thus simplifying identification of the compounds obtained by each solvent treatment.

Figure 2

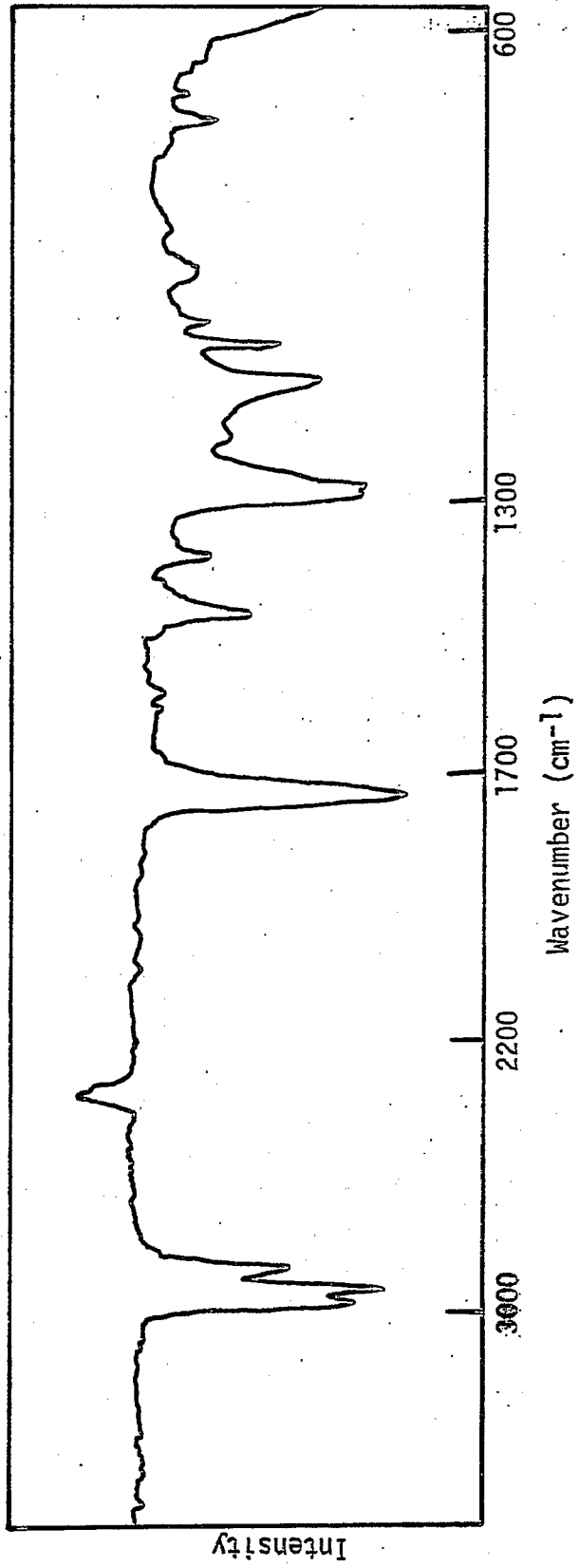
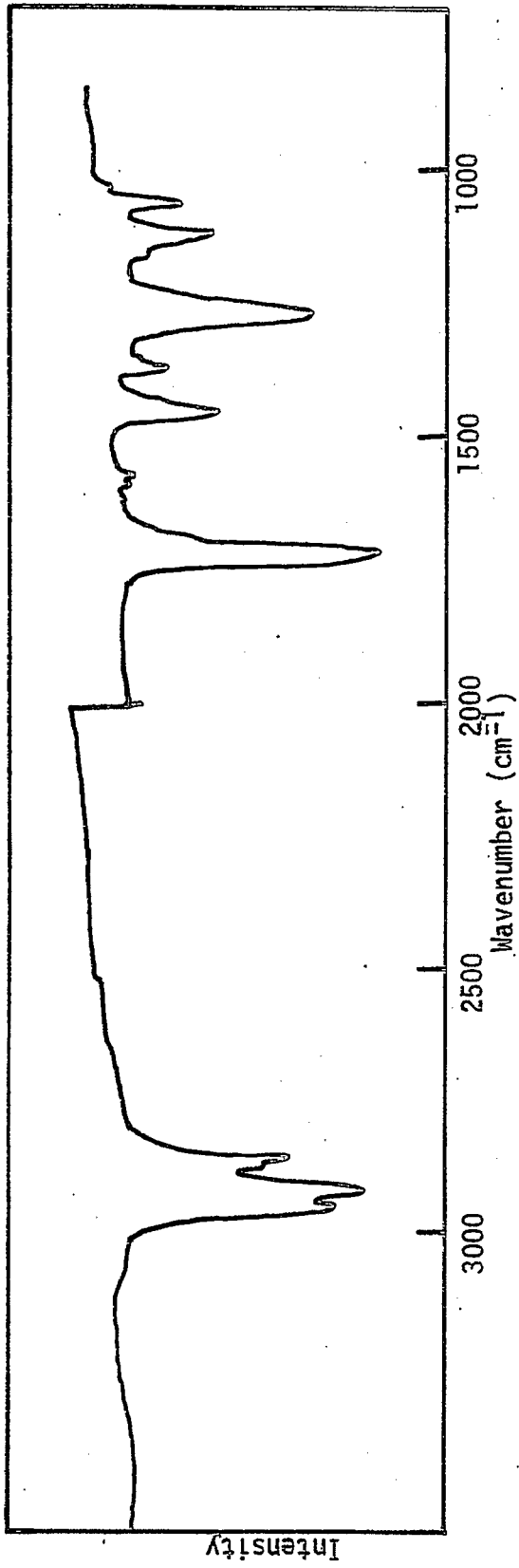


Figure 1

Project A-2

Solvent Treatment of Coal-Derived Liquids (CDL)

Faculty Advisor: L. L. Anderson
Graduate Student: Eun Kwang Chung

Introduction

The endeavor to separate CDL into chemically different fractions is being continued. Some extraction of paraffinic material from CDL has previously been reported. Also the possibility of dividing CDL into strong and weak hydrogen bonded fractions has been discussed. Further studies on these subjects are presented in this report.

Extractions with CHCl_3 , $\text{C}_2\text{H}_5\text{OH}$, aqueous NaOH and HCl solutions on certain fractions of CDL have been performed. The extraction products were examined by means of infrared (IR) and nuclear magnetic resonance (NMR) methods.

Chloroform, as well as acetone, exhibited a good precipitating quality for paraffinic material. The highly hydrogen bonded and less hydrogen bonded fractions were obtained by ethanol extraction. The NMR spectra of these fractions revealed their different structural features as was earlier observed in the IR spectra. When these fractions were treated further with NaOH or HCl solution, some interesting observations were made. Two of these were the appearance of carbonyl bands and the disappearance of hydrogen bonding peaks in the IR spectra. More work is being directed toward understanding these hydrogen bonding phenomena and its use in separating CDL.

Project Status

Experimental

Acetone soluble (AS) and acetone insoluble (AP) fractions were prepared from CDL as described in previous reports. One part of AP was extracted with four parts of CHCl_3 at 0°C , thereby precipitating paraffinic material. The chloroform soluble portion was treated again with acetone to separate out the remaining paraffins.

Ethanol was employed to separate a highly hydrogen bonded fraction from the AS. The soluble portion was named AS-ES and the insoluble, AS-EP. The ratio of solvent to sample was 4:1 and the extraction was done at 3°C . Samples of AS, AP, AS-ES and AS-EP were treated with 10% NaOH or 10% HCl solution.

The NaOH extractions were performed in separatory funnels. The CDL fractions floated though a very small portion remained

in the aqueous layer. The CDL phases were removed and extracted further with either acetone, benzene or ethanol. The HCl treatment resulted in phase separations of the samples in aqueous solution. The phases were separated by decantation.

Solvents were removed under a partial vacuum from each extraction product at the temperature of boiling water. Each product was analyzed by IR. Some were examined by NMR and MS. Only the results of AS-ES and AS-EP gave useful information. Others were found either to be too complex for NMR and MS methods or their spectra were essentially identical to each other.

Results and Discussion

The chloroform extraction gave more pure paraffinic material than did the acetone treatment. Under the same extraction conditions the IR spectra of the chloroform showed the same paraffinic absorption bands as the acetone extraction as shown in the last report but the nonparaffinic bands were smaller. This suggests that chloroform has a stronger solvent power than acetone for all the components in AP. The solvent power of chloroform for paraffinic materials is weak and therefore precipitates them. Some paraffinic material, however, remained in the solution but was separated out with acetone. Using these separation methods, the paraffinic content of CDL was calculated to be about 7% by weight.

AS-ES shows a different hydrogen bonding absorption band than AS-EP as shown in Figure 1. AS-ES has a large bell-shaped absorption band with its maximum absorption appearing at around 3400 cm^{-1} which indicates much hydrogen bonding, while AS-EP exhibits little sign of hydrogen bonding. The ^{13}C -NMR spectra of these samples also display marked differences (Figure 2). AS-ES has different unsaturated carbons, more heteroatoms, and more branching in the saturated structure than AS-EP. To understand more about the differences, the fractions were treated with NaOH or HCl solution.

NaOH treatment of AS-ES resulted in the disappearance of the hydrogen bonding band in the IR spectra (Figure 3). The band at 880 cm^{-1} appears to be due to Na_2CO_3 , which came from the solvent washing. It is also likely that the bands of Na_2CO_3 have affected the bands around 1300 , 1460 , 1600 and 3400 cm^{-1} .

When AS-EP was treated with NaOH solution, a carbonyl band (1700 cm^{-1}) appeared in the IR spectra with some alteration of the band around 3400 cm^{-1} (Figure 3). Absorption peaks for sodium carbonate did not appear in the spectrum. A satisfactory explanation for the presence of the carbonyl band has not been yet found. The different responses of AS-ES and AS-EP to NaOH treatment indicates again the dissimilarity of the two fractions as observed in the IR and NMR spectra. Continued investigation of this dissimilarity will hopefully shed more light on the nature of CDL.

In aqueous HCl solution, AS and its fractions showed a phase separation. The IR spectra of the two phases were different from each other (Figure 4). For example, with the AS, the bottom phase had a flat hydrogen bonding band though the other bands were unchanged. The IR spectrum of the upper phase indicates the presence of little organic material and much hydrogen bonding. The lower and upper phases were about 85% and 10% of AS respectively. Upon analyzing AS-EP, the lower phase did not show a significant spectral change.

The disappearance of hydrogen bonding in AS with both HCl and NaOH treatments is interesting. Sternberg et al. observed that it would be impossible for asphaltenes to have an amphoteric structure.¹ This disappearance has to be investigated more, but in contrast it suggests the presence of amphoteric configuration in the asphaltenes of CDL.

Future Work

Since the hydrogen bonding phenomenon appears to be invaluable for the fractionalization of CDL, the observations made in this quarter will be examined in further detail. The extent or depth of interaction between the fractions and NaOH or HCl solution will be investigated. Extraction, distillation and/or other means will be used. Attempts will be made to identify the functional groups and/or chemical structures involved in the interactions.

The CDL has been separated into at least three chemically distinctive fractions so far and the whole separating scheme will be repeated for more quantitative data. Also to check the usefulness of the scheme a reactivity study for each fraction will be planned. The study will be primarily on the hydrogenation or oxidation of CDL and its fractions.

References

1. H. W. Sternberg, R. Raymond and F. K. Schweighardt, Science, 188, 49 (1975).

Figure 1
I.R. Spectra of AS-ES and AS-EP

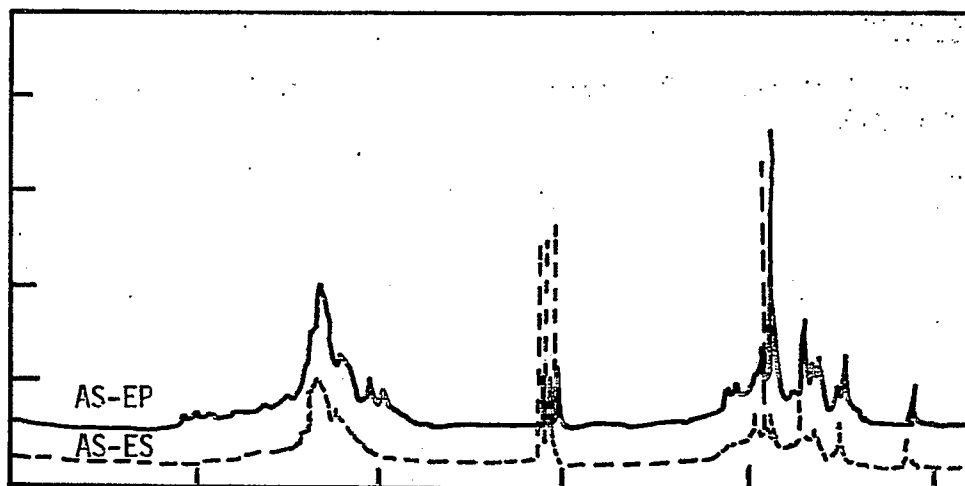
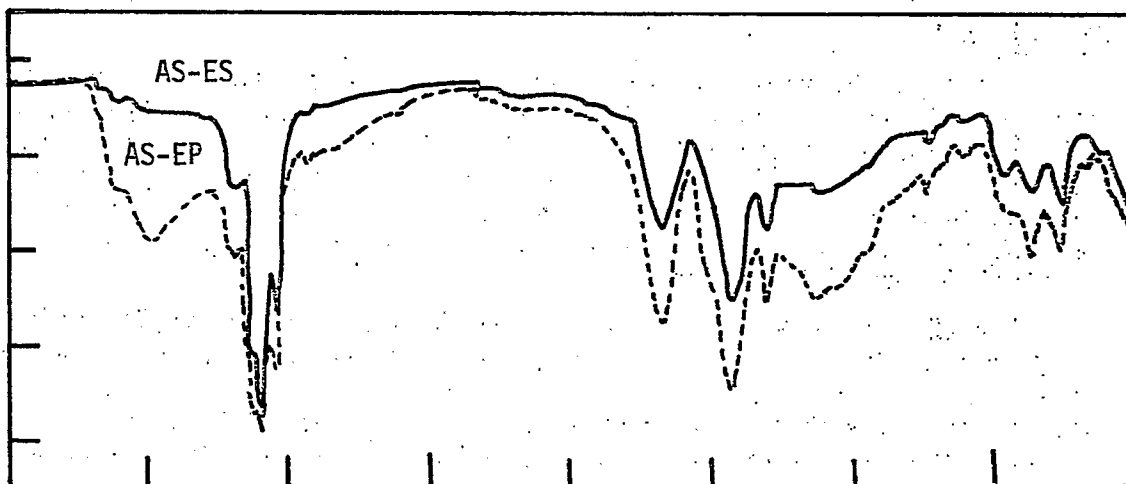


Figure 2
¹³C-NMR Spectra of AS-EP and AS-ES

Figure 3
I.R. Spectra of Products of NaOH
Treatment of AS-EP and AS-ES

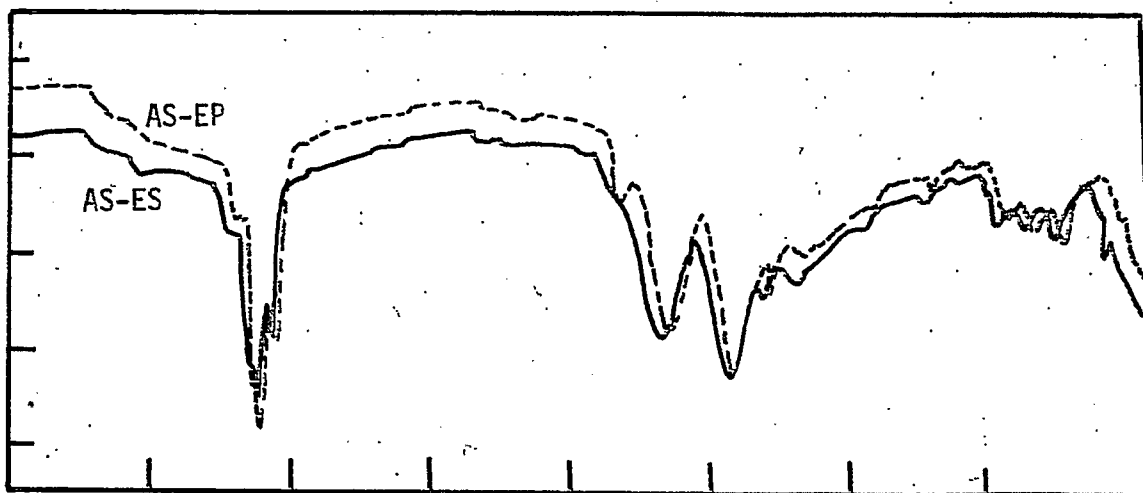
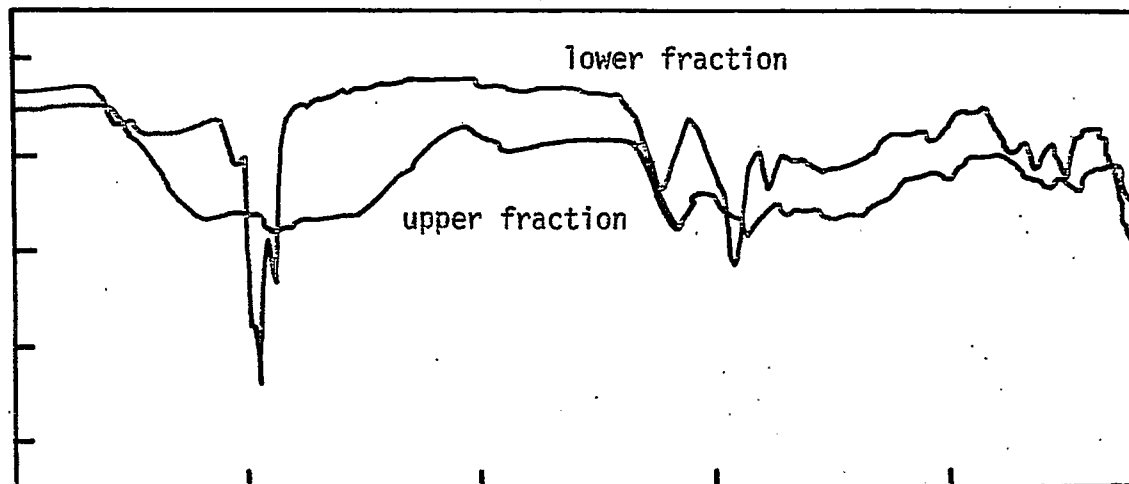


Figure 4
I.R. Spectra of HCl Treatment Products of AS



Project A-4

Steam Reforming of Aromatic Compounds

Faculty Advisor: A. G. Oblad
Graduate Student: Shri Goyal

Introduction

Coal-derived liquids are a complex mixture of a variety of chemical compounds of which 70% are aromatic hydrocarbons. Therefore, some fundamental studies of steam reforming of simple aromatic hydrocarbons have been initiated. The general reforming process and details of the equipment have been previously reported.

Project Status

The steam generator, preheater and reactor have been tested for temperature and pressure leakage and are now working well. The pressure control valve (pneumatic) has some leakage and is being repaired. A bypass line and micro-valve have temporarily been installed. The flow meter for the gases has also been installed.

Future Work

After the assembly of the equipment has been completed and the lines insulated, the entire test set-up will be tested and calibrated. Finally, methane will be steam reformed on Girdler G56-B steam reforming catalyst to confirm the workability of the process equipment.

Project A-6

Production of Hydrogen from Char Produced in Coal Hydrogenation under High Pressure

Inactive at Present

Project A-7

Study of Thermal and Vapor Phase Upgrading of Coal Liquids

Faculty Advisor: A. G. Oblad
Graduate Student: R. Ramakrishnan

Introduction

Various commercial processes exist to produce high purity benzene from toluene by thermal hydrodealkylation. Most of the thermal dealkylation studies in the literature have been limited to alkylbenzenes and alkylnaphthalenes. Very little work has been done on three or more ring aromatic compounds. The main objective is to see if coal-derived liquids can be upgraded by thermal hydrogenolysis or by using vapor phase catalysts.

Project Status

Equipment fabrication was very difficult due to the high temperature (600°C+) and high pressure needed for the thermal reactions to occur. After several reactor concepts were tried a coil wound around a grooved isothermal metal block was selected. This reactor was tested at maximum reaction conditions of 700°C and 1000 psi and was found to have essentially a constant temperature of 700°C throughout the entire reaction coil.

Preliminary experiments with toluene have given results comparable to those available in the literature. This indicates that the reactor and the analytical methods are satisfactory. Experiments with benzene indicate some cracking. A procedure for analyzing the products from pure compound studies is being developed. The results obtained from the cracking of pure compounds will be used to plan research in the upgrading of coal liquids.

Project A-8

Synthesis of Light Hydrocarbons from CO and H₂

Faculty Advisor: A.G. Oblad
Postdoctoral Fellow: M.K. ZamanKhan
Graduate Student: Chen-Hsyong Yang

Introduction

The purpose of this project is to develop suitable catalysts for hydrogenation of carbon monoxide to C₂-C₄ gaseous lower molecular weight compounds particularly olefinic hydrocarbons. Catalyst life and stability of meritorious catalysts will also be studied on a laboratory scale.

In previous reports an evaluation of a series of cobalt catalysts containing various amounts of copper as an activity and selectivity modifier were examined. In addition to that, nickel and iron catalysts were synthesized in order to compare them with cobalt. The nickel catalyst was tested but proved to be undesirable for the synthesis of light C₂-C₄ hydrocarbons. As expected it was an excellent methanation catalyst.

During this quarter the work was divided into three areas: I. the further evaluation of cobalt-copper catalyst, II. studies of the effect of pretreatment on catalyst activity and selectivity, and III. the evaluation of iron catalysts.

Project Status

I. Cobalt-copper catalyst

(1) To continue the study on the effect of cobalt content on the activity and selectivity of the cobalt catalyst for hydrogenation of CO, the following samples of cobalt-copper catalysts were prepared by coprecipitation.

Co-A	Co	-	Cu	-	Al ₂ O ₃	-	Na ₂ O
	6.1%		7.35%		-		-
ZK-15	Co	-	Cu	-	Al ₂ O ₃	-	Na ₂ O
	15%		7.35%		-		-
Co-A ^{II}	Co	-	Cu	-	Al ₂ O ₃	-	Na ₂ O
	12%		15%		-		-

In addition to the previously prepared cobalt-copper catalysts, the catalysts Co-A and ZK-15 were evaluated under similar conditions to determine differences in activity and selectivity.

It was found that the higher cobalt content catalyst, ZK-15, showed higher CO conversion than other cobalt catalysts (Table 1). However, it also proved to be unstable during the activity test. Catalyst ZK-15 deactivated faster than other cobalt catalysts in the series. The catalysts having higher cobalt content had high initial activity but may be much more sensitive to sintering than lower cobalt containing catalysts. The reasons for the instability will be investigated in future work.

In comparisons of catalysts of different cobalt compositions, it was found that a cobalt to copper ratio of 1:1 showed more promising results than other cobalt catalysts (Table 1). Because of its activity, stability and selectivity, catalyst Co-A was chosen for a comparison of the two different pretreatment methods (Table 2). Cobalt and nickel each as a primary metal component in K-4A and Ni-A were tested and compared. It was found that the nickel catalyst produced more CO₂ and CH₄ but less C₂ to C₅ and C₅+ hydrocarbons. Also the olefin and paraffin ratio was lower for the nickel catalyst than for the cobalt catalyst (Table 3 and Figure V).

(2) To study the effect of copper on the activity and selectivity of cobalt-copper catalysts, a fixed cobalt content series of catalysts with various amounts of copper were prepared.

ZK-14	Co - Cu - Al ₂ O ₃ - Na ₂ O
	6.1% 0.5% - -
ZK-12	Co - Cu - Al ₂ O ₃ - Na ₂ O
	6.1% 3% - -
Co-A	Co - Cu - Al ₂ O ₃ - Na ₂ O
	6.1% 7.35% - -
ZK-13	Co - Cu - Al ₂ O ₃ - Na ₂ O
	6.1% 12% - -
ZK-25	Co - Cu - Al ₂ O ₃ - Na ₂ O
	12% 15% - -

Evaluation of the above catalysts is continuing.

(3) To study the effect of alkali (Na₂O) on the selectivity of cobalt-copper catalyst, two catalysts, ZK-10 and ZK-11 were prepared by coprecipitation using NH₄OH which also adjusted the pH values of the fresh catalysts.⁴ ZK-10 had a pH of 9 and ZK-11 had a pH of 7. Both of these catalysts resulted in very low activities compared with catalyst Co-A at 275°C, 750 psig and a hydrogen-to-carbon atom ratio of 2:1. However selectivities remained almost the same for all the cobalt catalysts including those without sodium (Table 4 and Figures III and IV). The reasons for the low activities of these catalysts will be studied further.

(4) The influence of various supports on the activity of cobalt-copper is also being tested by preparing the following catalysts.

Co-A Co - Cu - Al₂O₃ - Na₂O
 6.1% 7.35% 3 -

Co- Co - Cu - on Molecular Sieve Type-y
 6.1% 7.35%

Co- Co - Cu - on SiO₂ - Al₂O₃
 6.1% 7.35% -

(5) To study the effect of mode of preparation of cobalt-copper catalysts with a fixed metal ratio, the catalyst was prepared by both coprecipitation and impregnation methods. Evaluations of these catalysts are continuing.

(6) Some insight into the selectivity and product distribution of hydrogenation by the cobalt-copper catalysts was sought by replacing the copper with chromium. Both catalysts were prepared by coprecipitation.

Co-A' Co - Cr - Al₂O₃ - Na₂O
 6.1% 7.35% -

Testing of this catalyst will be done.

II. Studies of the effect of pretreatment on catalyst activity and selectivity

Previous experiments have shown that catalyst with alumina as a support and pretreated by heating in air at 500°C for 2 hr followed by reduction in hydrogen at 300°C for 4 hr have higher activities than catalysts reduced in hydrogen at 300°C. This difference in activity may be due to the alumina support changing into γ -alumina during the 500°C treatment. However, the activity of alumina supported catalysts reduced in hydrogen at 500°C has been compared with catalysts calcined in air at 500°C and then reduced in hydrogen at 300°C. Catalysts reduced in the hydrogen at 500°C only show higher activity for CO conversion. This catalyst preparation step was adopted as standard pretreatment for cobalt catalysts. Selectivity of the catalysts remained almost constant regardless of the pretreatment. See Table 2 and Figures I, II, III and IV.

III. Iron catalysts

To explore the possibility of an iron catalyst for hydrogenation carbon monoxide, a commercial ammonia synthesis catalyst, CASC-I, was tested for two different pretreatments. CASC-I gave very promising and challenging results. The olefin/paraffin ratio of C₂-C₄ product ranges from 2:4 which

is very high. This catalyst is, however, very unstable. It lost 90% of its initial activity (CO conversion per pass) every 3 hr yet CASC-I was almost completely dead after 6 hr in the reaction streams. As the reactor temperature was raised 25°C the activity increased to the previous level (Table 5).

CASC-I reduced in hydrogen at 450°C at 5000 cc/g hr without being nitrided in NH₃ showed lower activity than those that were nitrided. Even after the NH₃ nitrided catalyst was reduced again in hydrogen at 450°C, it showed higher activity than the hydrogen reduced iron catalyst. Selectivities of CASC-I showed that a higher percentage of CO was converted to CO₂ even at 10 to 20% CO conversion. Cobalt catalysts showed lower selectivity of CO to CO₂ conversion.

The iron catalysts

ZK-22	Fe - Cu - K ₂ CO ₃
	83.7% 16% 0.3%
ZK-23	Fe - Co - Kieselguhr
	45% 10% 45%
ZK-26	Fe ₃ O ₄ - Cu - CaO - MgO - Al ₂ O ₃ - K ₂ O
	84% 10% 2% 0.3% 2.5% 0.8%
K-3	Fe on Al ₂ O ₃
	12% -

were tested giving improved results with the same pretreatment and reaction conditions. ZK-26 is the same as CASC-I except that it contains 10% copper. This catalyst showed slower deactivation as compared to CASC-I. It takes about 10 hr to lose 90% of its activity. However its selectivity is the same as CASC-I (Tables 5 and 6).

ZK-22 is not as active. It has about 1% of the activity of CASC-I and ZK-26 at 225°C, 750 psig, hydrogen-to-carbon monoxide of 1:1. As the reactor temperature was raised to 265°C the activity was increased to 50% CO conversion. The selectivity of ZK-22 is the same as the other iron catalysts. The regeneration of ZK-22 in hydrogen restores some of its activity (Table 7).

ZK-23 has a composition of iron, cobalt and Kieselguhr in the ratio of 45:10:45 respectively. Its activity is approximately the same as CASC-I on a basis of unit iron metal content. This catalyst appeared stable in activity in the reaction stream though the reason is unknown (Table 8).

Research will continue on improvement of the iron catalyst's stability without changing its activity and selectivity

toward light olefins. We have many ideas for accomplishing this.

Future Work

Work will continue on the Cobalt-copper/alumina- Na_2O series of catalysts to determine composition optimum for both activity and selectivity. The effects of the main process variables will be determined for the optimum catalysts of the series. Some attempts will be made to estimate catalyst stability of these very interesting catalysts.

Exploratory work to develop new catalyst compositions not yet studied will be done. We have a number of ideas in this area.

Table 1

Activity and Selectivity of ZK-15 Catalyst

Temperature °C	225	250	275
Pressure (psig)	750	750	750
Space velocity (cc/g/sec)	0.77	0.77	1.54
H ₂ /CO (molar ratio)	2	2	2
% CO conversion	10.04	36.38	72.06
<u>Product Distribution (%)</u>			
CO ₂	25.66	4.85	49.10
CH ₄	29.23	34.86	24.14
C ₂ -C ₄	33.34	37.56	22.39
C ₅ ⁺	11.78	22.73	4.36
Olefins to Paraffins Ratio (O/P)	1.166	0.538	0.0180
R.OH	2.00	1.241	0.10
H ₂ O	1.485	1.773	1.26
Water	-	90.87	86.961

Table 2
Evaluation of Co-A for Hydrogenation of Carbon Monoxide

	PRE-TREATMENT OF Co-A											
	Co-A reduced in H ₂ at 520°C for 4 hr						Co-A calcined in air at 520°C followed by reduction at 275°C for 4 hr					
	250		275		750		250		275		750	
Temperature °C	500	750	500	750	500	750	500	750	500	750	500	750
Pressure (psig)	0.77	0.77	0.77	0.77	0.77	0.77	0.77	0.77	0.77	0.77	0.77	0.77
Space velocity (cc/g/sec)	2.33	1.50	1.50	2.33	2.33	1.50	2.33	1.50	1.50	2.33	1.50	2.33
% CO conversion	7.11	3.84	13.55	51.35	5.74	6.37	13.73	34.29	0.0	11.60	3.78	10.83
<u>Product distribution (%)</u>												
CO ₂	0.0	0.00	6.58	10.79	0.0	28.08	43.30	37.36	38.35	37.60	33.77	17.05
CH ₄	42.54	36.02	38.88	37.42	42.20	44.43	37.36	34.08	16.31	13.01	21.64	0.18
C ₂ -C ₄	15.25	19.55	17.17	17.70	0.46	0.76	0.43	0.16	1.94	0.42	0.14	0.18
C ₅ ⁺	-	-	-	-	-	-	-	-	-	-	-	-
O/P	-	-	-	-	-	-	-	-	-	-	-	-
H ₂ O	-	-	-	-	-	-	-	-	-	-	-	-
R. OH	-	-	-	-	-	-	-	-	-	-	-	-
Water	-	94.65	-	98.0	-	-	-	-	-	-	-	87.89

Table 3

Comparison in Activity and Selectivity
of Nickel and Cobalt Catalysts

	Ni-A Ni = 8.1%, Cu = 7.35%		K-4 Co = 8.1%, Cu = 7.35%	
	275		275	
Temperature °C				
Pressure (psig)	22	750	22	750
Space velocity (cc/g/sec)	0.11	0.77	0.11	0.77
H ₂ /CO (molar ratio)	1	2.33	1	2.33
% CO conversion	11.16	18.29	20.4	39.40
<u>Product distribution (%)</u>				
CO ₂	58.47	63.07	22.46	20.77
CH ₄	26.70	24.41	19.46	28.14
C ₂ -C ₄	7.79	9.71	29.28	34.45
C ₅ ⁺	7.04	2.80	28.80	16.63
O/P	0.131	0.062	1.681	0.850
H ₂ O	2.0	2.28	1.89	1.96
R.OH	-	-	-	-
Water	-	95.4	-	89.4

Table 4
Activity and Selectivity of
ZK-10 and ZK-11

	ZK-10 (pH 9)		ZK-11 (pH 7)	
Temperature °C	275	300	275	300
Pressure (psig)	750	750	750	750
Space velocity (cc/g/sec)	0.77	0.77	0.77	0.77
H ₂ /CO (molar ratio)	1.5	1.5	1.0	1.5
% CO conversion	9.87	27.03	2.57	8.09
<u>Product distribution (%)</u>				
CO ₂	0.43	10.61	0.65	5.10
CH ₄	41.71	41.42	44.84	42.37
C ₂ -C ₄	39.43	34.83	32.39	41.10
C ₅ +	18.43	13.14	22.12	11.43
O/P	0.841	0.322	-	0.220
H ₂ O	1.81	1.91	0.32	0.43
R.OH	0.37	1.43	0.01	0.44
Water	-	-	-	-

Table 5

CASC-I Iron Catalyst for Hydrogenation of CO

	CASC-I reduced in H ₂ at 550°C for 20 hr followed by nitriding with NH ₃ at 325°C for 6 hr			CASC-I reduced in H ₂ at 450°C for 20 hr		
	1st hour	6th hour	regenerated	1st hour	6th hour	regenerated
Temperature °C	225	250	250	250	250	250
Pressure (psig)	750	750	750	750	750	750
Space velocity (cc/g/sec)	1.54	1.54	1.54	1.54	1.54	0.77
H ₂ /CO (molar ratio)	2	1	1	1	1	1
% CO conversion	89.39	5.68	75.59	75.91	5.53	18.08
<u>Product distribution (%)</u>						
CO ₂	39.40	23.72	50.35	57.85	35.33	45.97
CH ₄	11.73	10.64	7.46	2.50	8.57	6.42
C ₂ -C ₄	24.82	30.78	19.93	21.50	26.49	21.13
C ₅ ⁺	21.98	34.87	22.27	18.15	29.61	26.48
O/P	2.90	2.70	3.59	4.65	2.67	2.49
H ₂ O	0.54	0.76	1.15	0.55	1.46	0.68
R.OH	2.07	0.00	0.00	0.00	0.00	0.00
Water	89.54	87.72	92.27	-	-	-

Table 6

Activity and Selectivity of ZK-26 Iron Catalyst

	ZK-26 reduced in H ₂ at 500°C for 20 hr followed by nitriding with NH ₃ at 325°C for 6 hr		ZK-26 reduced in H ₂ at 450°C for 20 hr	
	1st hour	after 10 hours	1st hour	after 10 hours
Temperature °C	260	220	250	200
Pressure (psig)	750	750	750	750
Space velocity (cc/g/sec)	1.54	1.54	1.54	1.54
H ₂ /CO (molar ratio)	1	1	1	1
% CO conversion	94.73	$\frac{\text{heated}}{\text{in H}_2}$ 38.34	83.77	$\frac{\text{heated}}{\text{in H}_2}$ 46.43
<u>Product distribution (%)</u>				
CO ₂	64.71	39.34	69.74	44.77
CH ₄	8.32	4.90	4.34	5.02
C ₂ -C ₄	17.46	15.66	14.12	20.71
C ₅ ⁺	8.68	31.81	10.18	29.52
O/P	1.24	3.63	2.62	3.76
H ₂ O	1.51	1.85	1.21	1.15
R.OH	0.83	8.29	1.61	0.18
Water	83.07	71.41	71.41	77.29

Table 7

Evaluation of ZK-22 Iron Catalyst for Hydrogenation of CO

	ZK-22 reduced in H ₂ at 500°C for 20 hr and nitrided in NH ₃ at 325°C for 6 hr			ZK-22 regenerated at 450°C in H ₂ for 20 hr		
	225	250	265	250	250	265
Temperature °C	225	250	265	250	250	265
Pressure (psig)	750	750	750	750	750	750
Space velocity (cc/g/sec)	1.54	0.77	0.77	0.77	0.77	0.77
H ₂ /CO (molar ratio)	1	1	1	1	1	1
% CO conversion	0.84	20.71	47.69	15.94	60.31	62.28
<u>Product distribution (%)</u>						
CO ₂	0.00	49.89	54.33	42.47	62.28	62.28
CH ₄	25.86	8.11	8.51	6.08	4.28	4.28
C ₂ -C ₄	51.60	23.05	22.13	23.75	18.16	18.16
C ₅ ⁺	22.54	17.44	12.14	27.16	15.21	15.21
O/P	2.22	1.81	1.62	2.31	2.82	2.82
H ₂ O	0.49	1.15	0.55	0.85	0.53	0.53
R.OH	-	1.51	2.89	0.54	0.07	0.07
Water	-	79.55	79.55	84.44	84.44	84.44

Table 8

Activity and Selectivity of ZK-23

	ZK-23 reduced in H ₂ at 500°C for 20 hr and nitrified at 325°C in NH ₃ for 6 hr		ZK-23 regenerated in H ₂ at 450°C for 20 hr	
	<u>1st hour</u>	<u>overnight</u>		
Temperature °C	225	275	225	
Pressure (psig)	750	750	750	
Space velocity (cc/g/sec)	1.54	1.54	0.77	
H ₂ /CO (molar ratio)	1	1	1	
% CO conversion	57.64	9.27	35.85	
<u>Product distribution (%)</u>				
CO ₂	51.61	9.88	56.29	
CH ₄	15.82	7.49	4.30	
C ₂ -C ₄	18.68	32.81	20.39	
C ₅ ⁺	10.28	49.82	18.52	
O/P	2.0	2.45	2.14	
H ₂ O	1.23	0.49	2.88	
R.OH	3.63	0.00	0.0	
Water	91.62	88.19	-	

Figure I
Selectivity and Activity of CO-A Reduced
in H₂ Only

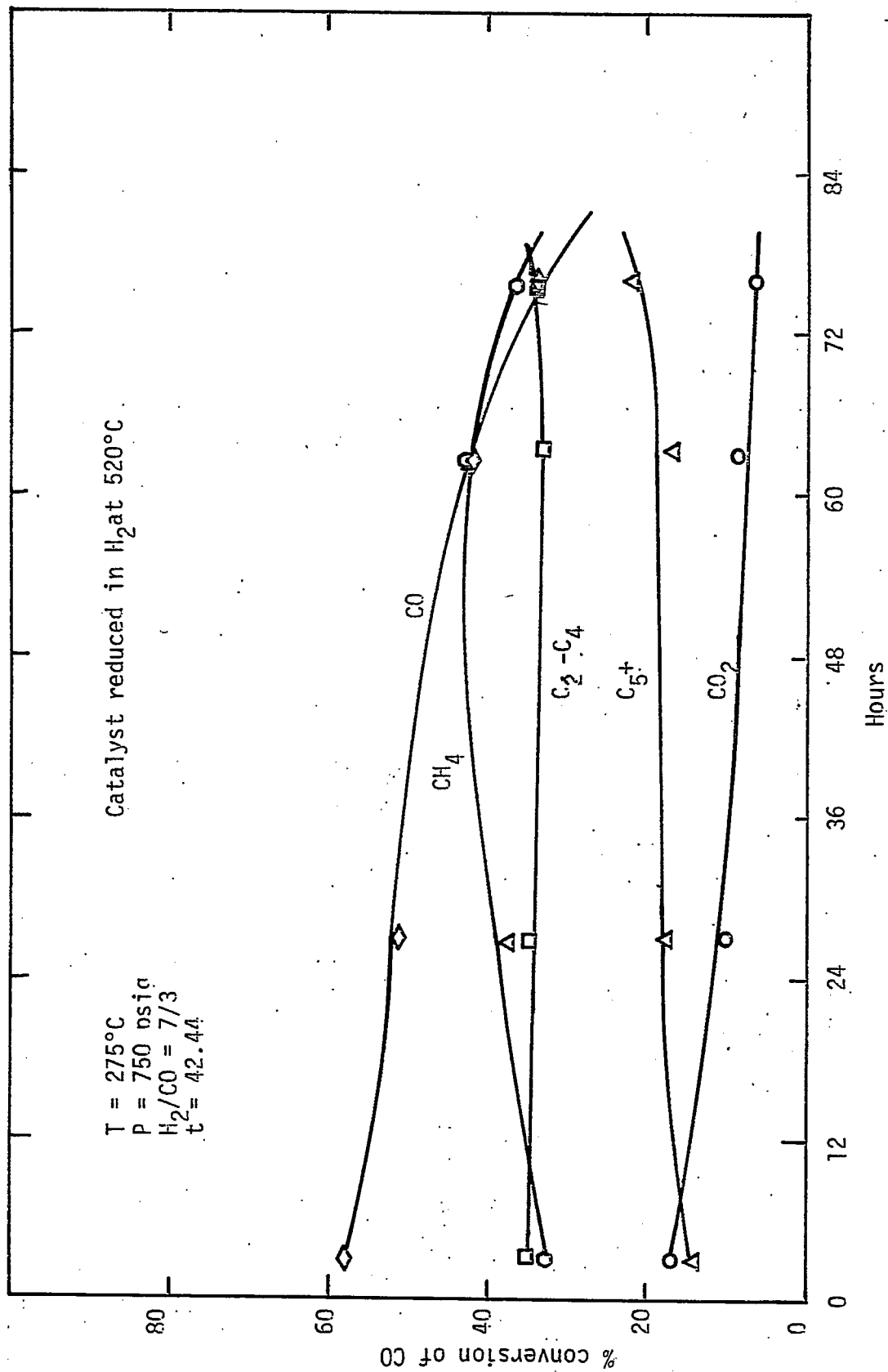
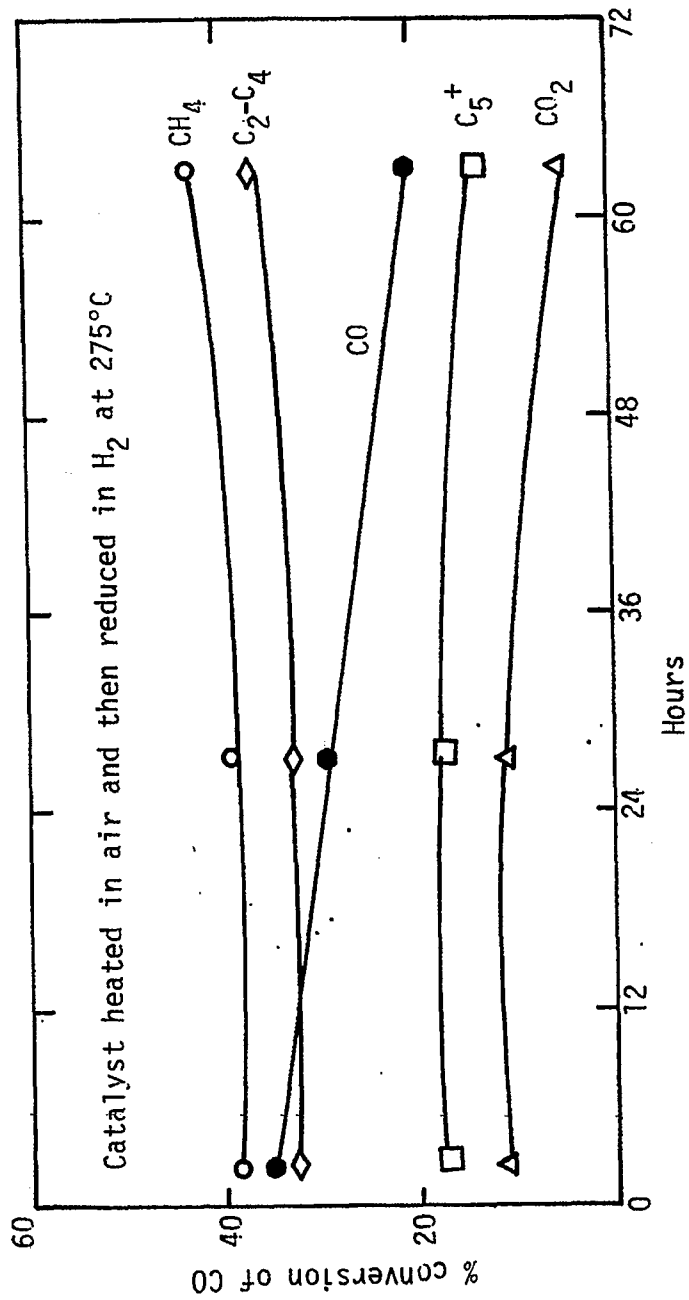


Figure II

Selectivity and Activity of Co-A



T = 275°C
P = 750 psig
H₂/CO = 7/3
t = 42.44

Figure III

Effect of Cobalt Content on
Selectivity and Activity

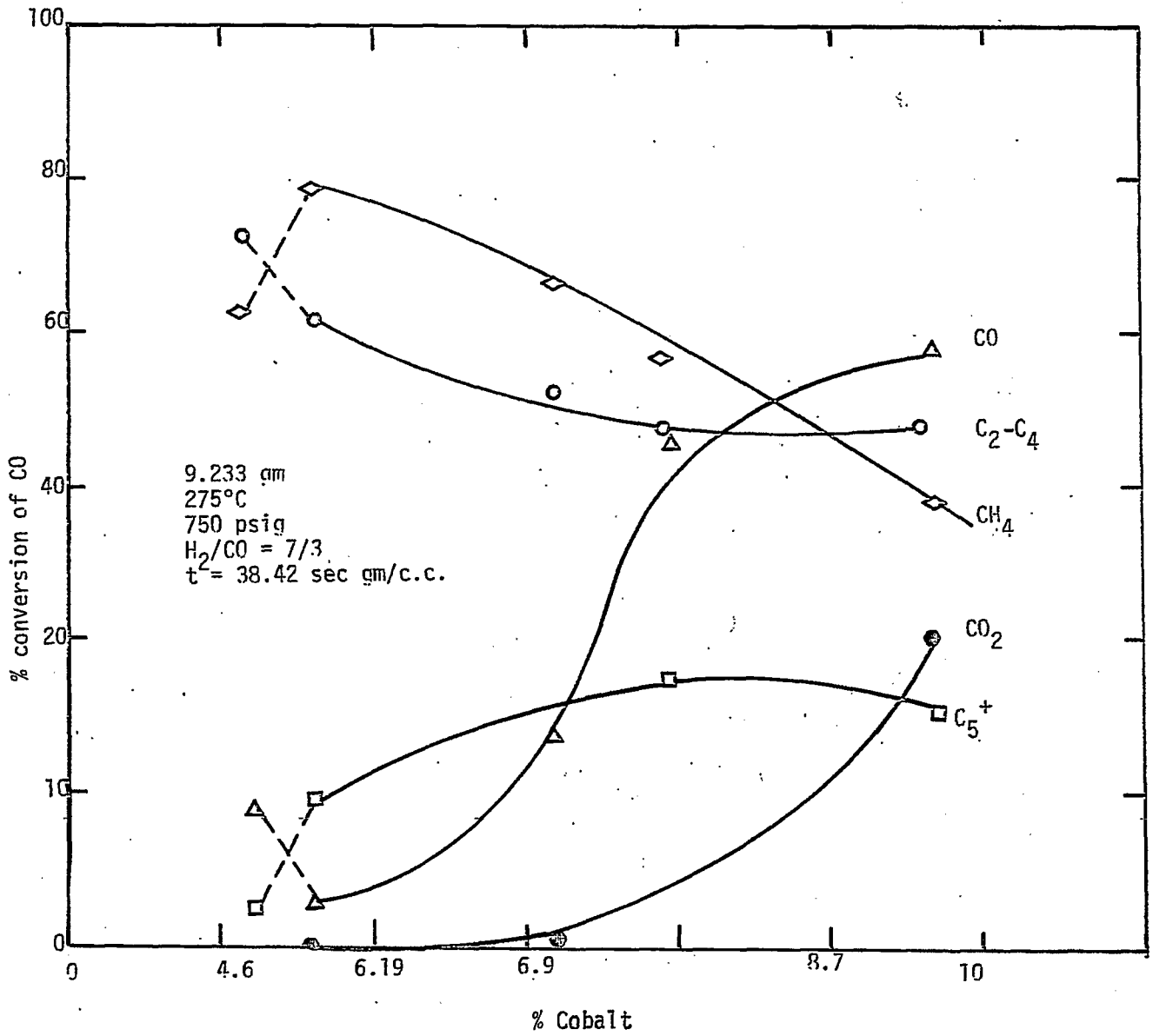


Figure IV
Effect of Cobalt Content on
Selectivity and Activity

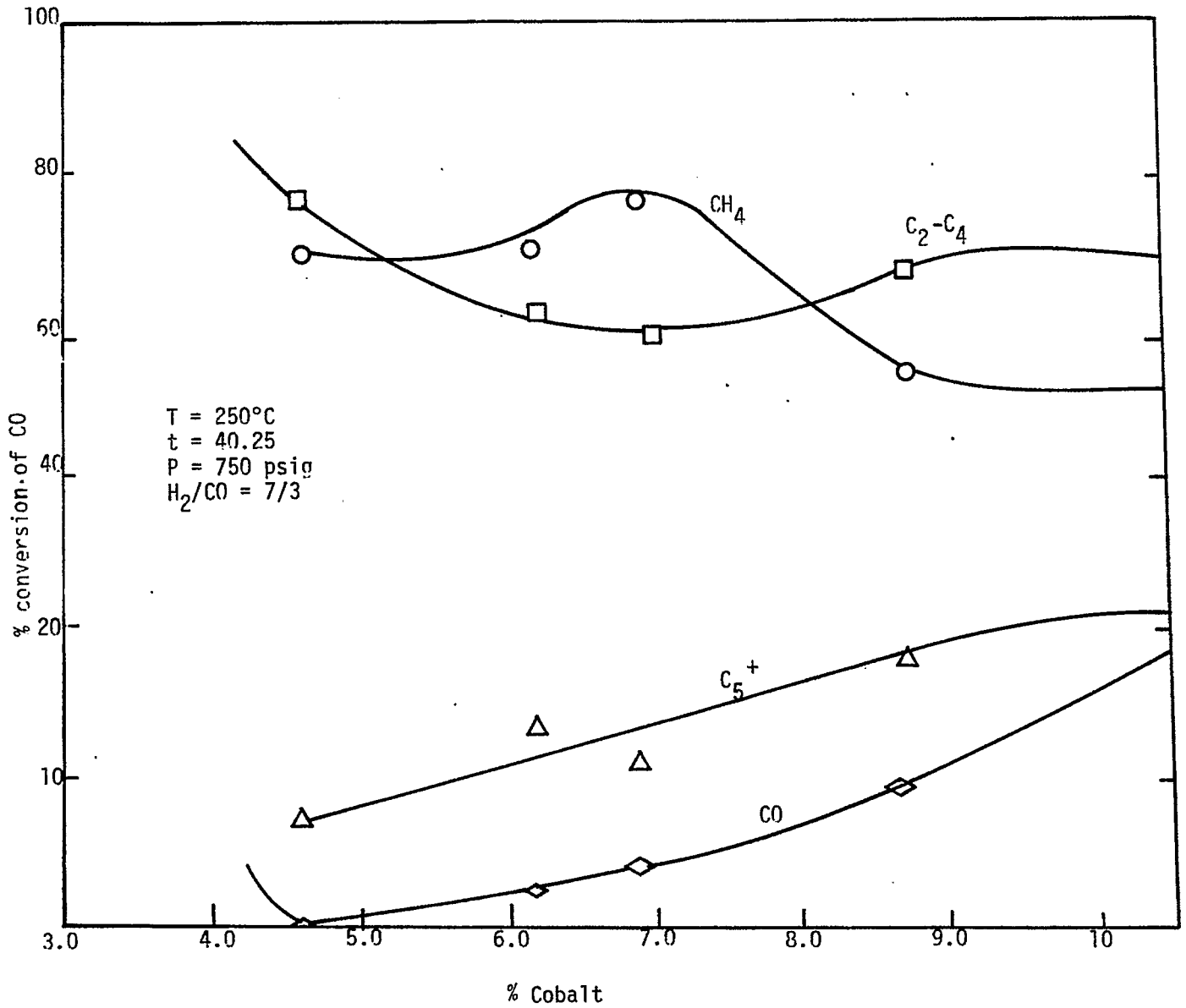
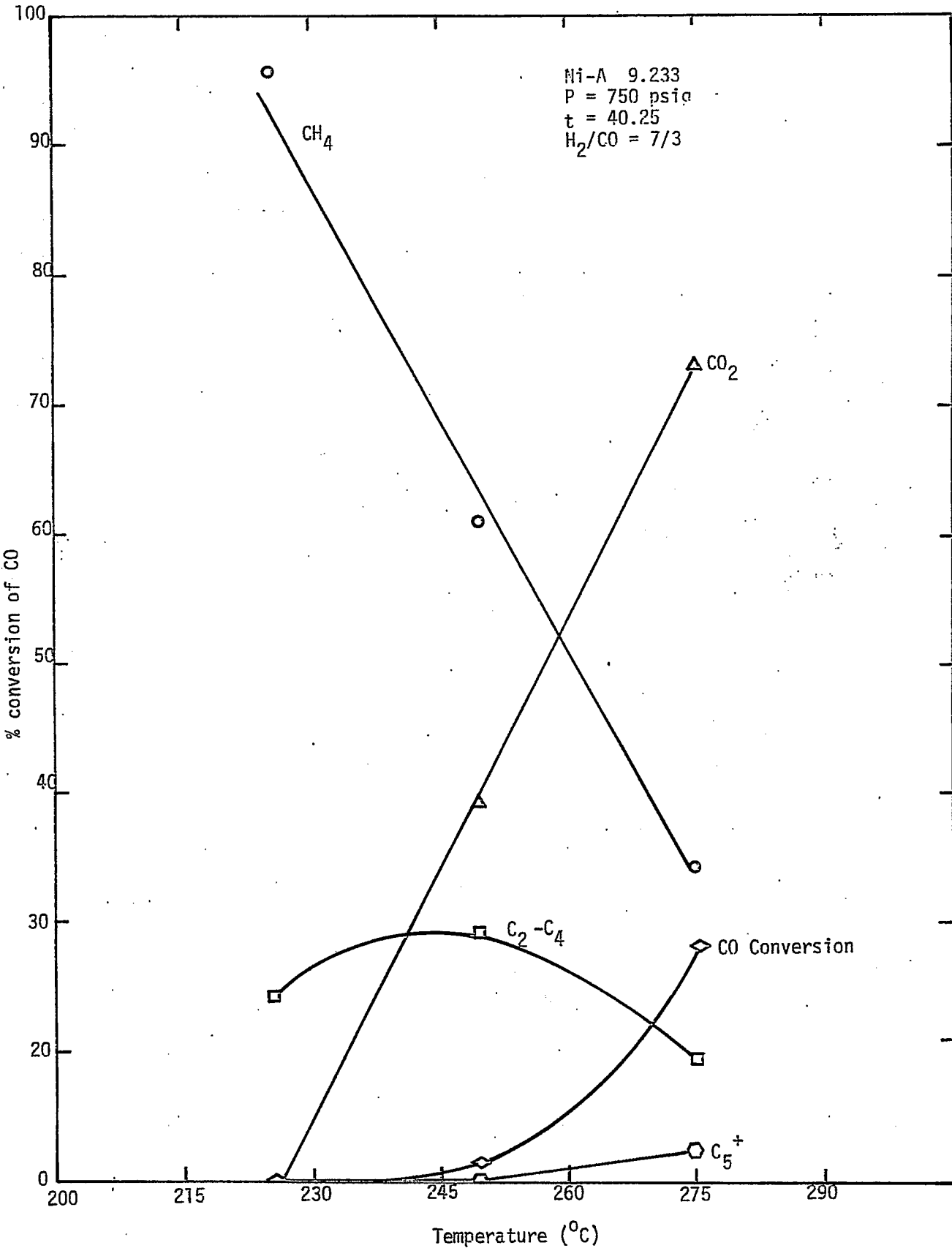


Figure V.



Project A-8

Synthesis of Light Hydrocarbons from CO and H₂ (Continued)

Catalyst Characterization Studies

Faculty Advisor: F. E. Massoth

Introduction

This phase of the project is intended to supplement the reactor studies by detailed examination of the catalyst properties which enhance catalyst activity and selectivity. This is accomplished by characterization studies performed on the same catalysts which have been run in the reactor. Of particular interest are metal areas, evidence for alloy formation, phase structures and catalyst stability. Also, variables in catalyst preparation and pretreatment are examined to establish effects on catalyst properties. Finally, in-situ adsorption and activity studies are undertaken under modified reaction conditions with a number of well-characterized catalysts to obtain correlating relationships.

Project Status

During this quarter, characterization tests were made on a number of new catalysts that had been evaluated in the high pressure reactor. These catalysts showed large differences in catalyst activity. The catalysts consisted of copper and cobalt supported on a sodium-alumina matrix, and were prepared by a coprecipitation technique. They were then oven-dried and given a hydrogen pretreatment at 500°C in the reactor prior to starting a run.

In the tests described below, each of the original oven-dried catalysts was subjected to a hydrogen treatment at 450°C for several hours, followed by cooling down to 0°C in a N₂ purge flow. Then air was admitted to determine the amount of oxygen chemisorbed. Next, the catalyst was reheated to 450°C in H₂ and finally oxidized in air at 450°C to determine the extent of reduction. This sequence was carried out in a flow microbalance. Both the apparatus and procedure have been described in earlier reports.

It has previously been shown that adsorption of oxygen at low temperature provides a good relative measure of active metal area present on the reduced catalyst.¹ Weight loss occurring in the initial reduction step is due to water loss from the alumina support and to the reduction of the copper and cobalt carbonates and oxides present. Therefore, a high temperature redox cycle is necessary to measure the extent of reduction of the metal components after having determined the oxygen

adsorption of the reduced catalyst. The metal dispersion is then defined as the ratio of the weight change obtained in the adsorption step to that in the high-temperature oxidation step. It should be pointed out that the dispersion calculated in this manner is only approximate. It is based on the assumption that one oxygen atom is adsorbed per metal surface atom at low temperature. This surface stoichiometry seems reasonable but has not yet been confirmed. A complicating factor is that different stoichiometries may pertain to copper and cobalt. Thus, the surface composition must be known. It is extremely difficult to determine because the surface composition may be different from the bulk composition in alloys.² Furthermore, the high temperature oxidation is taken to represent oxidation of the reduced metals to CuO and CoO. This is a simplification since at 500°C, Co₃O₄ is the stable state of cobalt oxide in air.³ Nevertheless, the corrections are not expected to be large due to these factors, and the simplified metal dispersion values can be taken as a rough guide for comparative purposes.

The catalysts tested are given in Table I. They represent preparations having different cobalt to copper ratios and different metal levels. In the normal preparation, sodium carbonate solution is used to effect coprecipitation of the metals and alumina. A small amount of sodium oxide is incorporated in the catalyst by this procedure. In two cases, ammonium carbonate was used for the precipitation, thus, eliminating sodium from the catalysts. In one of these catalysts, the pH of the solution was maintained at 7 (a pH of 9 was used for all the others). In addition, some were prepared with high purity materials and others with a practical grade of cobalt nitrate. The latter catalysts had exhibited lower catalytic activities than the former in the high pressure reactor. One reason for instigating these tests was to determine if this effect was due to different metal areas in the two cases.

Given in Table I are the catalyst conversions obtained in the high-pressure reactor under a standard set of conditions and the results of the catalyst measurements. Extents of reduction from the high-temperature oxidation weight changes were appreciably higher than predicted from the nominal compositions in some cases. The reason for these discrepancies is not known at present. The calibration of the microbalance was rechecked and found to be accurate. It would appear that the nominal compositions are too low. Analyses of these samples by atomic absorption were too erratic to give reliable results. Further analyses will be made using X-ray fluorescence later. In view of these uncertainties, it is possible that some of these catalysts are reduced to a lesser degree than others.

The amount of adsorption shows only a very rough relationship to the total metal present on the catalyst. This is not surprising in view of the complexity of this catalyst system. The adsorption, being a measure of the total metal surface area per gram, will depend on reducibility and on the degree of dispersion of the metal, as well as on total metal content.

The dispersions show more systematic trends than the adsorptions. Figure 1 shows the variation of metal dispersion with metal levels.

Figures 1A and 1B show that dispersion increased with Co content at constant Cu, and decreased with Cu content at constant Co. This would suggest an optimum ratio, and such an effect is shown in Figure 1C. The end points in Figure 1C were obtained from earlier experiments with only Co or Cu in the catalysts.¹ Although the data show some scatter, the optimum ratio for best dispersion is about 2 Co/Cu (atomic basis). This appears to be independent of metal loading, at least up to 20 wt % metals. The catalysts without sodium present gave low dispersions, suggesting that sodium may help metal dispersion. The use of the practical grade cobalt nitrate seems not to have affected metal dispersions.

Overall, the results confirm the earlier finding of a synergism in the system with respect to dispersion of the metal phase. For instance, addition of one metal to the other greatly increases the resulting dispersion of the metal. From the results of Figure 1C, small amounts of Cu added to Co seem to have a greater effect than the reverse situation.

Since the reaction of CO and H₂ depends upon the presence of reduced metal, the catalytic activity would be expected to be proportional to the free metal area in the reduced catalyst. Such a correlation is shown in Figure 2. It is obvious that a simple proportionality is not adequate; rather, there are two distinct correlations that can be drawn. The upper line represents more active catalysts than the lower line. Of interest, the catalysts of the upper curve were prepared with analytical grade chemicals (except for catalyst-14) whereas those of the lower line were prepared with practical grade cobalt nitrate. This suggests that an impurity in the practical grade material has rendered these catalysts less active. It is significant that this impurity did not affect metal areas as measured by oxygen adsorption. Two explanations are possible. First, the impurity may cover metal sites and lower CO or H₂ adsorption at reaction conditions, but it may also adsorb oxygen in the low temperature adsorption measurements. Thus, oxygen adsorption would not distinguish between uncovered and poisoned metal sites and therefore it would not give a true measure of effective metal sites available for reaction. Second, the impurity may adversely affect non-metal sites which are necessary for reaction, i.e., a dual site reaction mechanism may be operative. Hopefully, it will be possible to determine which explanation is correct by measuring CO chemisorption.

The catalyst without Na present (catalyst-10) fits better on the upper line of Figure 2. This suggests that Na has no catalytic role in the reaction. However, it is necessary to obtain good dispersion of the Co and Cu as discussed above. The other Na-free catalyst falls closer to the lower line and would appear to indicate that precipitation at a pH of 7 gives an intrinsically lower catalyst activity. However, these points need further checking with other catalyst formulations because of the low activities involved.

Future Work

Work on this project has been temporarily halted due to the loss of our technician. As soon as a graduate student or technician becomes available, work will resume.

Future work will involve further catalyst characterization of these and other catalysts now under consideration. The use of CO as an adsorbent will be investigated and compared with oxygen adsorption. In addition, in-situ testing for CO/H₂ reactivity in the microbalance will be undertaken with the objective of obtaining catalyst activity data in the same reactor in which metal areas are measured. This should provide better correlations between catalyst activity and their characterization.

References

- (1) F. E. Massoth and W. H. Wiser, ERDA Contract No. E(49-18)-2006, Quarterly Progress Report, Salt Lake City, Utah, March 1976, p 24ff.
- (2) J. Burton, E. Hyman and D. Fedak, J. Catal., 37, 106 (1975).
- (3) A. F. Trotman-Dickenson, Ed., "Comprehensive Inorganic Chemistry," Pergamon Press, 1973, p 1071.

Table 1

Properties of Co-Cu Catalysts

Catalyst/Remarks	Composition (a)		CO Conversion % (b)	O ₂ Adsorption mg/g (c)	Oxidn. Weight Change mg/g (c)	Metal Dispersion (d)	Metal Reduc. % (e)
	Co wt %	Cu wt %					
Co A	6.1	7.4	66	6.3	30.2	.21	117
Co AB	5.1	7.4	36	5.6	30.2	.18	128
Co B	4.1	7.4	24	1.7	26.2	.06	127
10 no Na	6.1	7.4	10	1.6	24.6	.06	95
11 no Na, pH7	6.1	7.4	6	3.0	22.0	.14	85
12 } Practical	6.1	3.0	9	2.7	16.7	.16	86
13 } Grade	6.1	12.0	8	6.7	43.3	.15	132
14 } Co(NO ₃) ₂	6.1	0.5	35	4.3	14.7	.29	97
15 } Used	15.0	7.0	72	21.8	52.0	.42	117
16 }	6.1	7.4	29	7.2	32.0	.22	132

(a) Nominal values from preparation based on metals and Al₂O₃.

(b) Reactor conditions: 275°C, 2 H₂/CO, 750 psi, 0.77 cc/g.s

(c) Based on oven-dried charge.

(d) Based on ten adsorbed per surface metal atom and redox weight change at 450°C, both on oven-dried charge basis.

(e) Based on oxidation weight changes per g of reduced catalyst and nominal compositions assuming oxide states of CuO and Co₃O₄.

Symbols:

○ - Reagent grade

● - practical grade

△ - No Na

□ - No Na, pH = 7

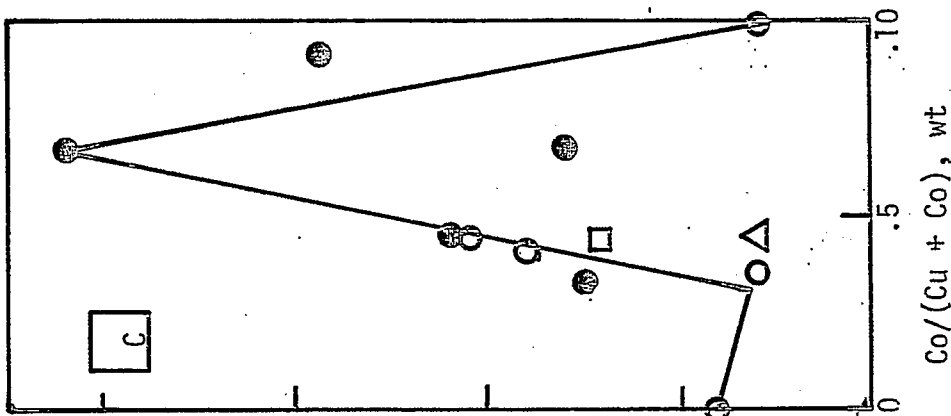
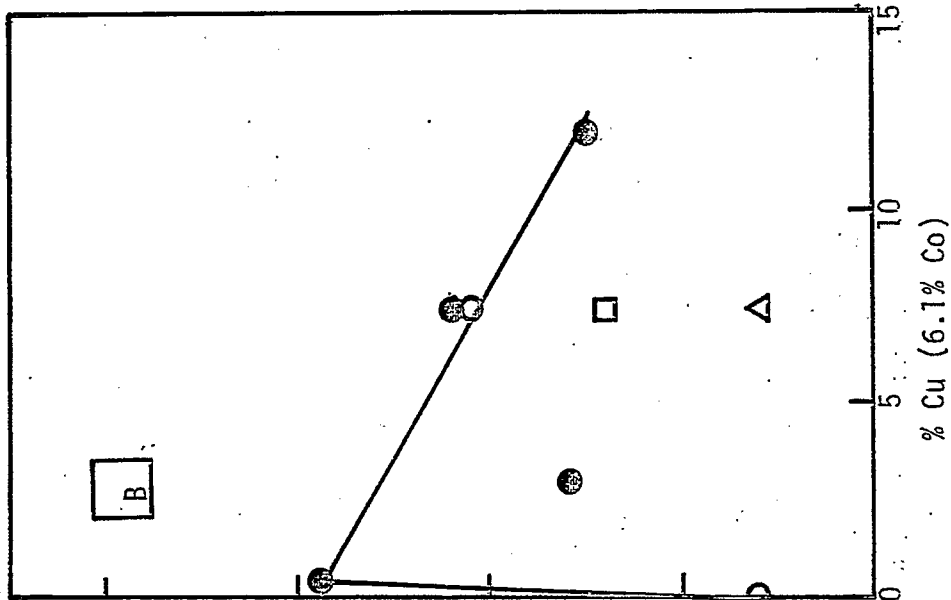
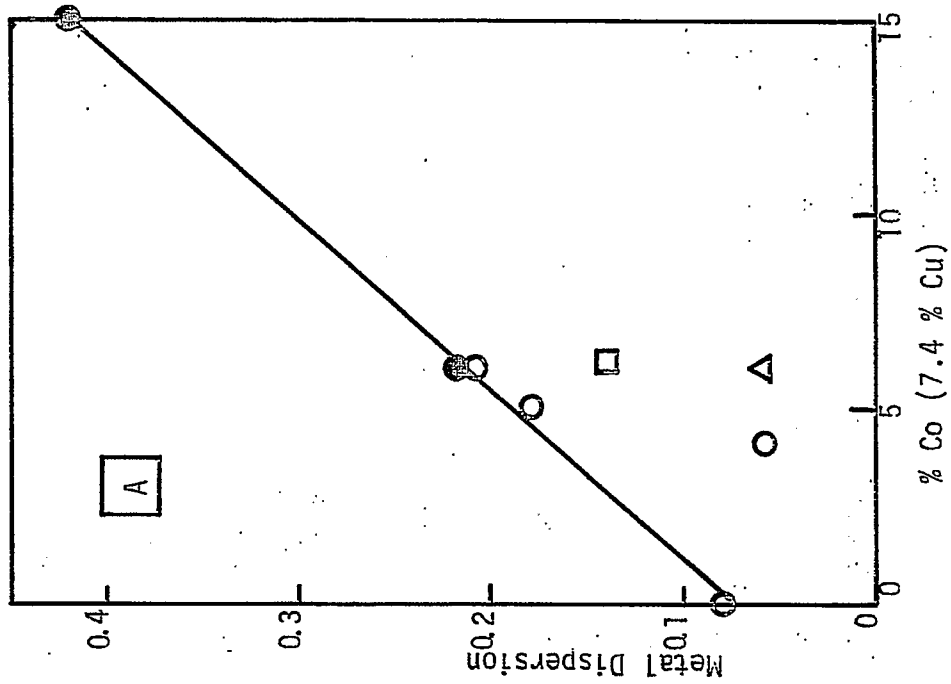
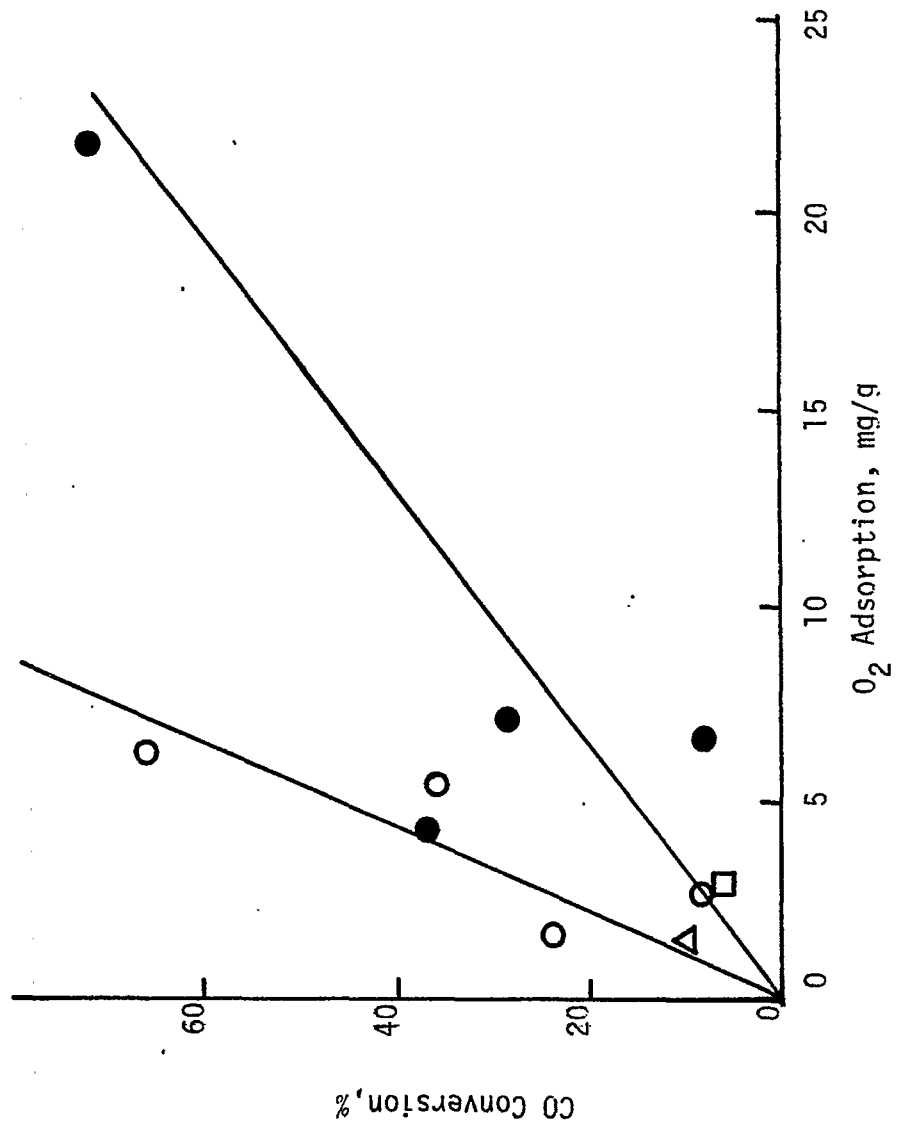


Figure 1. Effect of Co and Cu on Metal Dispersions

Figure 2. CO Conversion vs O₂ Adsorption

Symbols: Same as Figure 1.



Project A-9

Development of an Inexpensive Recycle Pump

Inactive at present

Project B-1

Development of Optimum Catalysts and Supports

I. Development of Technique

Faculty Advisor: F.E. Massoth
Graduate Student: M. Moora

Introduction

This project is concerned with diffusional resistances within amorphous cracking catalysts. Of primary concern is the question of whether the larger multi-ringed aromatics found in coal-derived liquids will have adequate accessibility to the active sites of typical hydrocracking catalysts. When molecular dimensions approach pore size diameters the effectiveness of a particular support is reduced owing to significant mass transfer resistance. A window effect, also known as configuration resistance, may even result when large diameter molecules are transported to smaller micropores of the catalyst.

Conceptually the diffusion of model aromatic compounds is carried out using a stirred batch reactor. The preferential uptake of the aromatics from an aliphatic solvent is measured using a U. V. spectrometer. Though the adsorbate molecules utilized thus far do not approach catalyst pore diameters, a substantial amount of necessary ground work is needed before more advanced studies involving larger molecules can be attempted.

Project Status

Current studies with different solvents produced some unexpected results, heretofore unmentioned in adsorption literature. When the solvent was varied from cyclohexane, n-heptane or cyclopentane, a change in equilibrium adsorption capacity as well as the kinetics of adsorption was noted. Table 1 summarized the uptake of chrysene from the three solvents. A $\gamma\text{-Al}_2\text{O}_3$ of 18 x 24 mesh size was used and the

initial adsorbate to catalyst ratio was the same. Two repeat runs were made. Although the duplicate runs show some variation, the uptake of chrysene in cyclohexane is clearly lower than in the other two solvents. The reason for this is not known at present.

In addition to adsorption capacities, some differences in fractional rates of adsorption were also noted. These were analyzed assuming simple Fickian diffusion in a sphere. A parameter D/a^2 can be obtained from the experimental data. Furthermore, the bulk diffusivity of a binary liquid can be used to calculate an effective diffusivity when considering a Wheeler type parallel pore model (provision is made for the void fraction and tortuosity of the internal surface).¹ Table 1 compares the values for the different solvents, where:

$$D/a^2 = \text{parameter calculated from initial slope of } \alpha \text{ vs. } (t)^{1/2}$$

where: α = fractional approach to equilibrium
 D = diffusion coefficient
 a = characteristic radius

$$D_{\text{eff}} = \frac{\theta D_B}{\tau}$$

where: θ = void fraction of catalyst
 τ = tortuosity of catalyst
 D_B = bulk diffusivity of solvent/solute combination
 r_p = particle radius

As calculated from the initial rate of uptake, D/a^2 is an order of magnitude lower than the estimated parameter D_{eff}/r_p^2 . Hence, the observed rate does not appear to be governed by bulk diffusion.

The role of the solvent in determining the equilibrium adsorption capacity is currently being investigated. Batch adsorption isotherms using several solvents and catalysts are underway and should provide some valuable information about this anomaly. In addition, since the catalyst/adsorbate ratios are close to those used in the stirred reactor, we hope to find exactly where on the isotherm the current kinetic tests are being run.

The effect of particle diameter was also studied during the last quarter. Figure 1 is a plot of fractional approach to equilibrium, α , versus time for particles of 30 x 60 mesh, 18 x 24 mesh and 14 x 18 mesh. The strong kinetic dependence on particle size clearly indicates an intraparticle diffusion resistance.

Iterative calculations were carried out to estimate effectiveness factors using the relations developed by Weisz and Hicks for spherical

particles.² By estimating the diffusivities for each radius from the slope of the fractional approach to equilibrium versus time curves, the values indicated in Table 2 were obtained. These values represent the approximate ratio of intraparticle diffusion rate to intrinsic adsorption rate, when adsorption is assumed to occur via a first order, irreversible reaction. The lack of agreement between the two sets of calculations indicate that a simple effectiveness factor approach is not sufficient to explain the results.

Another approach to explain the particle size effect involves a kinetic model of the contracting sphere type, as developed by Yagi and Kunii.³ Preliminary curve fitting to linearized versions of the "shrinking core" model produced good fits to 40-50% of the fractional uptake. For ease of calculation it was assumed that bulk adsorbate concentration remained constant during adsorption. This is, of course, unrealistic and the use of the more complicated relations expressing bulk concentration as a function of conversion (uptake) should provide a better fit.

Earlier plans called for the fabrication of a basket-impeller or Carberry-type reactor for use during this quarter. Delays in delivery of the glass vessel have prevented such work. The purpose of such a reactor is to promote better film transfer between the catalyst surface and bulk liquid. The existing reactor was, however, evaluated for the mixing effectiveness in an attempt to estimate the magnitude of such resistance with regard to the rate data already obtained.

Figure 2 represents the bulk concentration change versus time plot when mixer rpm was varied between 0 and 530 rpm (maximum). A clear change in the slope was observed when the rpm was increased from 0 to 210, but nearly indistinguishable changes occurred when further increases were made. For this particle size, 18 x 24 mesh, it may be concluded that bulk transfer resistance appears to be negligible at rpm's greater than 300-350. However, for smaller particles, mixing may be more ineffective and the use of a Carberry reactor should prove beneficial.

Future Work

Mathematical modeling will be continued in an attempt to elucidate a controlling mechanism. Primary emphasis will be placed on the contracting sphere approach since a satisfactory fit was obtained for a portion of the approach to equilibrium. Other models to be considered will include surface diffusion, Crank's solution to Fick's 2nd law for various geometries and series models involving possible combinations of mass transfer resistance in the film, macropores and micropores.⁴

Batch isotherm tests will also be continued during the next quarter. By utilizing various solvent-adsorbate-catalyst combinations the

magnitude of the solvent effect, as well as the shape of the adsorption isotherms will be determined.

Kinetic testing will continue as soon as the necessary reactor vessel is received. It is hoped that a better understanding of the adsorption and counter diffusion processes will be obtained through the use of this system.

Literature Cited

1. A. Wheller, in P. H. Emmett (ed.) "Catalysis," Vol. III, Reinhold Publ. Corp., 1955, Chapter 2.
2. P. B. Weisz and J. S. Hicks, Chem. Eng. Sci., 17, 265 (1962).
3. S. Yage and D. Kunii, Chem. Eng. Sci., 16, 364 (1961).
4. J. Crank, "The Mathematics of Diffusion," Clarendon Press, 1975.

Table 1

Effect of Solvent on Capacity and Rate of Uptake of Chrysene

Catalyst: $\gamma\text{-Al}_2\text{O}_3$, 18 x 24 mesh

Solvent	Adsorption (mmol/g)	$\frac{D_2/a^2}{(\text{cm}^2/\text{sec} \times 10^5)}$	$\frac{D_{\text{eff}}/r_p^2}{D/a^2}$
n-heptane	.017 .021 <u>.019</u>	3.15 3.72 <u>3.4</u>	61 52 <u>57</u>
cyclohexane	.013 .009 <u>.011</u>	2.46 4.15 <u>3.3</u>	32 19 <u>26</u>
cyclopentane	.022	4.15	36

Table 2

Effectiveness Factor Calculations

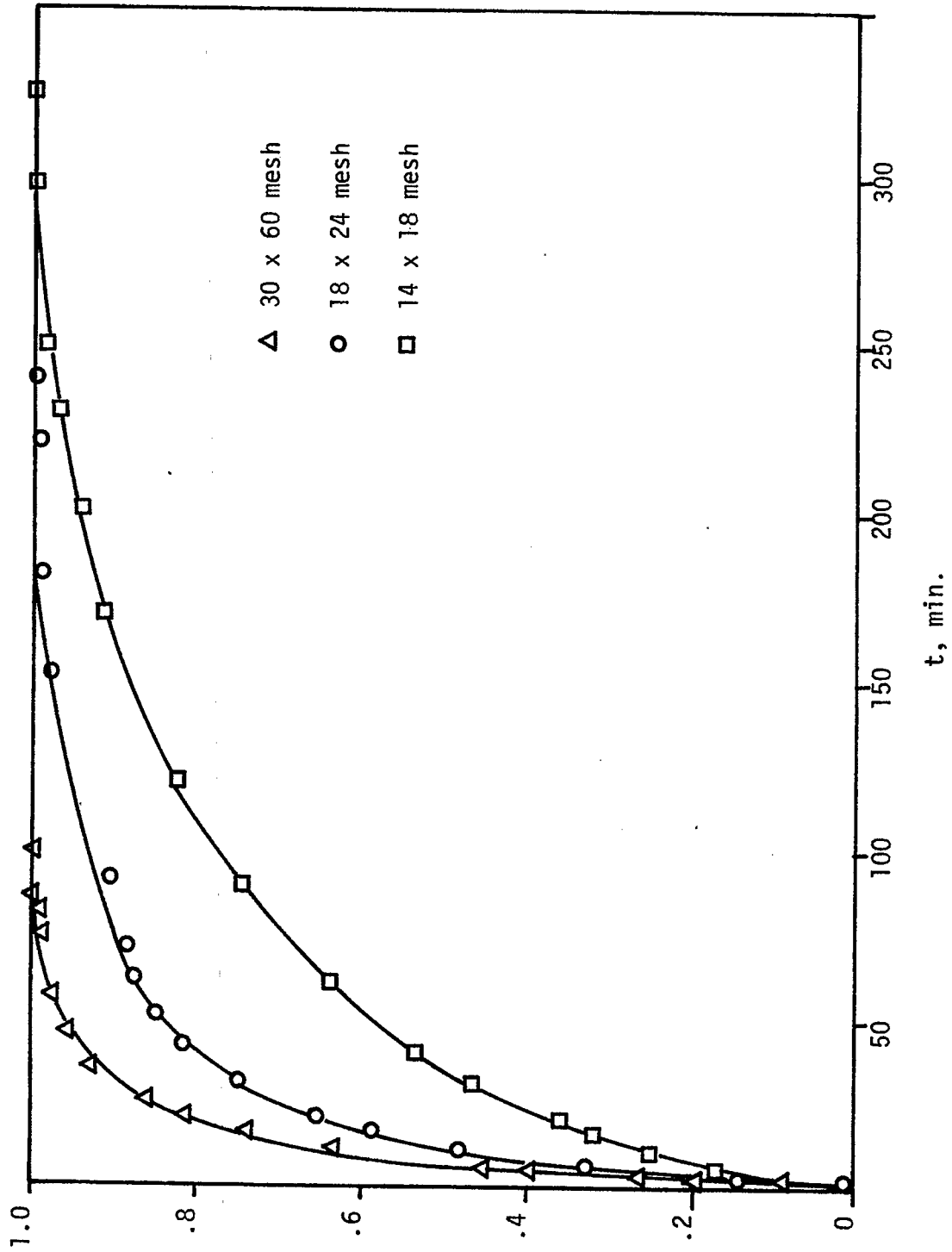
Adsorbate: Chrysene

Catalyst: $\gamma\text{-Al}_2\text{O}_3$

Set	Particle Size	Effectiveness Factor
1	30 x 60 mesh	.691
	18 x 24 mesh	.396
2	30 x 60 mesh	.355
	14 x 18 mesh	.103

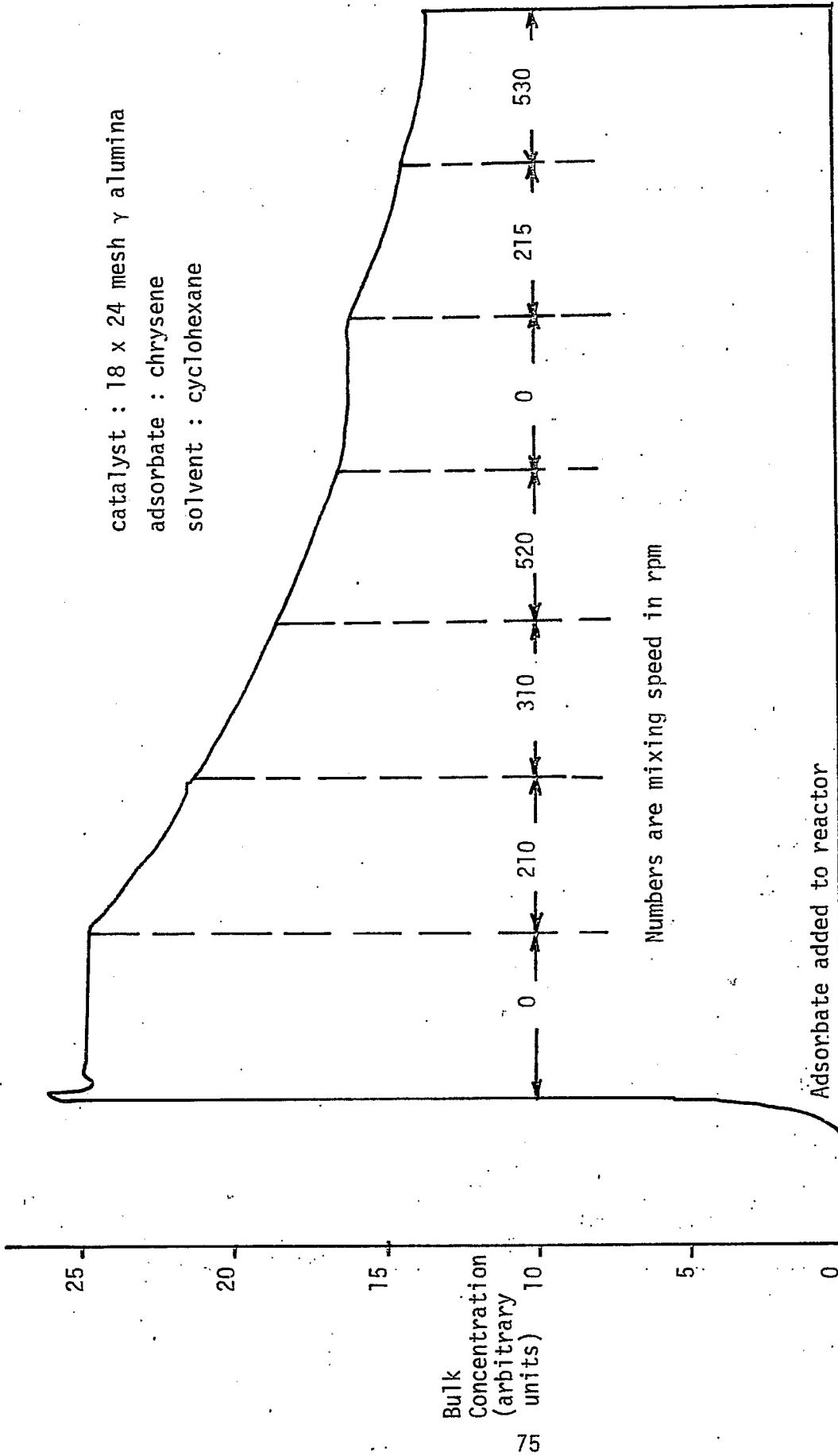
Figure 1

Fractional Approach to Equilibrium vs. Time for 3 Particle Sizes



Effect of Mixing Speed on Adsorption Kinetics

catalyst : 18 x 24 mesh γ alumina
adsorbate : chrysene
solvent : cyclohexane



Time (arbitrary units)

Project B-1

Development of Optimum Catalysts and Supports

II. Application to Large Molecules

Faculty Advisor: F. E. Massoth
Student: C. S. Kim

Introduction

Since coal liquids may contain rather large molecules, this phase of project B-1 extends the research to larger molecules. The primary emphasis of this study is to assess the diffusional characteristics of macromolecules in realistic catalyst supports. Findings from previous work will be compared to the present results to determine if simple extension of principles derived therefrom will apply to the larger molecules. Similar experimental techniques as developed in the first phase are employed here, though experiments may have to be run at higher temperatures to achieve adequate solubility and diffusional rates.

Project Status

This study aims to use a homologous series of hydrocarbon macromolecules as model compounds of coal-derived liquids. However, only a few homologue series of compounds appeared as reasonable candidates after reviewing their physical and chemical properties, availability and detectability by analytical instruments.

As one of the possibilities, a series of polycyclic ethers (crown ethers, molecular size ranging from 10 to 30 Å) have been reviewed. Discussion with Drs. Bradshaw and Izatt of Brigham Young University at Provo, Utah revealed that these polycyclic compounds actually change their molecular size in the presence of solvent, thus making it difficult to estimate exact molecular size.^{1,2} We will check further the possibility of estimating molecular dimensions of these materials.

A series of multiring aromatic compounds is being considered. The largest commercially available are still not as large as desired, but will suffice for the time being. The structures of four of the largest found with their approximate critical dimensions are shown in Figure 1. Several of the intermediate sized compounds between those above and chrysene will be added to obtain a series of compounds of varying molecular size. These will be tested with several commercial aluminas having average pore diameters ranging from 50 to 150 Å. Catalyst supports having smaller dimensions are being sought.

Although most commercial catalysts have rather large average pore diameters compared to the model compounds now available, complete utilization of their internal structure may nevertheless be restricted. This could be caused by two factors. First, the commercial catalysts generally have a wide range of pore sizes. Thus, an appreciable fraction of their internal surface (catalytically active sites) could be in rather narrow pores, thereby excluding entry of some macromolecules. This is equivalent to the configurational regime discussed by Weisz for zeolite catalysts.³ Second, when catalyst pore size are several fold larger than molecular size, an effective resistance to diffusion may be expected. This is due to the increased frictional drag on the molecule in close proximity to the pore walls.⁴ The first effect can be assessed by adsorption capacity experiments whereas the second effect can be determined by adsorption rate experiments. Because of the complexity of the systems involved, experiments will be made with as large a range of molecular sizes and catalyst pore sizes as possible. Ultimately, we wish to define a relationship between molecular size and pore size that will allow us to predict how diffusional resistance will restrict catalyst utilization.

Future Work

Characterization of catalyst supports will be started with the alumina on hand. This will involve a complete nitrogen adsorption-desorption isotherm to determine pore size distribution as well as surface area and pore volume. As other catalyst supports become available, they will be similarly characterized.

When the pure compounds which have been ordered arrive, they will be tested for solubility in various solvents. Also, their U.V. spectra will be run to determine suitable ranges for analysis.

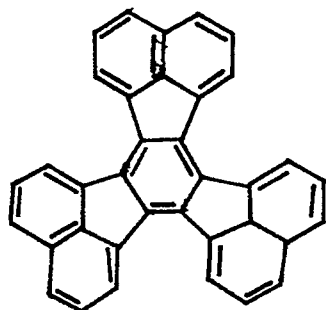
From the above tests, several combinations of molecules and support systems will be chosen for initial studies. These will take the form of adsorption capacity measurements and adsorption rate measurements.

References

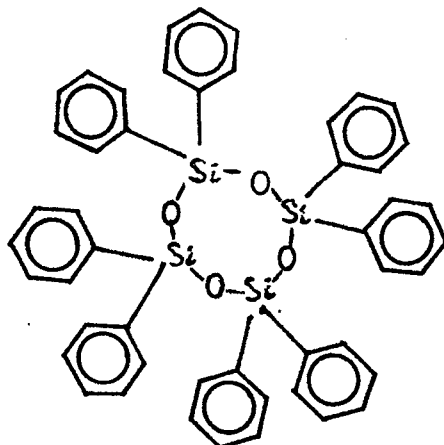
1. J. J. Christensen, J. O. Hill, and R. M. Izatt, Science, 174 (4008), 459 (Oct. 1971).
2. J. J. Christensen, D. J. Eatough, and R. M. Izatt, Chem. Rev., 74, 351 (1974).
3. P. B. Weisz, Chem. Tech. (Berlin), 498 (1973).
4. C. K. Colton, C. N. Satterfield and C. Lai, AIChE J, 21 289 (1975).

Figure 1

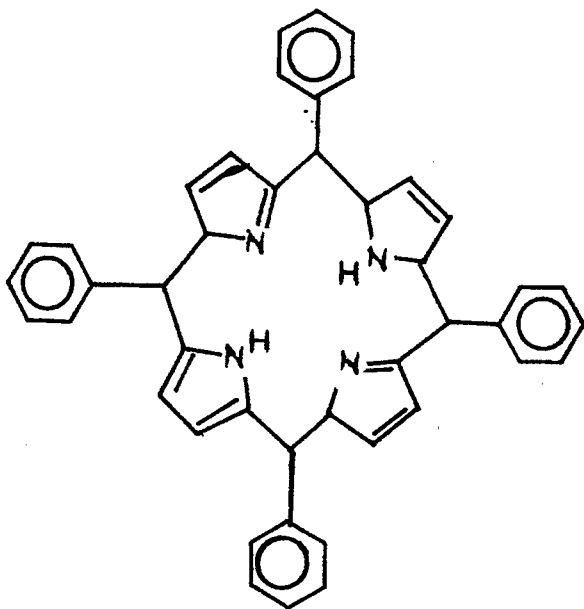
Aromatic Structures and Approximate Critical
Molecular Diameters



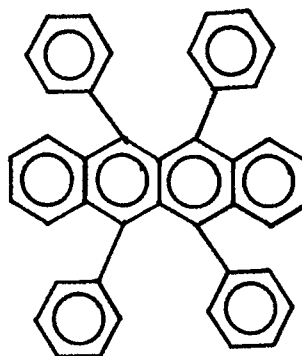
Decacyclene
(14 Å)



Octophenylcyclotetrasiloxane
(16 Å)



Meso-Tetraphenylporphine
(20 Å)



Rubrene
(13 Å)

Project B-2 (alternate)

Effects of Coke and Poisons upon the Desulfurization Activity of Cobalt Molybdate Catalysts

Faculty Advisor: F. E. Massoth
Postdoctoral Fellow: S. W. Cowley

Introduction

The importance of cobalt molybdena catalysts for hydrotreating and hydrodesulfurization of petroleum feed stocks is well known. These catalysts are also being studied in the hydrodesulfurization and liquifaction of coal slurries and coal-derived liquids. However, these complex feeds result in rapid catalyst deactivation. The aim of the current project is to gain insight into the deactivation mechanism. The approach involves detailed kinetic studies on the model compound benzo-thiophene, assessing the effects of poisons and coke precursors on the kinetics of the reaction. The studies are carried out in a stirred microbalance reactor, which allows simultaneous measurements of catalyst weight change and activity.

Project Status

During this period several preliminary experiments were completed. A standard set of conditions was compared against a variety of other reaction conditions to evaluate changes in catalyst weight and benzo-thiophene conversion.

Experimental

The catalysts studied were γ -Al₂O₃, 8% Mo/ γ -Al₂O₃ and 1% Co-8% Mo/ γ -Al₂O₃. These were pretreated in the stirred microbalance reactor as follows:

- (1) The catalyst was heated to 415°C in nitrogen to remove excess water until a constant catalyst weight was obtained. (The Al₂O₃ was cooled to 360°C and then used without further pretreatment).
- (2) The catalyst was presulfided for two hours with a H₂S/H₂ mixture containing 8% hydrogen sulfide.
- (3) The catalyst was purged with nitrogen until a constant catalyst weight was obtained.

- (4) The reactor temperature was lowered to 360°C prior to the introduction of benzothiophene and hydrogen under the standard conditions. Flow through the reactor was maintained at 40 cc/min. Reactor details and run procedures were described in the last report.

The benzothiophene desulfurization products were analyzed via gas chromatography using a flame ionization detector. The column was 1/8" by 8' stainless steel, packed with 3% SE-30 on Gas Chrom Q. Ethylbenzene was the major product, with only small amounts of styrene, toluene and benzene also being produced. A product with a longer retention time than benzothiophene was also detected but not identified and could possibly be dihydrobenzothiophene.

Temperature Effects

The effects of temperature on benzothiophene desulfurization were studied over both Mo/Al₂O₃ and Co-Mo/Al₂O₃ catalysts. The results are given in Tables 1 and 2, respectively. Benzothiophene desulfurization over Mo/Al₂O₃ showed a moderate temperature dependence, i. e., desulfurization decreased with decreasing temperature. The difference in catalyst weight and conversion from the initial to final standard conditions indicates that some change in the catalyst had occurred during the series. This could be due to either coking or additional sulfiding of the catalyst.

In the case of the Co-Mo/Al₂O₃ catalyst, temperature had very little effect upon the catalyst activity and suggests that cobalt has appreciably lowered the activation energy for the reaction. It is interesting to note that there was no change in catalyst weight from the initial to final standard conditions; however, there was a slight decrease in conversion. It is apparent that the Co-Mo/Al₂O₃ catalyst does not undergo as much change as the Mo/Al₂O₃ catalyst during changes in reaction temperature.

It should be noted that substantial changes in catalyst weight occurred over the temperature ranges run with the two catalysts. These weight changes were predominantly reversible, indicating rather large changes in reversibly adsorbed species on the catalyst. The negative trend obtained with temperature would indicate a reversible adsorption equilibrium is occurring between the catalyst surface and the gas-phase compositions of benzothiophene and/or hydrogen sulfide.

Effects of H₂S, H₂ and Benzothiophene Partial Pressures

Changes in H₂, H₂S and benzothiophene partial pressures over the Mo/Al₂O₃ catalyst produced marked changes in the benzothiophene conversion and catalyst weight, as shown in Table 3. Increasing the benzothiophene partial pressure produced a decrease in conversion and suggests a reactant and/or product inhibition. Similar results were obtained by increasing the hydrogen sulfide partial pressure, indicating a substantial product inhibition by hydrogen sulfide. This is in line with the large

weight gains realized in the presence of added H_2S . These findings agree with results previously reported. 1,2,3

Decreasing the hydrogen partial pressure decreased the conversion, which indicates a direct dependence of the reaction upon hydrogen. The weight increase of the catalyst from initial to final states could either be due to catalyst sulfiding or coking.

Corrosion of the safety plug on the hydrogen sulfide cylinder produced a severe leak and the tank had to be vented. For this reason, it was not possible to repeat this series for the Co-Mo/ Al_2O_3 catalyst, and the remaining preliminary experiments were performed without the use of hydrogen sulfide.

The effect of hydrogen partial pressure on benzothiophene conversion over the Co-Mo/ Al_2O_3 catalyst was studied. The results are given in Table 4. Conversion greatly decreased with a corresponding decrease in hydrogen partial pressure. However, the conversion and catalyst weight remained unchanged from the initial to final standard runs. This suggests that catalyst sulfiding and not coking may have been responsible for the changes that occurred from the initial to final standard runs in the series with Mo/ Al_2O_3 (Table 3).

Effect of Ethylbenzene Partial Pressure

The partial pressure of ethylbenzene was increased to determine if the reaction was product inhibited. This was done by adding extra ethylbenzene to the feed by means of a separate bubbler in the H_2 feed line. The results are given in Table 5. The calculated conversion is based upon the absolute benzothiophene peak areas from the gas chromatograms. Ethylbenzene appears to have very little effect upon conversion. An exact value for conversion in run SC-13-20 was not possible because of the sampling technique used, and therefore, a range is given. There was no significant change in catalyst weight from the initial to final standard runs, and this suggests that ethylbenzene is reversibly adsorbed.

Coking Effects

As discussed previously (Table 4), no coking of the Co-Mo/ Al_2O_3 catalyst with benzothiophene was observed even at a hydrogen partial pressure of 0.11 atm. Only when hydrogen was completely replaced by nitrogen did coking occur. The results are given in Table 6. Coking under these conditions was not immediate; an induction period of about 60 minutes was required before coking commenced. The conversion dropped rapidly during this induction period but did not reach zero until coking began. It is apparent that adsorbed hydrogen remained on the surface of the catalyst and was titrated from the surface by its reaction with benzothiophene. This indicates that the coking process can then proceed only after the adsorbed hydrogen has been removed. The amount of benzothiophene converted during this induction period can be related to the amount of hydrogen that was adsorbed on the catalyst. Calculations based upon this information showed that about 0.9 atoms of hydrogen/molybdenum atom were present on the catalyst. This is in close agree-

ment with previously reported results for the hydrogen content of sulfided catalysts.⁴

Coking was allowed to proceed until 9 mg of coke was deposited on the catalyst. Assuming that a benzothiophene molecule occupies about 60 Å², then 9 mg of coke represents a surface area of about 70m²/g (assuming coke is a monolayer). This means that about 40% of the surface is covered with coke. It has been estimated that about 50% of the catalyst surface is covered with a monolayer of molybdena.⁴ The molybdenum monolayer is responsible for the catalyst activity, so the covering of a substantial fraction of this active surface should result in an appreciable drop in conversion. However, the conversion dropped only slightly. This is an indication that coke may not be monolayered but instead layered to form coke particles. Another possibility is that some coke may be formed on the exposed alumina surface. Therefore, the drop in conversion could be the direct result of coke occupying desulfurization sites or could be due to an indirect electronic effect of coke occupying adjacent, inactive desulfurization sites. In the first case, the adsorption constants for reactant and products would remain unchanged, although the number of active sites would decrease. In the latter case, a change in these constants should occur with the number of active sites being the same. The kinetic analysis of a carefully controlled experiment should distinguish between the two cases.

Weight profiles of the coke precursors used in this study over the pure γ -Al₂O₃ support alone and the Mo/Al₂O₃ catalyst are shown in Figure 1. It is interesting to note that benzothiophene coked over γ -Al₂O₃ in the presence of either hydrogen or nitrogen, and none of this coke was removed in a nitrogen purge. Ethylbenzene, however, did not coke over γ -Al₂O₃ in either hydrogen or nitrogen. Both benzothiophene and ethylbenzene coked over the Mo/Al₂O₃ catalyst in nitrogen, but did not coke in hydrogen. It appears necessary to have an olefinic substance such as benzothiophene or styrene to initiate coke formation. Ethylbenzene can dehydrogenate over the Mo/Al₂O₃ or Co-Mo/Al₂O₃ catalysts to form styrene, a likely coke precursor.^{5,6} The dehydrogenation of ethylbenzene to styrene does not occur over γ -Al₂O₃; therefore, no coking is observed. Both γ -Al₂O₃ and the molybdate catalyst have sites for the formation of coke. However, only the molybdate catalyst has a hydrogenation function that can prevent coke formation in the presence of a coke precursor.

Poisoning Effects

A drop in the benzothiophene conversion resulted from poisoning the Co-Mo/Al₂O₃ catalyst with pyridine. This was expected since pyridine is known to be a strong poison for the hydrodesulfurization reaction.^{7,8} The results are given in Table 7. The introduction of pyridine produced an immediate weight gain by the catalyst, followed by a gradual increase

to a constant weight of 3.3 mg. An increase in the pyridine partial pressure resulted in an additional weight gain of 0.9 mg for a total of 4.2 mg. A nitrogen purge of the system produced a gradual weight loss of only 1.3 mg. At this point, it appears that pyridine is reversibly adsorbed on some sites, but irreversibly adsorbed on others. When pyridine was passed over the catalyst in hydrogen, a weight gain of 4.1 mg was observed. This is close to the weight gained in nitrogen. A nitrogen purge of the system resulted in a weight loss of 1.9 mg. The increased weight loss may have resulted from additional reduction of the catalyst in the absence of H₂S, rather than loss of adsorbed pyridine.

Gas chromatographic analysis of the exit stream showed the formation of a new compound when pyridine was passed over the catalyst in nitrogen. This compound was absent when nitrogen was replaced by hydrogen. It is suspected that this new compound is a dimer of pyridine formed in the absence of hydrogen. It is possible that polymers of higher molecular weights are also being formed but remain on the catalyst. In other words, pyridine may also be a coke precursor as well as a selective poison. If this is the case, then some of the irreversibly adsorbed pyridine may be in the form of coke on the catalyst. Therefore, it is necessary that future poisoning studies be done in the presence of hydrogen. Furthermore, to prevent some reduction of the catalyst in hydrogen alone, poisoning studies must be done under steady-state reaction conditions.

Effects of Water

The results of Table 3 clearly show a strong inhibition of benzothiophene conversion in excess hydrogen sulfide. It was of interest to know if water produced a similar result. Water was introduced at increasing partial pressures during the steady-state desulfurization of benzothiophene. The results are given in Table 8. Benzothiophene conversion was only very slightly affected by the presence of water in the vapor inlet stream, although some catalyst weight gain was experienced. Water adsorption was completely reversible as evidenced by the return of the catalyst to its original weight and activity. Apparently, water neither readily competes for active sites nor incorporates itself into the catalyst structure under the reactor conditions employed in these runs.

Future Work

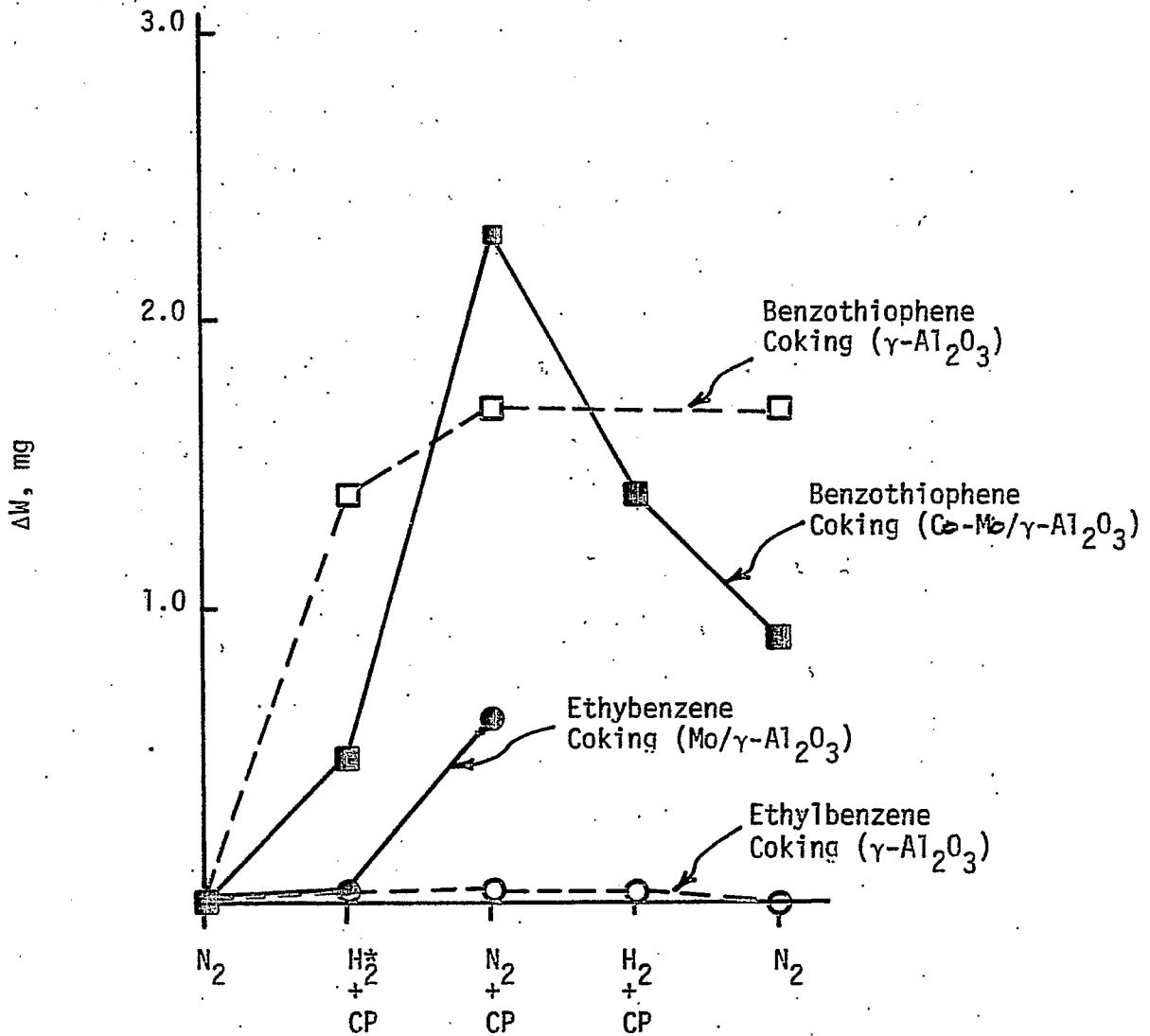
A new tank of hydrogen sulfide has arrived. Detailed kinetic studies can now be made to determine the general rate expression for the benzothiophene desulfurization reaction. Further analysis based upon this general rate expression will provide values for the adsorption constants of the reactants and products involved. The effect of coking and poisoning on these adsorption constants will then be studied. This will provide valuable information about the mechanisms involved in coking and poisoning of HDS catalysts.

References

1. P. J. Owens and C. H. Amberg, Adv. Chem. Ser., 33, 182 (1961).
2. C. N. Satterfield and G. W. Roberts, AIChE J., 14, 159 (1968).
3. O. Weisser and S. Landa, "Sulphide Catalysts, Their Properties and Applications," Pergamon, New York, 1973, p 228.
4. F. E. Massoth, J. Catal., 36, 164 (1975).
5. S. W. Cowley, Ph.D. Dissertation, Southern Illinois University, Carbondale, Illinois, 1975.
6. E. H. Lee, Catalysis Reviews, 8, 285 (1973).
7. P. Desikan and C. H. Amberg, Can. J. Chem., 42, 843 (1964).
8. C. N. Satterfield, M. Modell and J. F. Mayer, AIChE J. 21, 1100 (1975).

Figure 1

Coking Profile of Benzothiophene and Ethylbenzene



Conditions Used (CP = Coking Precursor)

*In the case of ethylbenzene a 50:50 mixture of H_2/N_2 was used over the $Mo/\gamma-Al_2O_3$ catalyst

TABLE 1 EFFECT OF TEMPERATURE ON BENZOTHIOPHENE DESULFURIZATION

Catalyst = 8% Mo/ γ -Al₂O₃; Catalyst wt = 315.9 mg; P_T⁰ = 0.0050 atm^a; P_H⁰ = 0.875 atm^a

Run	SC-12-22 ^b	SC-12-23	SC-12-24	SC-12-25	SC-12-26 ^b
Reactor Temp, °C	365.5	428.3	325.5	272.0	366.0
% Conversion	51.6	57.4	27.0	10.2	34.0
ΔW , mg ^c	+0.4	-0.3	+1.3	+3.1	+0.7

a Subscripts represent H-hydrogen, T-benzothiophene.

b Standard conditions.

c Relative to initial weight before run.

TABLE 2 EFFECT OF TEMPERATURE ON BENZOTHIOPHENE DESULFURIZATION

Catalyst = 1% Co-8% Mo/ γ -Al₂O₃; Catalyst wt = 336.2 mg; P_T⁰ = 0.0032 atm^a; P_H⁰ = 0.877 atm^a

Run	SC-13-14 ^b	SC-13-15	SC-13-16	SC-13-17 ^b
Reactor Temp, °C	365.8	315.7	407.0	364.2
% Conversion	71.5	67.1	68.4	67.8
ΔW , mg ^c	+0.4	+1.3	+0.1	+0.4

a Subscripts same as in Table 1.

b Standard Conditions.

c Relative to initial weight before run.

TABLE 3 EFFECTS OF H₂, H₂S AND BENZOTHIOPHENE PARTIAL PRESSURES ON BENZOTHIOPHENE DESULFURIZATION

Catalyst = 8% Mo/γ-Al₂O₃; Catalyst wt = 315.9 mg; Reactor Temp = 365°C

Run ^a	SC-12-10 ^b	SC-12-11	SC-12-12	SC-12-13	SC-12-14	SC-12-15	SC-12-16 ^b
P _T ^o , atm	0.0050	0.0025	0.0025	0.0025	0.0025	0.0025	0.0050
P _H ^o , atm	0.879	0.882	0.852	0.519	0.549	0.882	0.879
P _N ^o , atm	0	0	0	0.332	0.332	0	0
P _S ^o , atm	0	0	0.030	0.030	0	0	0
P _E , atm	0.0025	0.0014	0.0009	0.0004	0.0010	0.0014	0.0023
P _S , atm	0.0025	0.0014	0.0310	0.0300	0.0010	0.0014	0.0023
P _T , atm	0.0025	0.0011	0.0016	0.0021	0.0015	0.0011	0.0027
P _H , atm	0.872	0.878	0.849	0.522	0.523	0.878	0.872
% Conversion	50.4	56.5	35.0	14.7	41.2	56.4	45.2
r _T , cm ³ /min-g	0.361	0.202	0.125	0.053	0.148	0.202	0.324
ΔM, mg	+0.4	-0.1	+1.1	+1.4	+0.9	+0.7	+1.1

a Subscripts represent: E-ethylbenzene, H-hydrogen, N-nitrogen, S-hydrogen sulfide, T-benzothiophene,
 b standard conditions.

TABLE 4 EFFECT OF HYDROGEN PARTIAL PRESSURE ON BENZOTHIOPHENE
DESULFURIZATION

Catalyst = 1% Co-8% Mo/ γ -Al₂O₃; Catalyst wt = 336.2 mg; Reactor Temp = 363°C

Run ^a	SC-13-29 ^b	SC-13-30	SC-13-31	SC-13-32 ^b	SC-13-33
P _T ⁰ , atm	0.0032	0.0032	0.0032	0.0032	0
P _H ⁰ , atm	0.881	0.220	0.110	0.881	0
P _N ⁰ , atm	0	0.661	0.771	0	0.884
% Conv.	66.5	22.5	12.1	66.7	0
ΔW , mg	+0.5	+0.6	+0.7	+0.5	0

a Subscripts same as in Table 3.

b Standard conditions.

TABLE 5 EFFECT OF ETHYLBENZENE ON BENZOTHIOPHENE DESULFURIZATION

Catalyst = 8% Mo/ γ -Al₂O₃; Catalyst wt = 315.9 mg; Reactor Temp = 364°C

Run ^a	SC-12-19	SC-12-20	SC-12-21
P _T ⁰ , atm	0.0025	0.0025	0.0025
P _H ⁰ , atm	0.882	0.875	0.882
P _E ⁰ , atm	0	0.0068	0
% Conv	57.4	55-63 ^b	56.6
ΔW , mg	+0.2	+0.5	+0.3

a Subscripts same as in Table 3.

b Conversion based upon the absolute area of benzothiophene peak in gas chromatogram.

TABLE 6 EFFECT OF COKING ON BENZOTHIOPHENE DESULFURIZATION

Catalyst = 1% Co-8% Mo/ γ -Al₂O₃; Catalyst wt = 336.2 mg; Reactor Temp = 365°C

Run ^a	SC-13-6	SC-13-7	SC-13-8	SC-13-9
P _T ^O , atm	0.0032	0.0032	0.0032	0
P _H ^O , atm	0.881	0	0.881	0
P _N ^O , atm	0	0.881	0	0.884
% Conversion	61.5	----	54.4	----
ΔW , mg	+0.5	+2.3	+1.4	+0.9

a Subscripts same as in Table 3.

TABLE 7 EFFECT OF POISONING ON BENZOTHIOPHENE DESULFURIZATION

Catalyst = 1% Co-8% Mo/ γ -Al₂O₃; Catalyst wt = 336.2 mg; Reactor temp = 363°C

Run ^a	SC-13-20	SC-13-21	SC-13-22	SC-13-23	SC-13-24	SC-13-25	SC-13-26	SC-13-27
P _T ^O , atm	0.0032	0	0	0	0	0	0	0.0032
P _H ^O , atm	0.881	0	0	0	0	0.880	0	0.881
P _N ^O , atm	0	0.884	0.883	0.880	0.884	0.	0.884	0
P _P ^O , atm	0	0	0.0009	0.0037	0	0.0037	0	0
% Conversion	72.6	----	----	----	----	----	----	60.7
ΔW , mg	+0.4	0	+3.3	+4.2	+2.9	+4.1	+2.5	+2.8

a Subscripts represent: P-pyridine; all others same as in Table 3.

TABLE 8 EFFECT OF H₂O ON BENZOTHIOPHENE DESULFURIZATIONCatalyst = 1% Co-8% Mo/ γ -Al₂O₃; Catalyst wt = 343.7 mg; Reactor Temp = 361°C

Run ^a	SC-17-8	SC-17-9	SC-17-10	SC-17-11	SC-17-12
P _T ⁰ , atm	0.0032	0.0032	0.0032	0.0032	0.0032
P _H ⁰ , atm	0.881	0.868	0.861	0.817	0.881
P _W ⁰ , atm	0	0.013	0.022	0.064	0
% Conversion	65.5	65.0	64.8	62.4	65.3
ΔW , mg	+0.7	+0.9	+1.0	+1.1	+0.7

a Subscripts represent: W-water; all others same as in Table 3.

Fundamental Studies on Hydrogen Transfer

Faculty Advisor: F. E. Massoth
Student: D. S. Moulton

Introduction

A viable process for producing coal liquids involves a high-temperature hydrogenation of coal impregnated by zinc chloride or similar substances. In this process, the zinc chloride acts as a catalyst but its role in the reaction is not fully understood. An important factor may be its hydrogen transfer characteristics. The object of this project is to determine the hydrogen transfer mechanism of the zinc chloride impregnated on coal in terms of the hydrogen transfer characteristics of various types of catalysts.

Hydrogen-deuterium exchange reactions are used to determine the mode of hydrogen transfer. Model reactions characteristic of exchange over different types of catalysts are studied in order to establish the catalytic function responsible for exchange on the zinc chloride. Reaction studies are carried out in a glass vacuum system using gas-phase reactions. The reactant gases are circulated around a closed loop, through the catalyst bed. Degree of exchange is determined by continuous analysis of the gas phase using a mass spectrometer.

Project Status

A modification of the glass vacuum system was made to facilitate direct sampling of the gas phase without ordinary sample transfer. A small auxiliary loop was placed in the system with provision for installing a capillary tube leading to the mass spectrometer. When the circulation gases are diverted through the auxiliary loop, they are swept past the capillary opening. With this arrangement, the direct sampling is representative of the gas stream.

The quadrupole mass spectrometer has been assembled. A heavy duty cart was constructed and wired the necessary electric components and accessories. Vacuum pumps, valves, switches, the analyzer and the control unit were all mounted directly on the cart. There is space for a recorder and there are provisions for adding an ionization gauge and controller. The entire unit is mobile and the inlet can interface with other laboratory systems.

Initial start up of the mass spectrometer is going smoothly. The system is capable of maintaining a vacuum of 5×10^{-7} torr, which is sufficient for operation. Degassing is continuing. Some preliminary observations of light gases indicate that the unit is operating properly.

Deuterated isobutane is to be prepared here. Undeuterated isobutane was prepared to gain familiarity with the method. Analysis of the product by gas chromatography indicated that it was about 96% pure. The impurities are solvent vapors which should be removable with distillation cycles.

Future Work

After tests to determine response time and other equipment factors, some preliminary runs will be made. Several catalysts of known acid type will be used. Deuterium gas will be used to deuterate the catalyst surface. After deuteration, isobutane will be passed over the catalyst and the extent of deuterium exchange will be followed with the mass spectrometer. Results from catalysts possessing Bronstead acidity only, Bronstead and Lewis acidity, Lewis acidity only and metal sites only will be compared.

Later on, similar tests will be made with zinc chloride and zinc chloride impregnated on coal. Isopentane or 3-methylpentane will be used with isobutane containing deuterium to study exchange between hydrocarbons.

Project B-4

Mechanism of Catalytic Hydrogenation by Metal Halide Catalysts Chemical Structure of Heavy Oils Derived by Coal Hydrogenation

Faculty Advisor: D. M. Bodily
Postdoctoral Fellow: S. Yokoyama

Introduction

The hydrogenation of coal using $ZnCl_2$ catalyst and the separation of the heavy oil into various fractions have been reported.^{1,2} Structural analyses of the hexane-soluble and the benzene-soluble/hexane-insoluble neutral oil fractions were performed, based on proton nuclear magnetic resonance (NMR) and elemental analysis.² A change in the concentration of $ZnCl_2$ catalyst affects the yield of various fractions, but does not affect the structure of the components of each fraction. The aromatic oil, asphaltene, and saturate fractions were separated by gel permeation chromatography (GPC). Carbon-13 NMR spectra were then obtained on these subfractions. The results for the saturate fraction have been reported.³

Carbon-13 NMR spectrometry has been applied for the determination of the structure of coal and petroleum products by several investigators.⁴⁻⁸ This technique is somewhat limited. It is difficult to obtain quantitative spectra because of the Nuclear-Overhauser effect and spin-lattice relaxation times. It is also difficult to assign absorption to the various types of carbons.

Project Status

Experimental

Carbon-13 NMR spectra for the aromatic oil and asphaltene subfractions are shown in Figures 1 and 2. Proton decoupling was employed. Spectra were measured on a pulse Fourier-transform spectrometer (Varian Associates XL-100 FTNMR), at a frequency of 25.16 MHz and a pulse interval of 0.4-0.8 seconds.

Carbon-13 Nuclear Magnetic Resonance

Absorption by aromatic carbons (100-160 ppm, TMS standard) and by aliphatic carbons (0-50 ppm) were integrated and used to estimate the carbon aromaticity, f_a . The results are shown in Figure 3 with respect to GPC elution volume and are compared with the results obtained previously by proton NMR. The ^{13}C NMR results are consistently lower. This could be due to the long relaxation times of carbons not bonded to a proton. This would reduce the intensities of bridgehead and alkyl substituted aromatic carbons. At the same time the intensity

of aliphatic carbons would be enhanced by the Nuclear-Overhauser effect. The value of f_a calculated from the ^1H NMR is based upon the assumption of a H/C ratio of 2 in the aliphatic portion of the molecule. This assumption could also account for part of the difference.

Bartle et al. have assigned adsorption in the aromatic region downfield from 129 ppm to internal and substituted aromatic carbons.⁵ Adsorption upfield has been assigned to aromatic carbons bonded to hydrogen, $\text{C}_{\text{ar-H}}$. This division was used to calculate the ratio of $\text{C}_{\text{ar-H}}$ to total carbon. The value of $\text{C}_{\text{ar-H}}$ should be equal to the hydrogens bonded to aromatic carbons, H_{ar} . A plot of $\text{C}_{\text{ar-H}}/\text{C}$ from ^{13}C NMR versus $\text{H}_{\text{ar}}/\text{C}$ obtained from ^1H NMR and elemental analysis for the subfractions is shown in Figure 4. The larger molecular weight fractions show good agreement, but the smaller molecular weight fractions eluted at longer times show substantial deviation from the expected results.

Figure 5 shows a plot of aliphatic carbons, C_{al} , and hydrogens bonded to aliphatic carbons, H_{al} (dotted line). Lines of constant $\text{H}_{\text{al}}/\text{C}_{\text{al}} = Z$ are also shown. The solid line represents the results from structural analysis using ^1H NMR. The values 1.5-2.0 indicate a predominance of naphthenic structures attached to aromatic ring systems.

Figures 3, 4 and 5 indicate that the ^{13}C NMR spectra are not quantitative and that the intensities of quaternary carbons, especially internal and substituted aromatic carbons, are low.

On the basis of the assignments of Bartle et al., the portion of the spectra due to aliphatic carbons was divided into carbons α to aromatic rings, C_α , and carbons β or further from aromatic rings, C_0 .⁵ The corresponding hydrogen, H_α and H_0 , were obtained from ^1H NMR spectra. These results are plotted in Figure 6 for the aromatic oil fraction. Although the ^{13}C spectra are expected to be quantitative in the aliphatic region, there may be overlap of the chemical shifts of C_α and C_0 carbons.

Because of the problems mentioned above, a good value of $\text{C}_{\text{al}}/\text{C}$ can not be obtained directly. Using the assignments previously noted, $\text{C}_{\text{al}}/\text{C}_{\text{ar-H}}$ was determined from ^{13}C NMR and $\text{C}_{\text{al}}/\text{C}$ was calculated from the following equation:

$$\frac{\text{C}_{\text{al}}}{\text{C}} = \frac{\text{H}_{\text{ar}}}{\text{H}} \cdot \frac{\text{C}_{\text{al}}}{\text{C}_{\text{ar-H}}} \cdot \frac{\text{H}}{\text{C}}$$

Values of f_a calculated by this equation are shown in Figure 7 and are compared with the results from ^1H NMR and elemental analyses. The values were then used to calculate $\text{H}_{\text{al}}/\text{C}_{\text{al}}$ and the structural parameters, $\text{H}_{\text{au}}/\text{C}_{\text{ar}}^*$ and σ^{**} . The values of $\text{H}_{\text{au}}/\text{C}_{\text{ar}}$ and σ are also shown in Figure 7 with numbers obtained from ^1H NMR, assuming $\text{H}_{\text{al}}/\text{C}_{\text{al}}$ equals 2. The combination of ^1H NMR, ^{13}C NMR and elemental analyses gives reasonable results. Further refinement will require clarification of the ^{13}C NMR spectra in the aromatic region.

The aromatic oil fraction is being separated into one, two and three to four ring fractions to provide more homogeneous samples.

- * H/C ratio in the hypothetical unsubstituted aromatic ring system.
- ** Degree of substitution.

References

1. W.H. Wiser et al., ERDA FE2006-1, Quarterly Progress Report, Salt Lake City, Utah, July-Aug 1975, p 22.
2. W.H. Wiser et al., ERDA FE2006-2, Quarterly Progress Report, Salt Lake City, Utah, Sept-Dec 1975, p 37.
3. W.H. Wiser et al., ERDA FE2006-3, Quarterly Progress Report, Salt Lake City, Utah, Jan-June 1976, p 52.
4. H.L. Retcofsky and R.A. Friedel, "Spectrometry of Fuels," Plenum Press, New York, N.Y., 1970, p 90.
5. K.D. Bartle, T.G. Martin and D.F. Williams, Chem. Ind. (London), 313 (1975).
6. Y. Maekawa, T. Yoshida and T. Imanari, J. Fuel Soc. (Japan), 54 (12), 21 (1975).
7. S.A. Knight, Chem. Ind. (London), 1920 (1967).
8. D.R. Clutter, L. Petrakis, R.L. Stenger, Jr., and R.K. Jensen, Anal. Chem., 44, 1395 (1972).

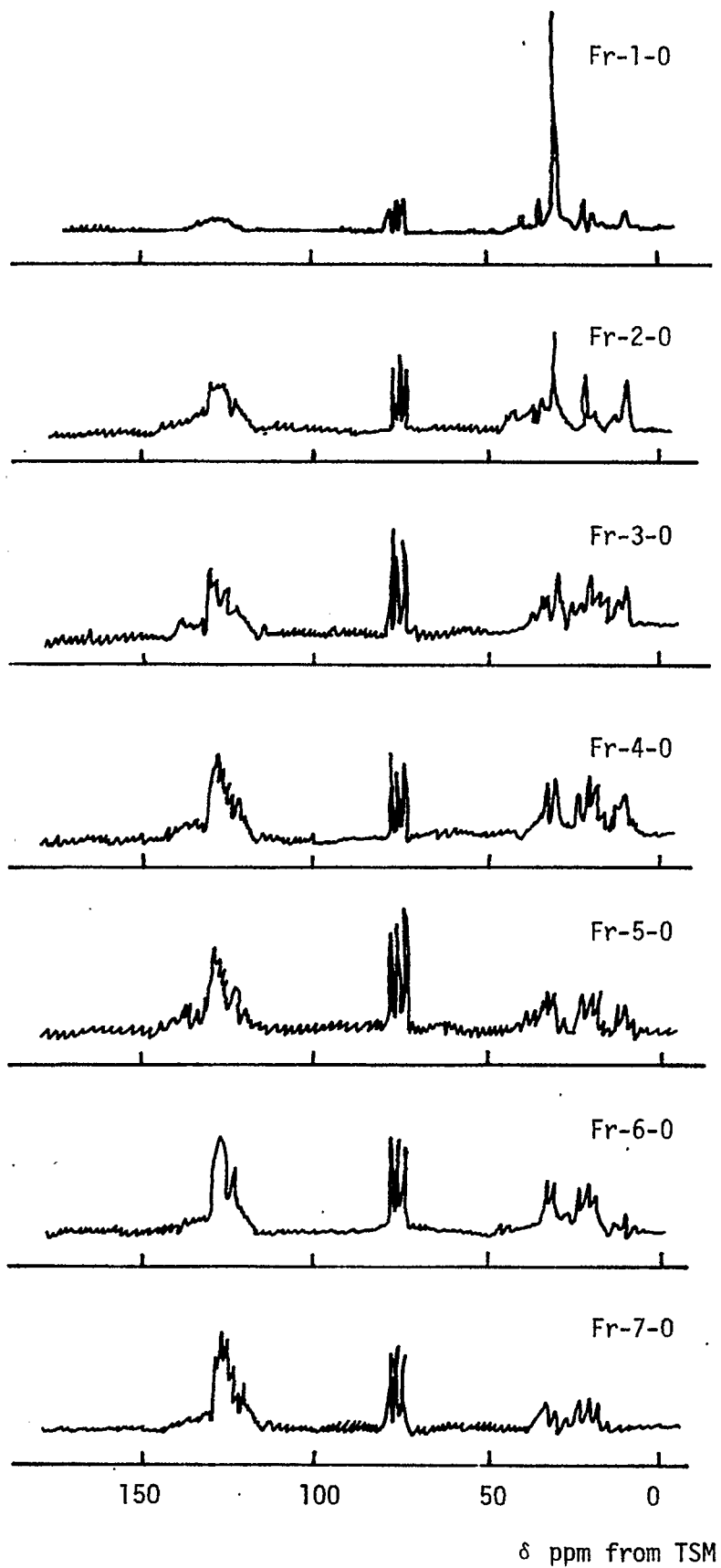
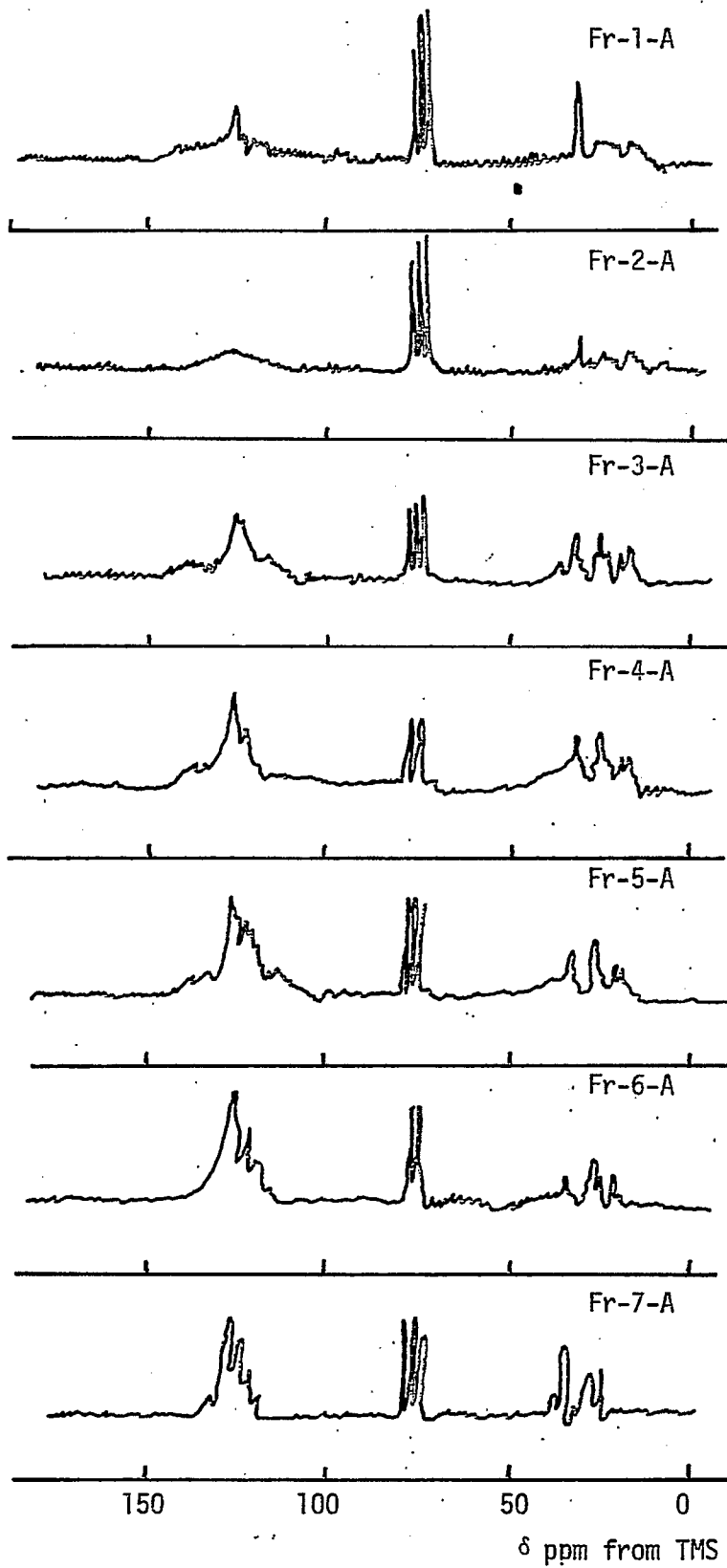


Figure 1
C-13 NMR Spectra for Oil Fractions

Figure 2



C-13 NMR Spectra for Asphaltene Fractions

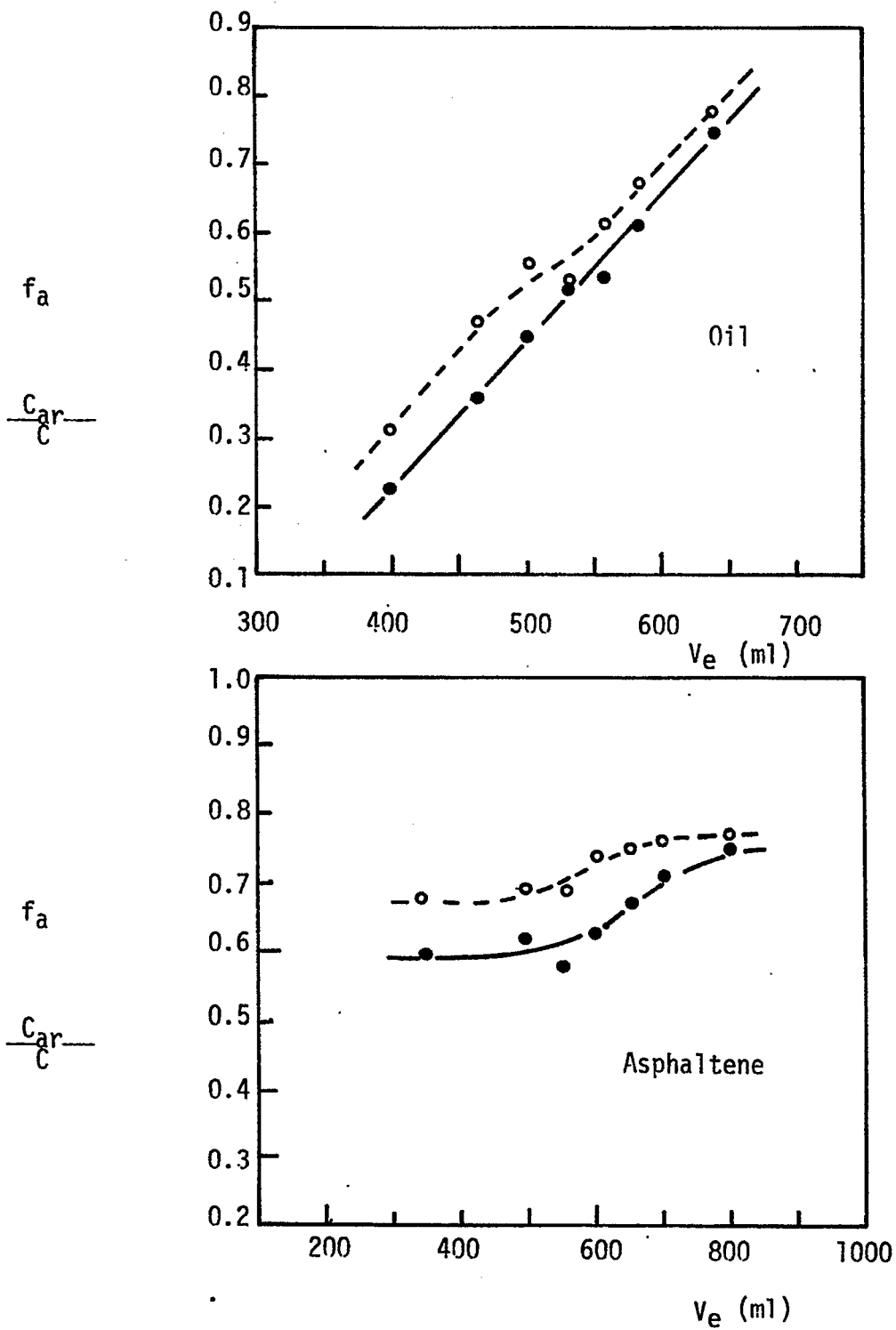


Figure 3

f_a From ^{13}C -NMR (solid line) and From ^1H -NMR (dashed line)

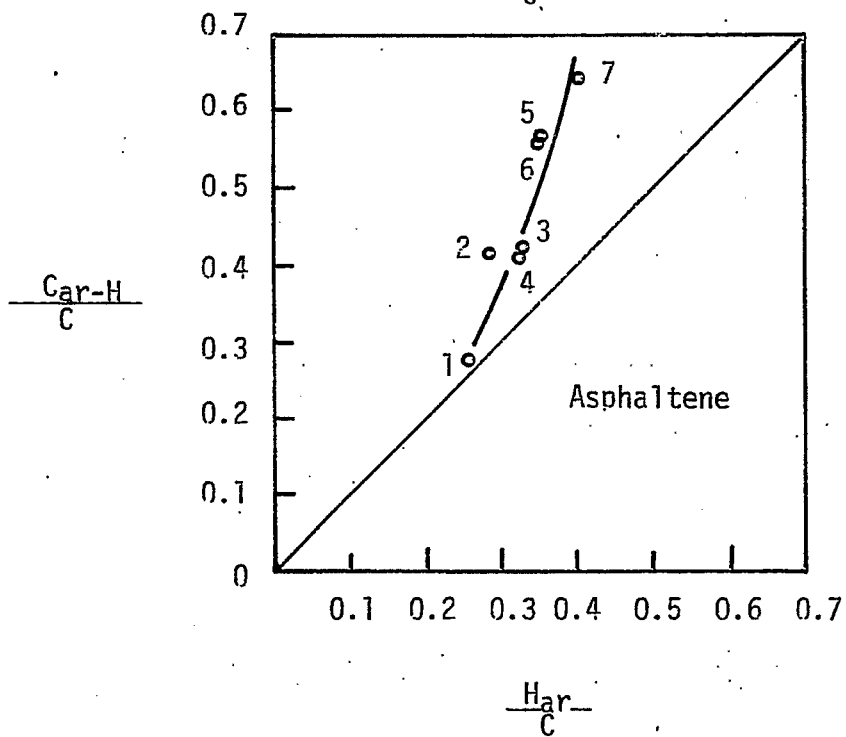
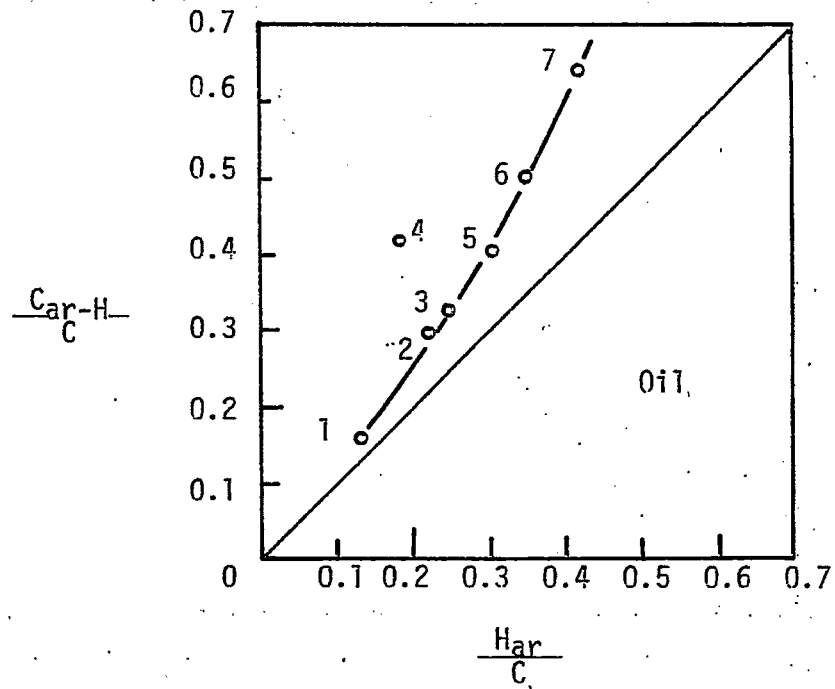


Figure 4

Relationship Between $\frac{C_{ar-H}}{C}$ and $\frac{H_{ar}}{C}$

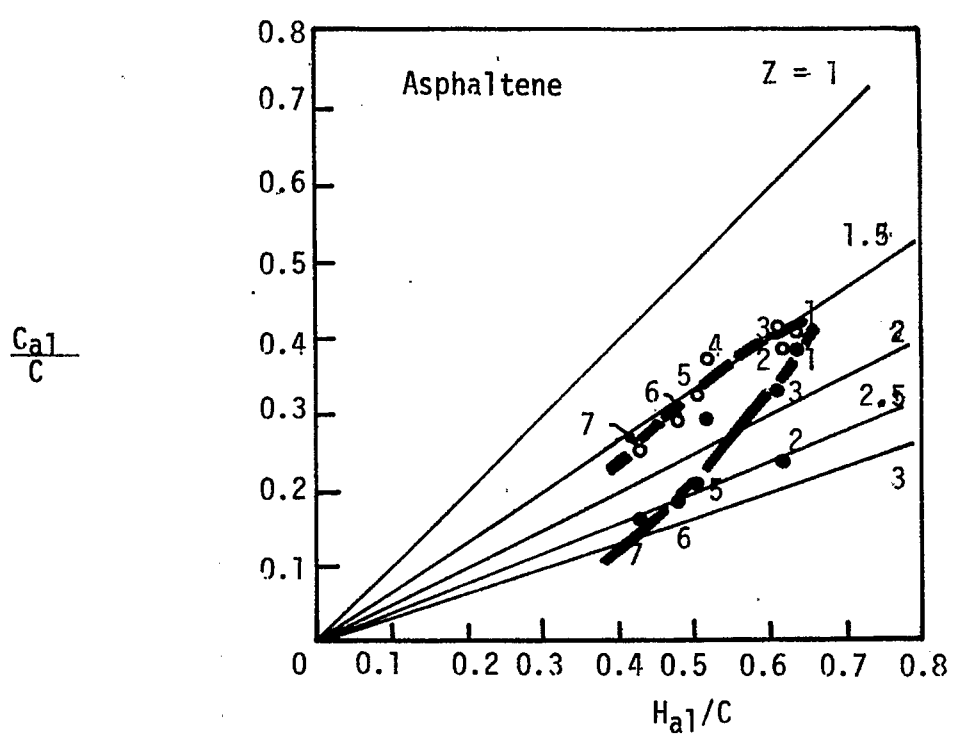
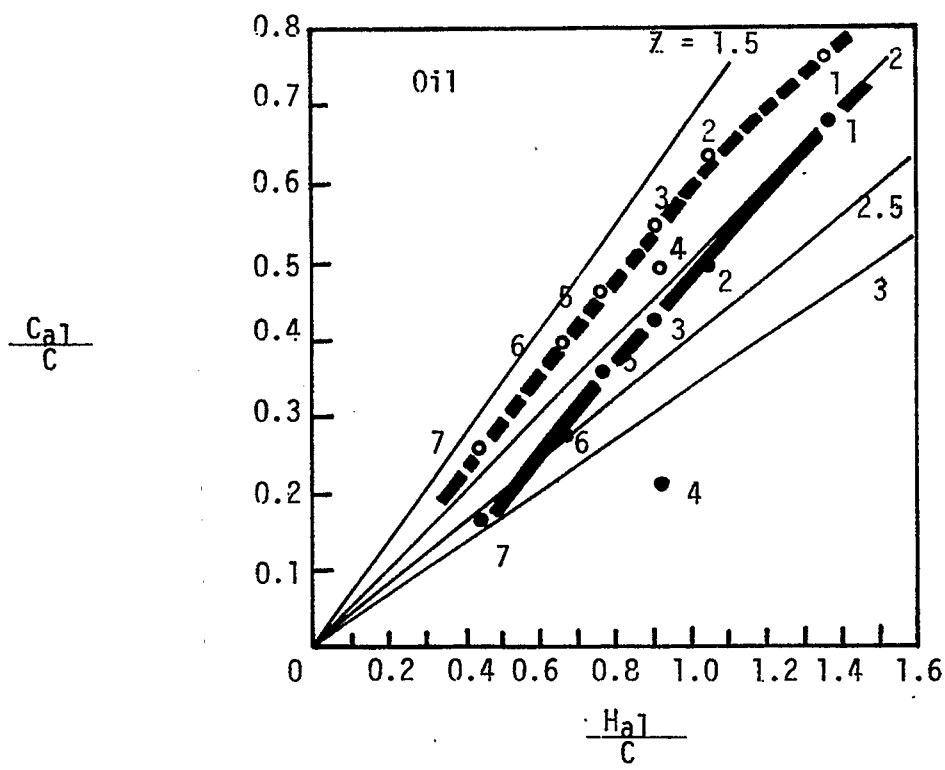


Figure 5

Relationship between Ca_1/C and Ha_1/C

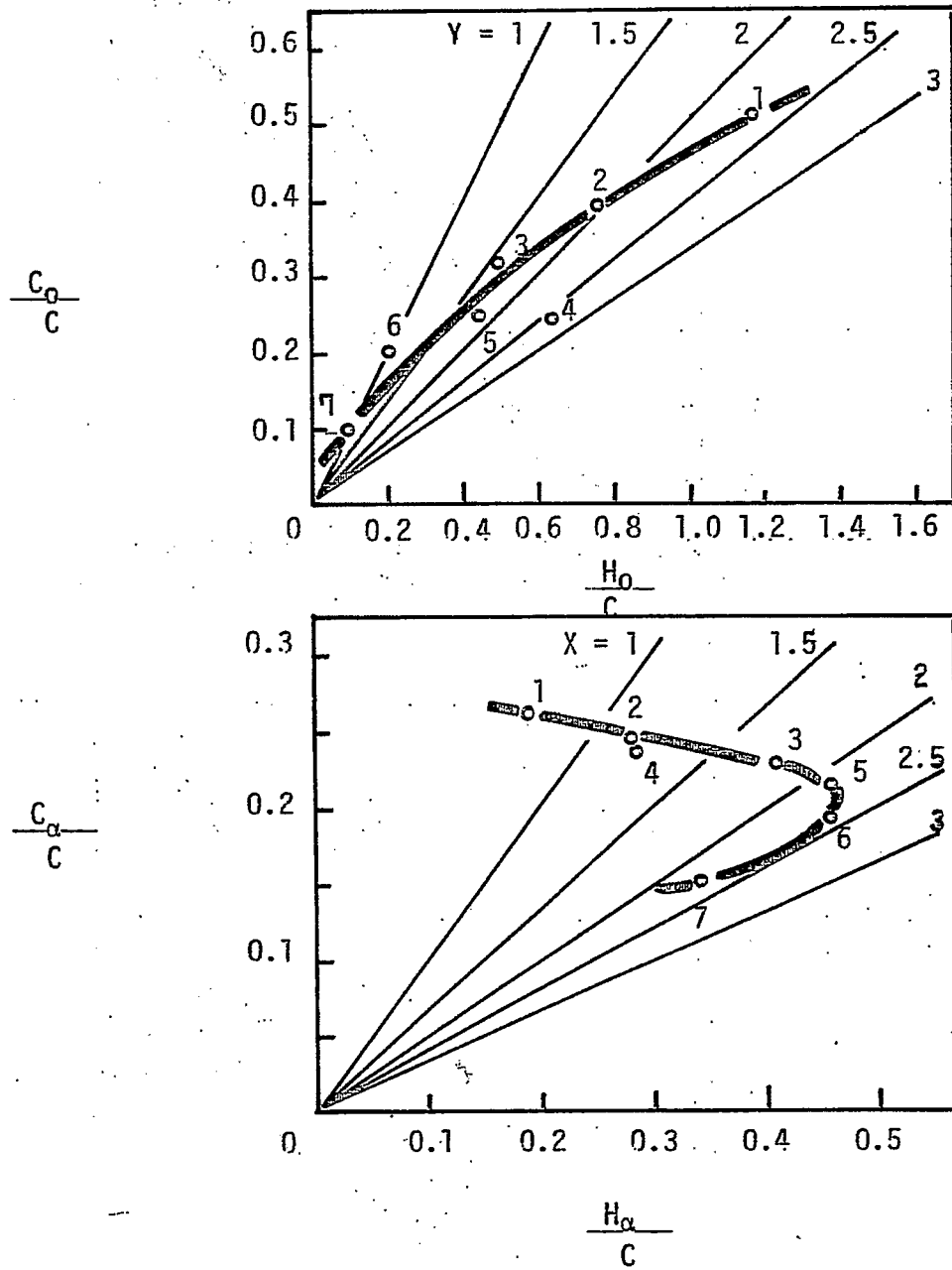


Figure 6

Relationship between C_0/C and H_0/C (above),
 C_α/C and H_α/C (bottom) for Oil GPC Sub-Fractions

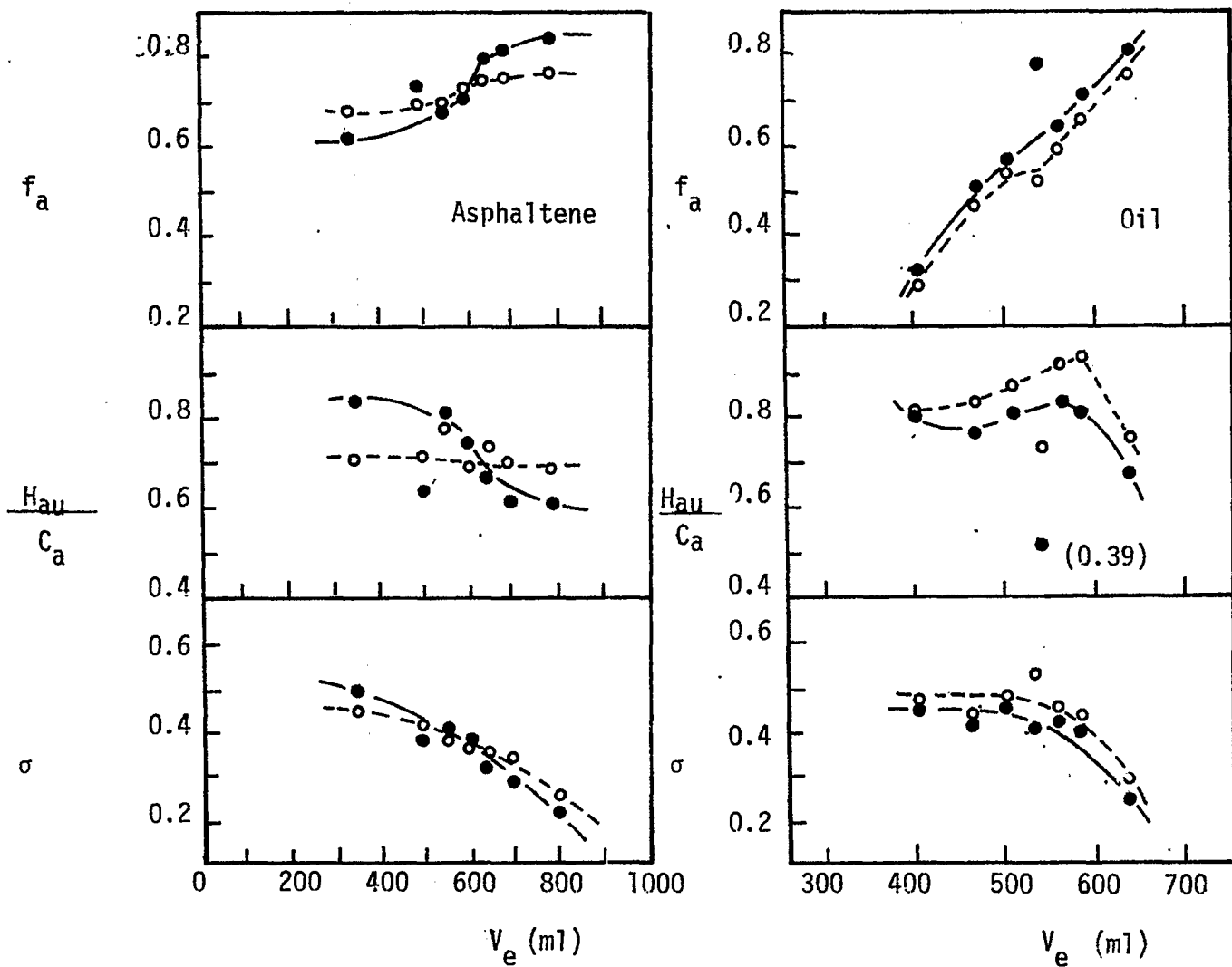


Figure 7
 Structural Parameters from ^{13}C -NMR
 (solid line) and from ^1H -NMR (dashed line)

Project C-2

Heat Transfer to Gas-Solid Suspensions in Vertical Co-Current Downflow

Faculty Advisor: J. D. Seader
Students: J. M. Kim, B. S. Brewster

Introduction

The University of Utah coal hydrogenation reactor involves co-current downflow of solids and fluid at high pressures and high temperatures. The mixture must be heated up to reaction conditions. Most research on heat transfer to flowing gas-solid suspensions has been conducted at low pressure in a vertical upflow system. Direct application of correlations to a vertical downflow system at high temperature and pressure is uncertain. Furthermore, even the fluid mechanics of suspensions in co-current downflow at such conditions are not understood. The purpose of this research is to carry out the fluid mechanics and heat transfer studies involving gas-solid suspensions in vertical downward co-current flow systems.

Project Status

In an earlier report, the design of an experimental apparatus was given for conducting preliminary studies. Most of the equipment and parts have been obtained and installed except for thermocouple wires. Also, preliminary analytical studies of the motion of single spherical particles in gas-solid suspensions were reported.

During this past quarter, installations of experimental apparatus has been continued. Some changes have been made in the location of the vibratory feeder and hopper. Tests with the vibratory feeder on top of the structure showed that the resonance, particularly above mid-range feeding rates, affected the whole structure. The feeder was then put on a bar across a large beam which completely separated it from the experimental structure. The solids hopper was made from a steel drum and was put on a weighing balance. This arrangement enables the measurement of the change of solids content in the hopper without attaching a sight glass to the hopper.

The air cylinders and four-way pneumatic valve have been acquired and installed. The compressed air lines are at 100 psig. Taking into account the weight of the slide and the friction between the slide and the shutter, the closing time with these air cylinders was calculated to be about 0.006 seconds. Actual closing time remains to be determined. The shutter body and the slide are now being fabricated in our machine shop.

The flanges, copper bus bars, and phenolic insulators needed for the heat transfer test tube have been made and are now ready for assembly. The copper bus bars will be silver-soldered to the tube. Detailed dimensions and thermocouple arrangement of the heat transfer test tube are shown in Figure 1.

Future Work

Plans for the next quarter are to complete the experimental apparatus and conduct trial runs to check the workability of the system.

Project C-1

Mechanism of Pyrolysis of Bituminous Coal - Inactive at present

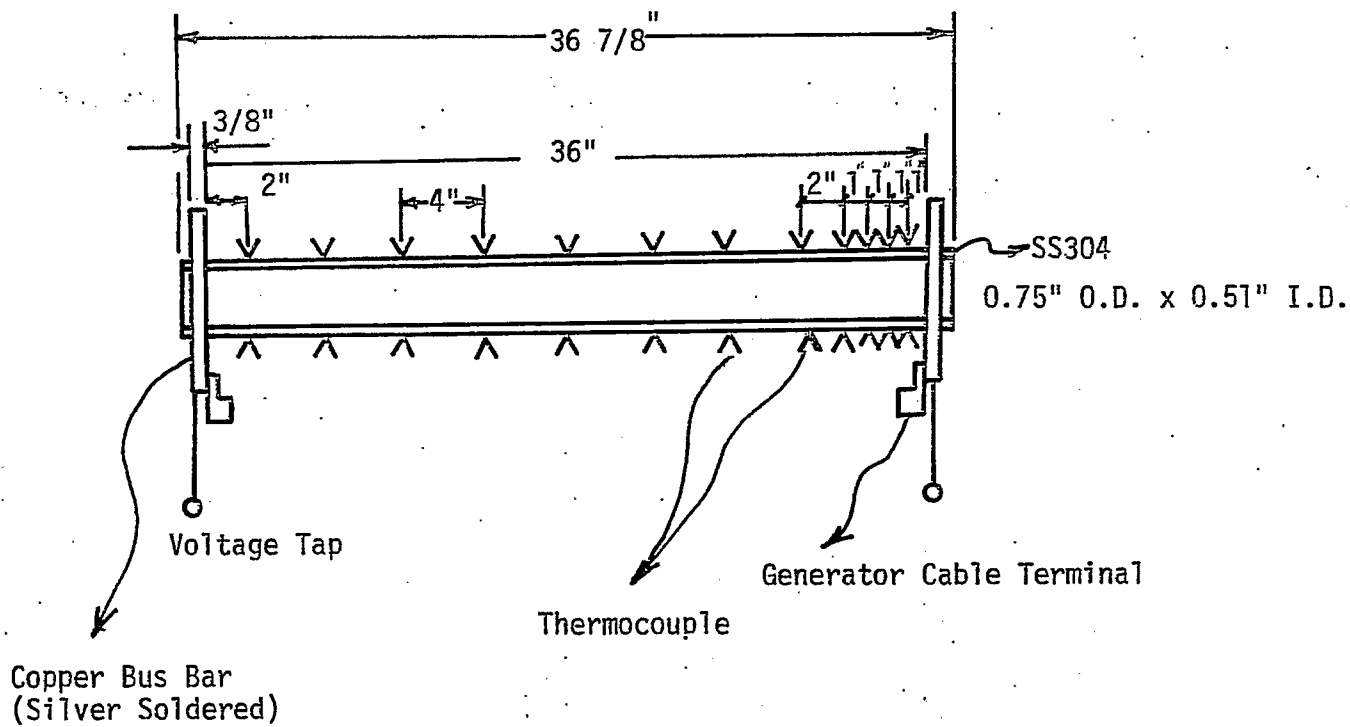


Figure 1
 Details of the Heat Transfer Test Tube

Project D-1

Coal Particle and Catalyst Characteristics for Hydrogenation Evaluation and Testing

Faculty Advisor: R. E. Wood
Graduate Student: J. M. Lytle

Introduction

This effort is related to the effects of coal particle size on coal hydrogenation. The existing hydrogenation equipment, of the OCR contract No. FE (49-18) - 1200, is being used. The reactor consists of a long coiled tube. It is heated from 700° to 1100°F and pressurized to medium pressure of H₂. A magnetic detection device has been fabricated. This, with the aid of an iron or magnetite ore tracer, will give information on residence time of the coal in the reactor. The reactor consists of 44' of 3/16" ID tubing for the preheater and 64' of 1/4" ID tubing for the reactor. A detector coil is placed at the beginning of the preheater and at the end of the reactor.

Project Status

Experimental

The residence time detection device has been tried using various particle sizes of iron with and without coal. This was done to determine the relationship between the residence time of the coal and of the iron. Small charges of iron and coal are physically mixed and fed into the reactor. Figure 1 shows the results of these tests. Line B indicates the effect of particle size on residence time of the iron without coal through the reactor. Line A shows that the residence time increases rather than decreases when 10 wt. percent iron is added to coal and catalyst. This is because of the resistance to flow of the hot plastic coal particles through the hot reactor. The larger iron particles seem to be less intimately associated with the coal so that the indicated residence time is reduced when larger particles of iron are added to the coal.

Results from Figure 1 indicate that smaller particle sizes of iron are more indicative of actual coal residence time. Figure 2 shows the residence time of an iron tracer vs. gas flow rate and particle size. Gas residence times are indicated in Figure 2. Iron particles more nearly approach the gas velocity as the particle size is reduced. The particle size was limited because screens smaller than 400 mesh were not available. Figure 3 shows the results of a similar study using magnetite ore as the tracer. The average specific gravity of the magnetite ore is 4.5 g/cc. Once again the smaller particle sizes are more easily

carried by the gas. Also the lower density magnetite is carried through the reactor more rapidly than the iron. This study indicates that the best tracer is -400 mesh or smaller, iron or magnetite. The scatter of points in Figures 2 and 3 is associated with a new system of gas flow control which has since been improved.

The ratio of coal to tracer and total sample size are important when determining the residence time of incremental samples of coal through the reactor. Line A of Figure 4 shows the relationship of sample size of -400 mesh iron tracer and residence time. The shorter residence time of the smaller sample sizes is related to the interaction of gas and iron particles. This means that the larger the sample size the more energy is required for the sample to travel from one detector to the next. Lines B, C and D of Figure 4 show the effect of adding coal to the iron. When coal is added the greater residence time is attributed to both the larger samples and the sticky nature of hot coal. The hot coal's resistance to flow through the hot reactor tube is especially apparent at higher temperatures as shown in Figure 5. It is noted that the residence time increases significantly with less iron tracer in the sample. This is the opposite effect noted in Figures 2 and 3 where the residence time was reduced with lower density magnetite and Figure 4 where the residence time was reduced with smaller amounts of iron added. This measurement could then become a measure of coal's resistance to flow through a heated reactor vs. temperature, catalyst type and percentage, particle size, coal type and pressure.

Several tests have also been done which involve a continuous feed of coal. The same equipment was used in these tests. The residence time measurement was made by injecting a small amount of iron tracer into the continuous feed of coal and hydrogen. The iron tracer was detected at the beginning of the preheater and at the end of the reactor. This procedure minimizes the relative percent iron in the coal and is a reliable measure of the actual residence time of the coal. Figure 6 shows residence time as a function of temperature and coal feed rate. No catalyst was used in these experiments. An increase in coal feed rate tends to increase the residence time of the coal at lower temperatures. However, at higher temperatures a difference in residence time is not detectable. This may be a result of a decreased bulk density of coal when subjected to a sudden temperature increase. Measurements have been made under these conditions where bulk density has been reduced by a factor of two or more. If catalyst is added to the system the results are somewhat different as shown in Figure 7. When catalyst is added the residence time increases with coal feed rate. It is expected that the catalyst may cause some of the coal to adhere to the wall of the reactor and thus increase the residence time.

Summary

The data obtained thus far indicates the need for smaller tracer particle size, low density tracer and a small percentage of tracer added to the coal. It is felt that an adequate sample would have approximately 10 wt. percent magnetite of -400 mesh or less than 38

microns particle size. During the process of obtaining the above data the sensitivity of the detection coils has deteriorated. To gain further data of this nature it is necessary to improve the sensitivity and longevity of the detection device.

Figure 1

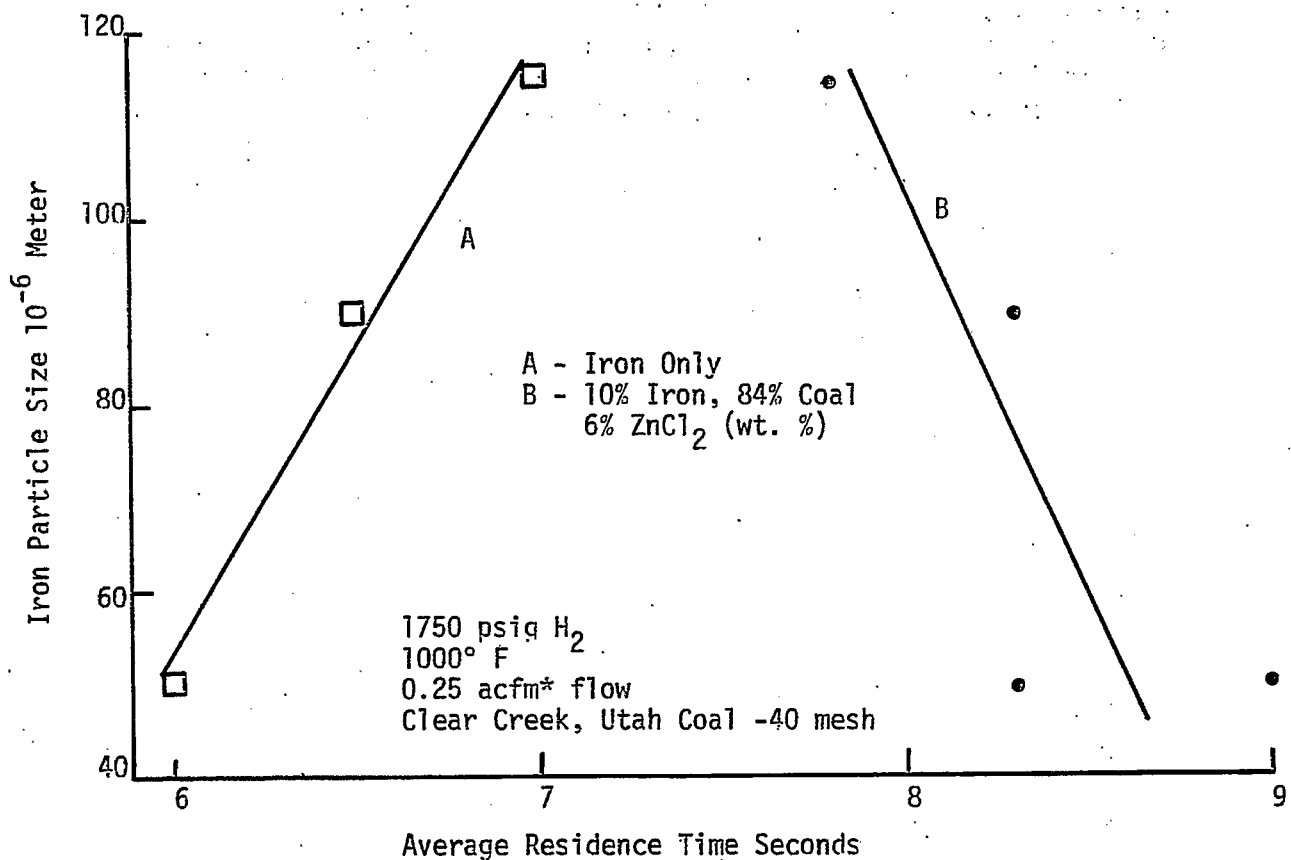
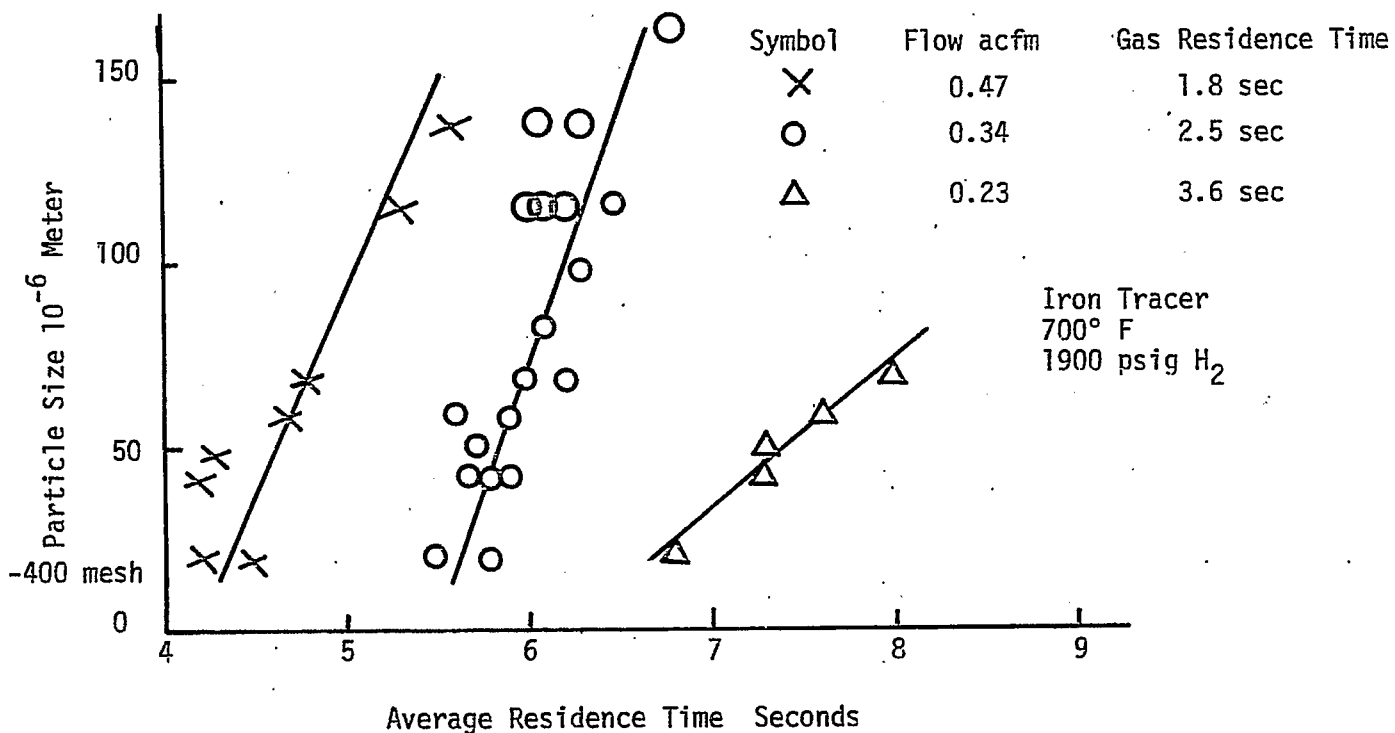


Figure 2



* Actual Ft³/min. at Actual Pressure Conditions and Room Temperature

Figure 3

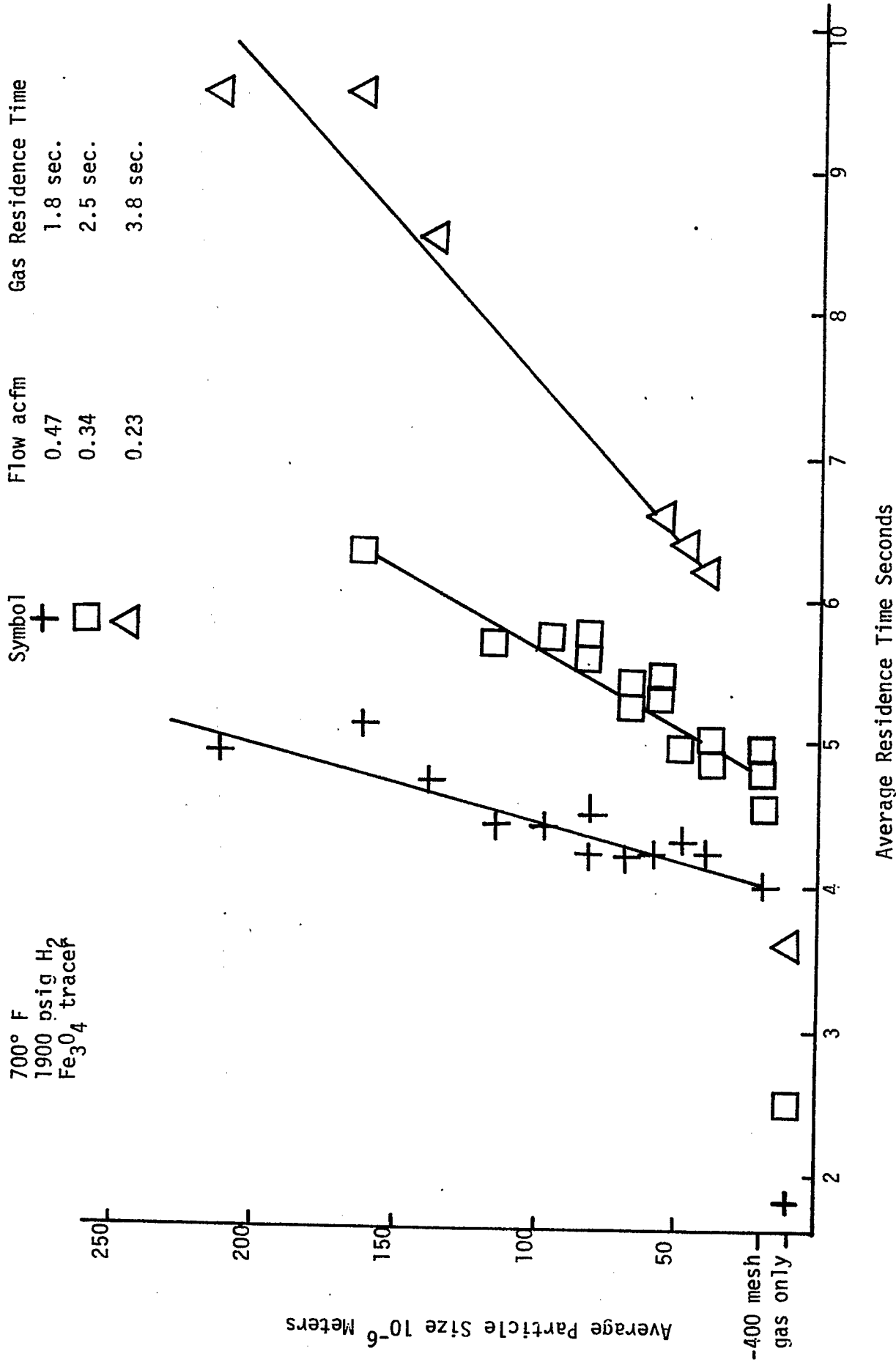


Figure 4

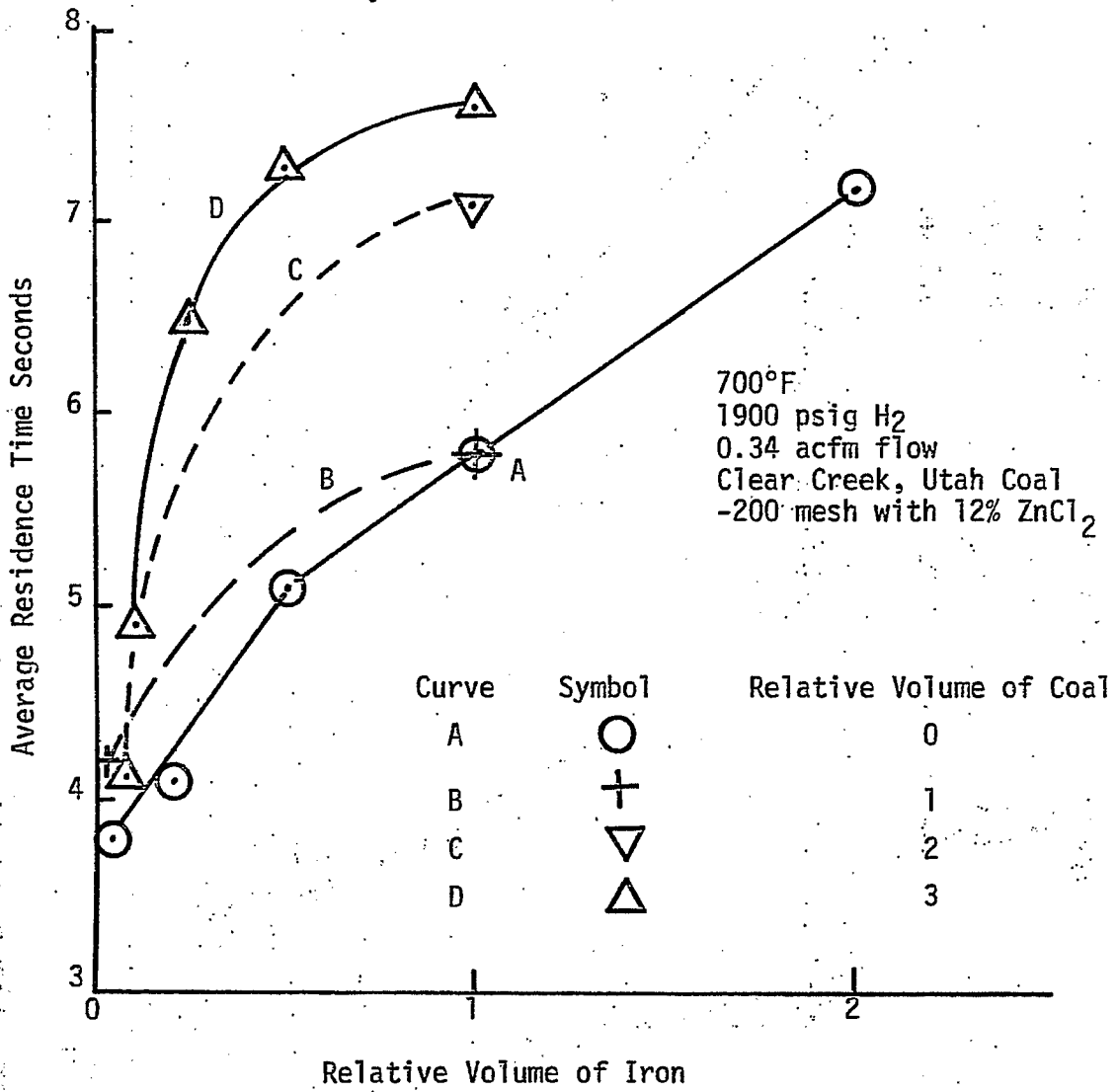


Figure 5

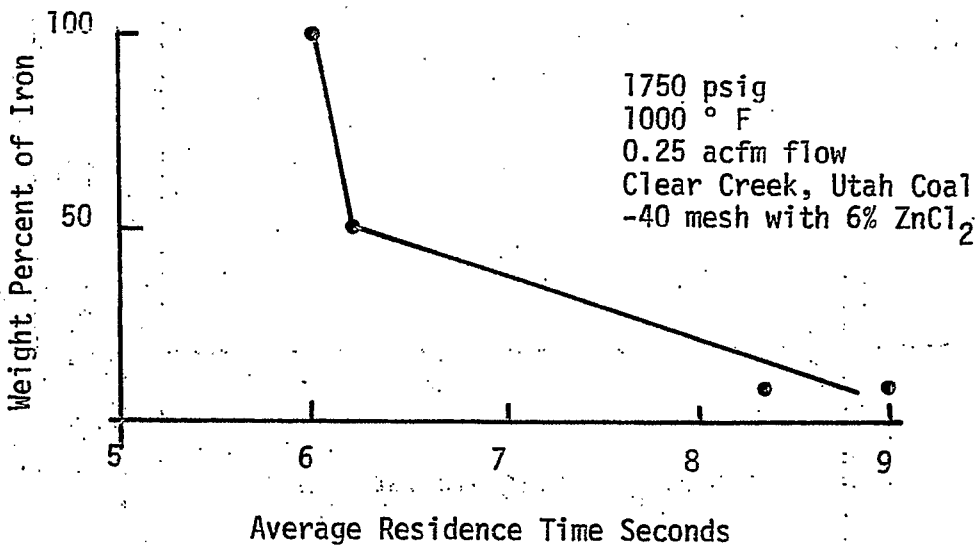


Figure 6

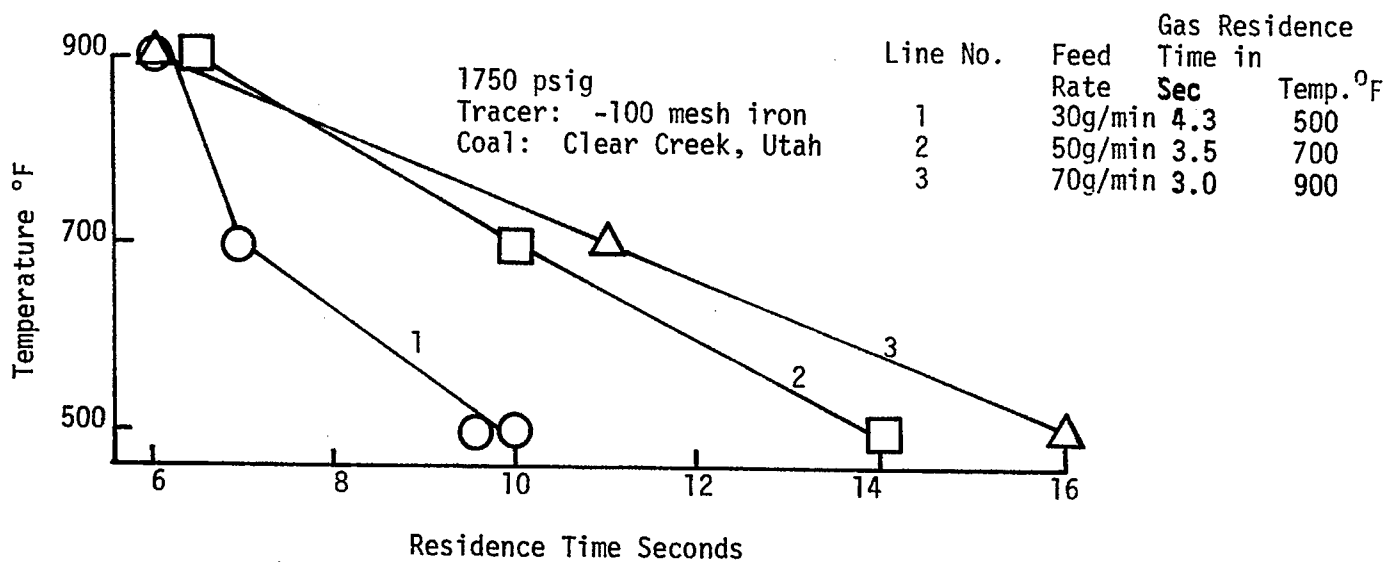
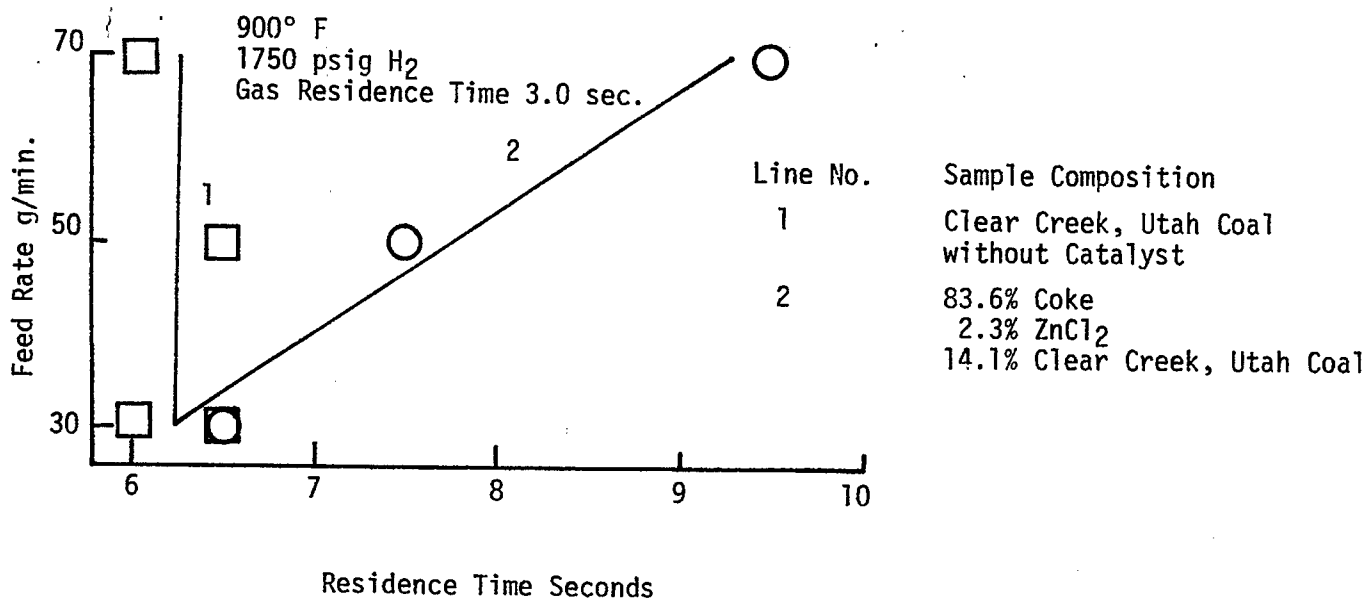


Figure 7



The Effect of Structure on Coal Reactivity

Faculty Advisor: D. M. Bodily
Student: B. Anderson

Introduction

Work has been previously done in an effort to define the effect of $ZnCl_2$ on coal.¹ In that study only one rank of coal was used. This study intends to further elucidate the action of $ZnCl_2$ on coal. This will be done by comparing coals of various ranks by Thermogravimetric Analysis (TGA) and analyses of pyrolysis gases from samples with different amounts of $ZnCl_2$.

Project Status

Samples were chosen from lignite, high volatile and medium volatile ranks. For the TGA, 10 mg samples of lignite and medium volatile coal, previously impregnated with 0%, 5%, 10% and 20% $ZnCl_2$, were heated to 900°C at a rate of 8°C/min. The atmosphere was pure nitrogen, flowing at a rate of 0.15 l/min. over the sample. The nitrogen carried the off-gases out and away from the apparatus. Weight changes were measured using the Cahn Electrobalance and a Rikandenki Recorder. The latter instrument also recorded temperatures from a chromel-alumel thermocouple placed next to the sample.

Samples of lignite, high volatile coal and medium volatile coal, each weighing 5 gm and having concentrations of 0%, 5% and 10% $ZnCl_2$, were heated from 110°C to 750°C. Pyrolysis gas samples were collected every 50°C starting at 250°C. These gas samples were analyzed on two gas chromatographs. Using an alumina column and a Packard Gas Chromatograph, hydrocarbons from one to six carbons were determined. Hydrogen quantities were measured using a molecular sieve column, a thermal conductivity detector, and argon carrier gas in an Antek Gas Chromatograph. Results will be reported after duplicate experiments are performed and after corrections are made for volatilization of $ZnCl_2$.

Future Work

High volatile coal and polystyrene will be run in the TGA. Polystyrene will be pyrolyzed with various amounts of $ZnCl_2$ for gas analysis. The polystyrene is to be used as a model for aliphatic linkage of aromatic rings.

References

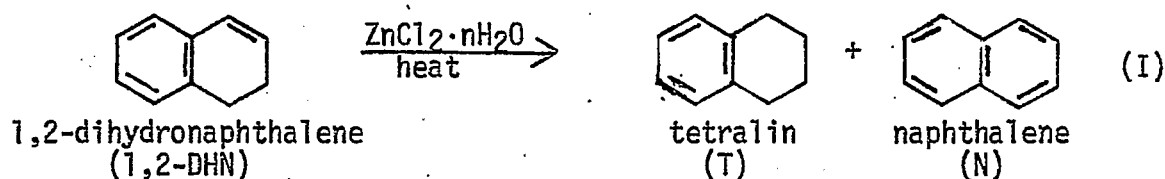
1. H. D. Lee, D. M. Bodily and W. H. Wiser, "A Thermal Study of Coal Impregnated with Hydrogenation Catalysts," Technical Report, Department of Interior, Office of Coal Research, June, 1974.

A Pyrolysis-Gas Chromatography Study of Coals and Related Model Compounds

Faculty Advisor: R. R. Beishline

Introduction

At the present time, this study is concerned with the catalytic effects of $ZnCl_2$ on the pyrolysis of coal-related model compounds. Specifically, reaction (I) is under investigation.



Reaction (I) occurs thermally in the absence of $ZnCl_2$, but the thermal reaction becomes very slow when the temperature is dropped to $300^\circ C$. In the presence of $ZnCl_2 \cdot nH_2O$, the reaction proceeds rapidly at temperatures as low as $150^\circ C$.

It is believed that the mechanism for reaction (I) is similar to one proposed by C. W. Zielke et al for the hydrogenation of coal, coal extracts, and polynuclear aromatic hydrocarbons in the presence of molten zinc chloride. The mechanism proposed by the author postulates that $ZnCl_2$ functions as a Lewis acid by coordinating a hydroxyl ion from water and releasing a hydrogen ion. This hydrogen ion protonates the position of the 3,4 -double bond in 1,2 -DHN to form a carbonium ion which becomes tetralin by abstracting a hydride ion from a second molecule of 1,2-DHN. The second molecule of 1,2-DHN, after loss of the hydride ion, ejects a proton to become N. This mechanism is shown in Figure 1.

The work presented in the penultimate Quarterly Progress Report demonstrated that water is necessary for reaction (I) to proceed, with the optimum value of n being near one. When n is much greater or less than one, the reaction is decelerated. A blank run with 1,2-DHN and water without $ZnCl_2$ (20 min, $165^\circ C$) gave no reaction. These data establish that both $ZnCl_2$ and water are necessary and furnish evidence in support of steps (A) and (B) of the proposed mechanism.

Project Status

If the mechanism proposed for reaction (I) (see Figure 1) is

correct, tetralin produced from 1,2-DHN and $ZnCl_2 \cdot D_2O$ should contain deuterium in the β position of the hydroaromatic ring. The work reported here establishes that this is actually the case.

The position and extent of deuteration were determined by nuclear magnetic resonance (NMR) and infrared (IR) spectroscopy. The presence of deuterium causes a loss in the integrated NMR peak area (integration loss) because deuterium absorbs in a different NMR spectral region than hydrogen and, therefore, is not seen when the instrument is set to observe hydrogen. Calculation of the integration loss from the difference between the areas of the respective undeuterated and deuterated peaks constitutes a quantitative determination of deuterium. For this method to be effective, the NMR absorptions of the hydrogens in question must be well resolved from adjacent peaks. This condition is met in the NMR spectrum of tetralin.

The position of deuteration was also determined from C-D stretching bands which appeared in the IR spectrum. In some cases, deuteration was quantitatively determined by using Beer's law to calculate the loss of C-H bond concentration from the decrease in C-H stretch intensity in the appropriate IR bands.

The integrated NMR values for undeuterated tetralin are listed at the top of Table 2 for comparison. A blank run was carried out (tube 101, Table 2, p 117) by heating undeuterated tetralin with $ZnCl_2 \cdot D_2O$. For this reaction, the IR spectrum showed no C-D stretch at 2170 cm^{-1} , which indicates that there was no aliphatic deuteration, i.e., tetralin, in the presence of $ZnCl_2 \cdot D_2O$ does not undergo H-D exchange at either the aliphatic α or β position. It should be noted that although the C-D stretch at 2170 cm^{-1} indicates aliphatic deuteration, it does not distinguish the α from the β position. Deuteration of the aromatic positions did take place, however, as indicated by the appearance of the aromatic C-D stretch at 2265 cm^{-1} in the IR spectrum, by quantitative Beer's law calculations based on intensity measurements of the aromatic C-H stretching band at 3020 cm^{-1} and also by the NMR integration loss at the 7.07 ppm (aromatic H) peak. This deuteration was expected since aromatic H-D exchange by an electrophilic aromatic substitution mechanism is well known. The electrophile, in this case, is the D^+ released when $ZnCl_2$ coordinates an OD^- from D_2O . This side reaction has no effect other than to use up part of the available deuterium. All three runs in which tetralin was produced from 1,2-DHN and $ZnCl_2 \cdot D_2O$ (see Table 2) show both aromatic and aliphatic β deuteration. In the 12 minute reaction (tube 102) the aromatic-deuteration is questionable from the NMR data alone, but the IR spectrum shows a small C-D stretching band at 2265 cm^{-1} and Beer's law calculations also indicate aromatic deuteration. For the last three runs of Table 1 (tubes 102, 103 and 104) it was arbitrarily assumed that the aliphatic α deuteration was zero and the NMR integrations for the α hydrogens were therefore normalized to 4.00. The IR data (Beer's law calculations), does not appear to have sufficient accuracy to indicate α deuteration.* (see following page) Although not highly accurate, the IR data of Table 1 agree reasonably well with and therefore serve as an

independent verification of the NMR data. Even if there were some α deuteration, the data show that β deuteration occurs to a greater extent. The experimental results therefore clearly support step (B) of the proposed mechanism (Figure 1).

Experimental

Tube Reactions:

The reactions in tubes 101-104 were carried out in sealed pyrex tubes (13mm x approx. 7 cm) which were prepared as follows: In a dry box, anhydrous $ZnCl_2$ (~ 1.000 g, 7.3×10^{-3} moles) was weighed into open tubes which were then stoppered with rubber caps. The tubes were removed from the dry box and the appropriate amount of D_2O (~ 0.132 ml, 0.146 g, 7.30×10^{-3} moles) added from a syringe. The tubes were again weighed to determine precisely the weight of water that had been added. In like manner the 1,2-DHN was added, i.e., from a syringe with subsequent weighing (~ 1.43 ml, 1.42 g, 0.0109 moles). The quantities were added to give $ZnCl_2:D_2O:1,2-DHN$ mole ratios of 1:1:1.5, respectively. The tubes were then degassed under vacuum using three freeze-thaw cycles and sealed off. To run the reaction, the sealed tubes were mounted in a small, horizontal rocking device and lowered into a $165^\circ C$ constant temperature bath. After rocking for adequate times, the tubes were withdrawn, quenched in a cooling bath to stop the reaction, opened, diluted with benzene and analyzed by GC. A column of $1/8" \times 6'$ ss was packed with 10% Carbowax 20 M on 80/100 mesh Chromosorb W. The GC analysis showed only 1,2-DHN, T, and N in the products. Previous calibrations have shown that the area percents of these compounds are equal to their mole percents. The percent reaction was calculated from the areas of unreacted 1,2-DHN. The results of the GC analysis are shown in Table 2.

Table 2
GC Analysis of Reaction (I) in the
Presence of D_2O

Tube no.	Reaction Temp ($^\circ C$)	Reaction Time (min)	% Reaction	% T	% Nap
102	165	12	15.8	8.6	7.2
104	165	20	79.4	45.5	33.9
103	165	40	96.2	57.4	38.8

*Assuming that IR data were accurate, then an aromatic D value (Table 1.) that was larger according to the IR data than the NMR data, would indicate that the NMR integration standard (the α hydrogens) had been chosen to be too large and should in fact be smaller than 4.00. The NMR values for aromatic H and βH would also be too large, and all the NMR D values would be too small. That the IR data is not sufficiently accurate to be used diagnostically in this way is indicated by the following fact. The aromatic D value (Table 2) for the blank run (tube 101) is larger according to the IR data than according to the NMR data, yet the NMR αH value of 4.00 must be correct, since the IR spectrum shows no aliphatic C-D stretching band at 2170 cm^{-1} .

NMR Analysis

The NMR spectrum of pure, undeuterated T was run, and the absolute values of the integrations for the α aliphatic hydrogens (2.76 ppm) were normalized to 4.00. The absolute values of the integrations for the aromatic (7.07 ppm) and β aliphatic (1.79 ppm) hydrogens were then scaled proportionately which gave them values of approximately 4.00 also (see Table 1). The α aliphatic hydrogens were chosen as the standard of comparison because a blank run carried out by heating undeuterated T with $ZnCl_2 \cdot D_2O$ showed no aliphatic deuteration (IR) and therefore no aliphatic H-D exchange at either the α or β aliphatic positions. Also, it was assumed that the α position was the least likely to be deuterated during the formation of T from 1,2-DHN. The values listed in Table 1 for undeuterated T are the averages of five integrations on each of two samples. Since the two samples were on different days, the standard deviations should be truly indicative of the errors introduced by instrument drift, operator error, etc. All other NMR values in Table 1 are the averages of five integrations on a single sample. All NMR spectra were run on micro samples, i.e., the sample was a column of liquid approximately one cm high in a standard melting point capillary.

IR Work

A. Calculation of the expected positions of the C-D stretching bands in tetralin.

The theory upon which these calculations are based is clearly set forth.² Briefly, the calculations were done as follows. The force constant for the particular C-H bond in question was calculated and the corresponding C-D force constant was assumed to have the same value.³ Using a new reduced mass for the C-D bond and the calculated force constant, the position of absorption (in cm^{-1}) of the C-D bond was calculated. The results are shown in Table 3.

Table 3
C-D Stretching Frequencies for Tetralin

C-H Stretch (cm^{-1})	C-D Stretch (cm^{-1}) (calc)	C-D Stretch (cm^{-1}) (obs)
Aromatic 3020	2248	2265
Aliphatic 2927	2180	2170
Aliphatic 2854	2130	2147 (shoulder on 2170)

B. Quantitative determination of the extent of deuteration

This work was based on Beer's law which quantitatively relates the absorption intensity of a given spectral band to concentration.

Beer's law can be expressed as:

$$\log\left(\frac{100}{\% \text{trans}}\right) = a b c$$

where: a = absorptivity
b = cell path length
c = concentration

The concentration of aromatic C-H bonds in undeuterated tetralin (moles C-H bonds/l) was calculated from the relationship:

$$\text{moles C-H bonds/l} = \frac{0.9702 \text{ g T}}{\text{ml T}} \times \frac{1000 \text{ ml}}{1} \times \frac{1 \text{ mole T}}{132.21 \text{ g T}} \times \frac{4 \text{ moles C-H bonds}}{\text{mole T}}$$

By measuring the % transmission of the 2030 cm^{-1} peak (aromatic C-H stretching) for undeuterated tetralin at several known values of b and by using the calculated concentration, the absorptivity was obtained. Using this absorptivity, the concentration of C-H bonds in deuterated tetralin was calculated from the measured % transmission (3020 cm^{-1}) at known b values. (See Table I -- note that concentrations in Table I are expressed as bonds/molecule rather than moles of bonds/l.) The concentration of C-D bonds was then obtained by difference. All measurements were made in a calibrated, variable path length cell.

Summary

A mechanism has been proposed for reaction (I) (see Figure 1). This



mechanism is supported by work reported in the last quarterly report and also by deuterium tracer work reported in this quarterly report.

Future Work

The investigation to determine the optimum value of n in reaction (I) is only partially completed and further work will be done in that area.

An attempt will be made to run reaction (I) to approximately 50% completion in the presence of D_2O and to determine whether or not there is D on the 1,2-DHN double bond at the 3 position. This will furnish evidence about the reversibility of step (B) in the proposed mechanism (Figure 1). This information will be valuable both as evidence for the proposed mechanism and in planning future kinetic studies.

References

1. C. W. Zielke et al, Ind. Eng. Chem., Process Des. Develop., 5, 51 (1966).

(continued)

References

2. C. J. Creswell, O. Runquist, and M. M. Campbell, "Spectral Analysis of Organic Compounds -- An Introductory Programmed Text," 2nd ed., Burgess Publishing Co., Minneapolis, Minn., 1972, pp. 62-66.
3. M. Avram and G. H. Mateescu, "Infrared Spectroscopy", Wiley-Interscience, New York, N. Y., 1972, p. 54.

Table 1
 Formation of Deuterated Tetralin from the Reaction of
 1,2-Dihydronaphthalene with $ZnCl_2 \cdot D_2O$

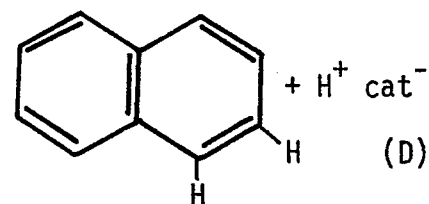
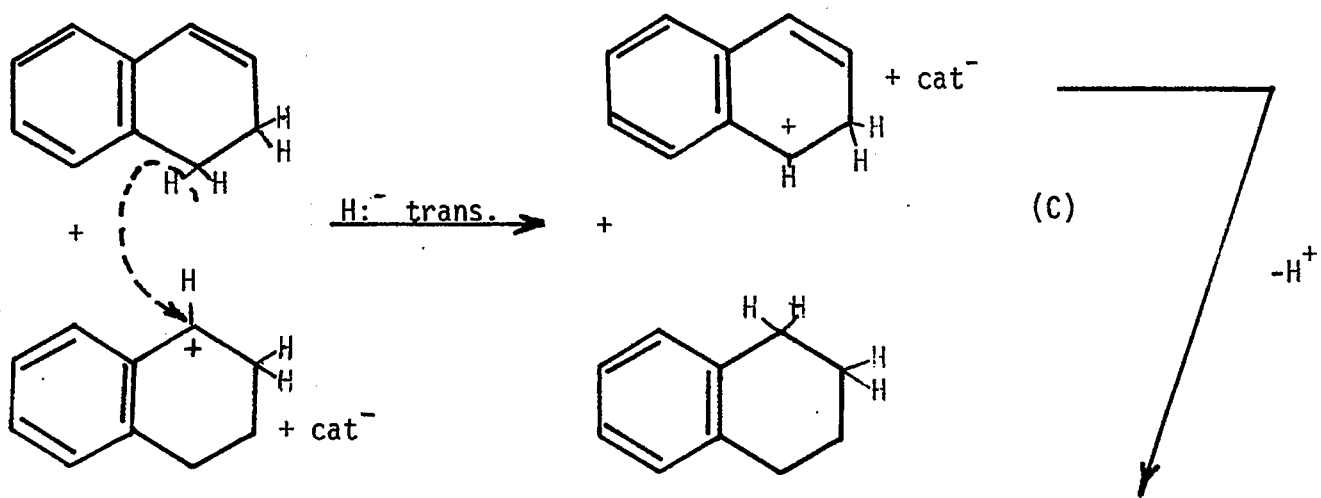
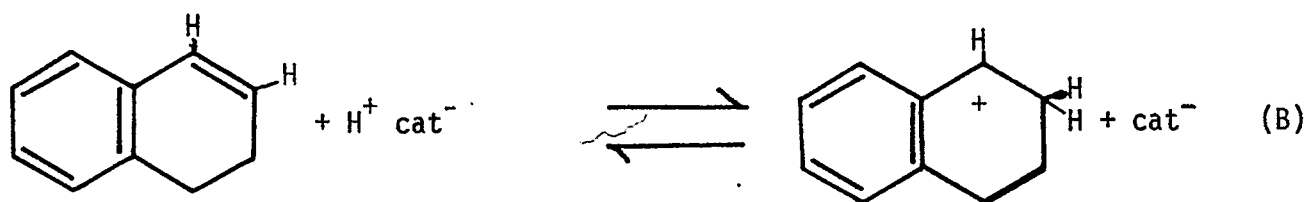
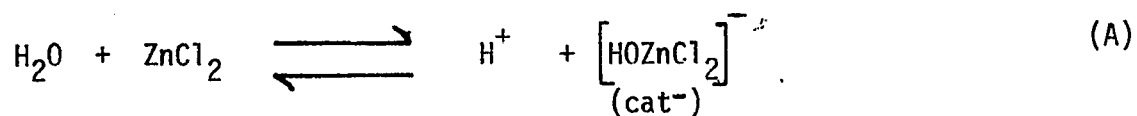
Sample	Retn time (min.) at 165° C	Average no. of Hydrogen or Deuterium Atoms per Molecule									
		Arom. H		Arom. D (by diff.)		αH NMR	αD (by diff.)	βH NMR	βD (by diff.)		
		NMR	I R	NMR	I R						
undeuterated tetralin	--	4.03 \pm 0.04	--	--	--	4.00 \pm 0.08	--	4.09 \pm 0.12	--	--	
tetralin + $ZnCl_2 \cdot D_2O$ (tube 101)	20	3.61 \pm 0.04	3.28 \pm 0.10	0.42 \pm 0.06	0.72 \pm 0.11	4.00 \pm 0.06	0.00*	4.16 \pm 0.02		-0.07 \pm 0.12*	
tetralin from rcn of 1,2-DHN with $ZnCl_2 \cdot D_2O$ (tube 102)	12	3.94 \pm 0.05**	3.79 \pm 0.07	0.09 \pm 0.06	0.21 \pm 0.07	4.00 \pm 0.03	0.00	3.63 \pm 0.04		0.46 \pm 0.13	
tetralin from rcn of 1,2-DHN with $ZnCl_2 \cdot D_2O$ (tube 104)	20	3.58 \pm 0.01	3.63 \pm 0.17	0.45 \pm 0.04	0.37 \pm 0.16	4.00 \pm 0.04	0.00	3.65 \pm 0.02		0.44 \pm 0.12	
tetralin from rcn of 1,2-DHN with $ZnCl_2 \cdot D_2O$ (tube 103)	40	2.62 \pm 0.08	2.53 \pm 0.13	1.41 \pm 0.09	1.47 \pm 0.14	4.00 \pm 0.23	0.00	3.08 \pm 0.07		1.01 \pm 0.14	

*The i r spectrum of this sample showed no aliphatic C-D stretch.

**The i r spectrum of this sample showed a small aromatic C-D stretch, as well as a larger aliphatic C-D stretch.

Figure 1

Proposed Mechanism for Reaction (I)



Pyrolytic Studies and Separation and
Characterization of Coal-Derived Liquids

The Separation and Characterization of Liquid Mixtures Derived
from Coal Hydrogenation

Faculty Advisor: R.R. Beishline

Introduction

This project deals with the investigation of promising methods for analyzing coal hydrogenation liquids. The work is primarily concerned with analysis of lighter fractions, since the gas chromatography (GC) and distillation equipment on hand is better suited to that range of boiling point. Last quarter the separation of a neutral coal hydrogenation fraction boiling from room temperature to 80°C was reported. This work indicated that a reasonably good GC separation of the room temperature to 80° fraction could be done on a column packed with Carbopack C/0.19% picric acid. The spinning band (SB) distillation column could also cut this material into smaller, less complex fractions making it easier to identify the individual components.

Project Status

The separation of a neutral hydrocarbon fraction boiling from 80° - 100° C at atmospheric pressure is currently in progress. This fraction came from a "light ends" coal hydrogenation sample obtained from the University of Utah coal hydrogenation reactor. The crude material was previously distilled, extracted with aqueous mineral acid and base and redistilled through a 1 x 16 cm column packed with 6 mm glass helices. The 80° - 100° C cut at atmospheric pressure from the redistillation furnished the starting material that is now being investigated.

The 80° - 100° C fraction was distilled through the SB column (54 ml pot charge) at a 200:1 reflux ratio, and the following fractions were obtained:

Fraction	Temp.(°C)	Vol.(ml)	Fraction	Temp.(°C)	Vol.(ml)
1+3	49-59	0.86	21+22	88-90	2.50
2	56.5-62.5	1.00	23	90-94	0.90
4	60.5-65	0.75	24	91-94	1.30
5+7	63.5-66.5	2.75	25+26+27	92-100	4.20
6	65-66.5	0.85	28	100-102	0.70
8	65.5-72	1.35	29	102-104	1.10
9+10+11	70-79	7.88	30	102-106	1.20
12+13+14	76-86.5	5.90	31	106-109	1.30
15+16	81.5-85	2.30	32	104-106	0.60
17+18	82.5-85	2.70	33	110-114	1.40
19+20	84.5-87	3.60			
					45.14
				pot residue	4.90
				volatility loss	3.96

Where a fraction is the sum of two or three numbers, it indicates that smaller fractions were combined since GC analysis has shown them to be very similar.

The problem previously encountered during distillation of the 25° to 80° C fraction was also evident during this distillation. When distillate was being taken off, only a few drops to 0.5 ml came off before reflux stopped. The column was run on total reflux until an acceptable reflux rate was reestablished and another small volume was taken until reflux stopped again. Due to the large number of components in the mixture the composition of the material distilling through the column changes rapidly. This upsets the adiabatic equilibrium in the silvered vacuum-jacketed column and causes reflux to stop. The temperature overlap of many of the above fractions (e.g., F23, 90-94°; F24 91-94°) is believed to be related to this same problem. When total reflux is established, the column is operating at near-equilibrium conditions and has its maximum fractionating capacity. As distillate is taken off, the composition of the material distilling changes rapidly, shifting the distillation off near-equilibrium conditions and causing the fractionating efficiency to drop. Higher boiling components that would be held back at maximum efficiency conditions are now allowed to reach the head and the temperature rises. The adiabatic equilibrium in the column is upset and reflux stops. When total reflux is reestablished, the column again operates at maximum fractionating capacity and the next fraction will come over at an initial temperature lower than the final temperature of the previous fraction. This temperature overlap is responsible for the scatter in the plot of the distillation (total volume distillate vs. temperature) which is shown in Figure 1. Conducting the distillation more slowly may help. However, this seems impractical since this distillation required ten working days to complete. The fraction boiling between 49° and 114°C obtained by fractionation of the material in the SB column had an apparent boiling range of 80 to 100° C when distilled in a 1 x 16 cm column packed with 6 mm glass helices.

GC analysis of the total fraction has shown it to contain about twenty-seven components. These analyses are being done on a 2 meter x 1/8" stainless steel column packed with 80/100 mesh Carbopack C/0.19% picric acid and also on a 3 meter x 1/8" stainless steel column packed with 10% sp 2100 on 80/100 mesh supelcoport. In the former column, the lower boiling components resolve better, but the higher boiling materials tail badly, while in the latter column, the lower boiling components do not resolve as well, but the higher boiling materials do not tail. Presently, an attempt is being made to use both columns to advantage and to interrelate the results obtained from them.

In the Oct - Dec 1975 Quarterly Progress Report, the preparation of five neutral hydrocarbon fractions from a "light ends" coal hydrogenation sample was described. The bromine numbers of these fractions have been determined and are shown in Table 1. Bromine number is a measure of unsaturation and is defined as the number of grams of bromine consumed by a one-hundred gram sample. The bromine numbers were determined by color-indicator titration according to ASTM method D1158-59T. This

method consists of dissolving the sample in carbon tetrachloride, treating it with an excess of standard bromide/bromate solution in the presence of glacial acetic acid, reducing the excess bromine with potassium iodide and titrating the liberated iodine to the disappearance of the starch-iodide blue color with standard sodium thiosulfate solution. The average number of carbon atoms per double bond (see Table 1) was taken as the n value in the C_nH_{2n} (empirical formula for a monoalkene) that gave a molecular weight nearest to the grams sample per mole of double bonds.

Table 1

Bromine Numbers of Neutral Hydrocarbon Fractions
Obtained from a "Light Ends" Coal Hydrogenation
Sample (University of Utah Coal Hydrogenation Reactor)

Fraction	Boiling Range (°C)	Bromine Number	Grams Sample per Mole of Double Bonds	Ave. No. of C Atoms per Double Bond
1	27-80 (atm)	89.57	178.4	13
2	80-100 (atm)	88.13	180.9	13
3	27-100 (100 Torr)	81.32	196.51	14
4	27-64 (10 Torr)	55.47	288.3	21
5	64-94 (10 Torr)	48.04	332.6	24

Summary

The separation of a coal hydrogenation liquid fraction (boiling range 80 - 100° C, at atmospheric pressure is now in progress. The separation is being done by a combination of SB distillation and GC.

The bromine numbers of five neutral hydrocarbon fractions from a "light ends" coal hydrogenation sample (see Quarterly Progress Report, Oct - Dec, 1975) have been determined.

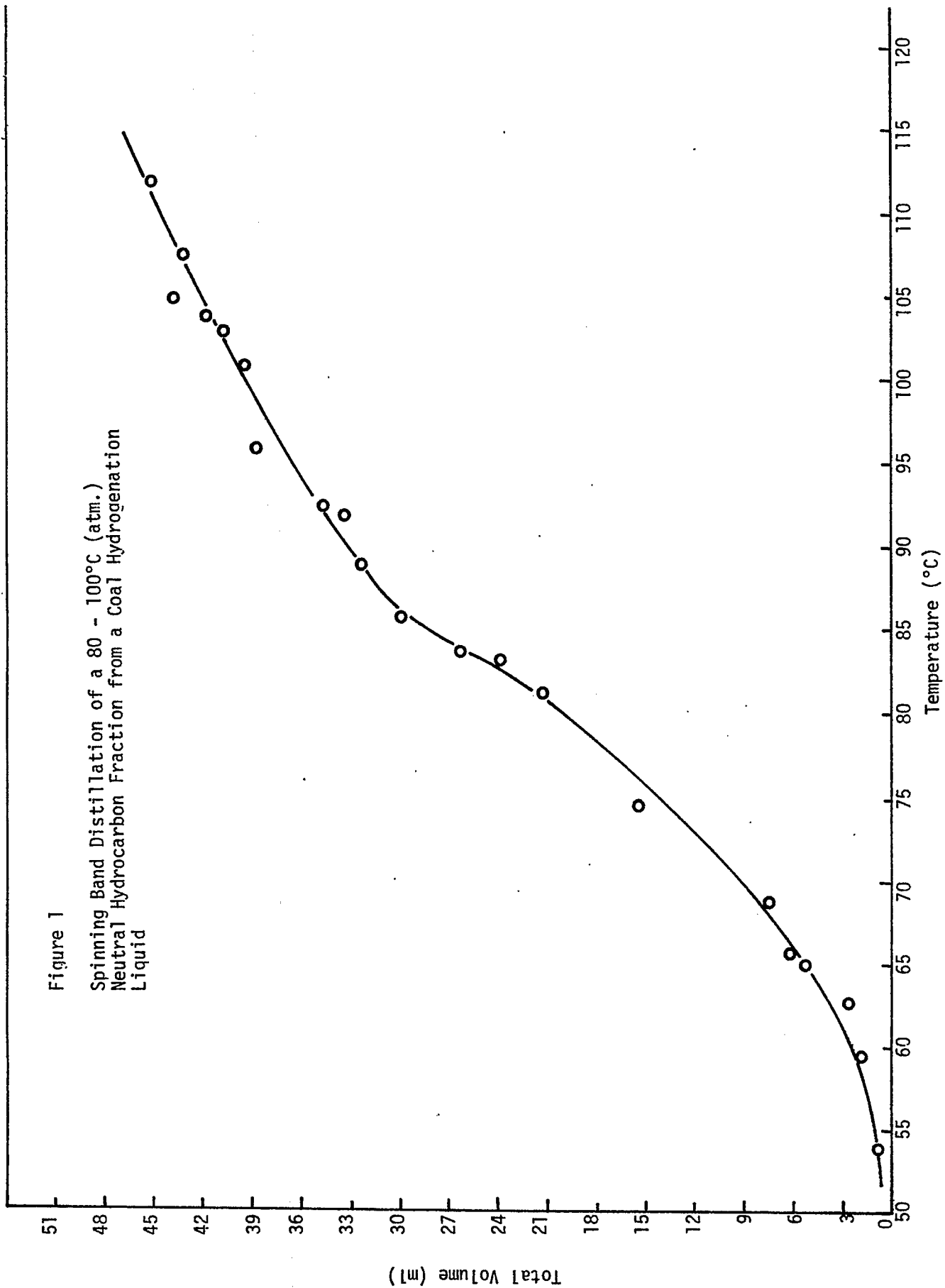
Future Work

The separation of a coal hydrogenation liquid fraction now in progress will be completed and the major components will be identified spectroscopically.

The quantity and identity of the alkenes present in coal hydrogenation fractions will be studied by mercuration, bromination, GC, SB distillation and spectroscopic techniques. These methods will be used in combinations which seem most appropriate to the samples being investigated.

Figure 1

Spinning Band Distillation of a 80 - 100°C (atm.)
Neutral Hydrocarbon Fraction from a Coal Hydrogenation
Liquid



V. Conclusions

Work is progressing satisfactorily on twelve projects. Four have not yet been initiated. Four projects which were continued from a previous contract. Students are now writing theses on three of these projects.

SATISFACTION GUARANTEED

NTIS strives to provide quality products, reliable service, and fast delivery. Please contact us for a replacement within 30 days if the item you receive is defective or if we have made an error in filling your order.

▲ **E-mail: info@ntis.gov**

▲ **Phone: 1-888-584-8332 or (703)605-6050**

Reproduced by NTIS

National Technical Information Service
Springfield, VA 22161

This report was printed specifically for your order from nearly 3 million titles available in our collection.

For economy and efficiency, NTIS does not maintain stock of its vast collection of technical reports. Rather, most documents are custom reproduced for each order. Documents that are not in electronic format are reproduced from master archival copies and are the best possible reproductions available.

Occasionally, older master materials may reproduce portions of documents that are not fully legible. If you have questions concerning this document or any order you have placed with NTIS, please call our Customer Service Department at (703) 605-6050.

About NTIS

NTIS collects scientific, technical, engineering, and related business information – then organizes, maintains, and disseminates that information in a variety of formats – including electronic download, online access, CD-ROM, magnetic tape, diskette, multimedia, microfiche and paper.

The NTIS collection of nearly 3 million titles includes reports describing research conducted or sponsored by federal agencies and their contractors; statistical and business information; U.S. military publications; multimedia training products; computer software and electronic databases developed by federal agencies; and technical reports prepared by research organizations worldwide.

For more information about NTIS, visit our Web site at <http://www.ntis.gov>.

The logo for NTIS, consisting of the letters "NTIS" in a bold, sans-serif font. The letter "i" is lowercase and has a dot above it.

**Ensuring Permanent, Easy Access to
U.S. Government Information Assets**



U.S. DEPARTMENT OF COMMERCE
Technology Administration
National Technical Information Service
Springfield, VA 22161 (703) 605-6000
